Titre: Title:	Dehydration of Glycerol to Acrolein in Fluidized Bed Reactor
Auteur: Author:	Marjan Dalil
Date:	2015
Type:	Mémoire ou thèse / Dissertation or Thesis
Référence: Citation:	Dalil, M. (2015). Dehydration of Glycerol to Acrolein in Fluidized Bed Reactor [Ph.D. thesis, École Polytechnique de Montréal]. PolyPublie. https://publications.polymtl.ca/1989/

UNIVERSITÉ DE MONTRÉAL

DEHYDRATION OF GLYCEROL TO ACROLEIN IN FLUIDIZED BED REACTOR

MARJAN DALIL
DÉPARTEMENT DE GÉNIE CHIMIQUE
ÉCOLE POLYTECHNIQUE DE MONTRÉAL

THÈSE PRÉSENTÉE EN VUE DE L'OBTENTION
DU DIPLÔME DE PHILOSOPHIÆ DOCTOR
(GÉNIE CHIMIQUE)
DÉCEMBRE 2015

UNIVERSITÉ DE MONTRÉAL

ÉCOLE POLYTECHNIQUE DE MONTRÉAL

Cette thèse intitulée :

DEHYDRATION OF GLYCEROL TO ACROLEIN IN FLUIDIZED BED REACTOR

présentée par : DALIL Marjan
en vue de l'obtention du diplôme de : Philosophiæ Doctor
a été dûment acceptée par le jury d'examen constitué de :

M. CICOIRA Fabio, Ph. D., président
M. PATIENCE Gregory S., Ph. D., membre et directeur de recherche
M. HENRY Olivier, Ph. D., membre
M. KALIAGUINE Serge, Ph. D., membre

DEDICATION

To my beloved husband Nima,
and to my parents...

ACKNOWLEDGEMENTS

I would like to convey my sincere and heartfelt gratitude to my Ph.D research supervisor, Professor Gregory S. Patience for having me provided with an exceptional support and assistance in the course of this project without which no achievement would have become possible. I am honoured to have had the opportunity to have studied as a student and worked as a Ph.D candidate under his professional supervision at École Polytechnique de Montréal. His patience, enthusiasm, motivation and accurate scientific attitude will never be forgotten.

I would also like to thank Dr. Jean-Luc Dubois for his full support, immense knowledge and professionalism. I am blessed to have worked under his direction and am extremely lucky to have learnt from him through his continuous professional assistance during this research project. In one sentence, Dr Dubois has always been there for me whenever I needed help in advancing the project.

I would also like to acknowledge Dr. Mahesh Edake and soon to be Dr Davide Carnevali who have greatly contributed to the accomplishment of the work. The large load of required laboratory work as well as scientific input was greatly overcome by the precious contributions of these two professionals.

I would like to individually thank Dr. Aline Auroux who kindly helped us with calorimetry experiments.

I thank Mr. Phillippe Leclerc and Dr. Redouane Boutrouka for their assistance with the elemental and FTIR analyses.

I'm grateful to Mr. Charles Bruel for his great help in translation of the abstract of this thesis to French.

I would also like to thank other professors and technical staff of the chemical engineering department of École Polytechnique de Montréal for providing the best assistance in the completion of this project. My deep gratitude goes to my friends and colleagues at École Polytechnique de Montréal, Cristian Neagoe, Cristian Trevisanut, Federico, Swathi, Camille, Mina, Niaz, and many more whose names I unintentionally forgot to mention, for their support in various aspects during this Ph.D thesis.

At the end, I would like to express my thanks to my husband, Nima, who have always supported me both personally and professionally. I'm grateful to his love, encouragement and kindness.

Finally, I would like to thank my parents for their love, patience and continuous support during these past four years.

RÉSUMÉ

L'acroléine, un intermédiaire d'importance pour l'industrie chimique, peut-être produite par déshydratation du glycérol. Son procédé commercial de production est actuellement l'oxydation du propylène, en une seule étape, dans un réacteur multitubulaire à lit fixe. Des considérations écologiques alliées aux réserves limitées de carburants fossiles ont toutefois encouragé les chercheurs à développer des substituts et/ou des additifs à ces derniers comme le biodiésel, le bioéthanol ou le biokérosène. Le biodiésel est produit par transestérification d'huiles végétales et de graisses animales. Le principal coproduit du procédé est le glycérol (10% massiques) dont le degré de pureté dépend du procédé employé. Les impuretés comprennent notamment de l'eau et du méthanol ainsi que des traces d'acides gras et de différents composés organiques et inorganiques. La purification du glycérol, par distillation, est l'étape préalable à toutes ses applications, lesquelles sont nombreuses du fait de sa structure multifonctionnelle. Toutefois, l'augmentation rapide de la production de biodiésel n'a pas coïncidé avec celle de ces applications et l'absence de débouchés en volumes suffisants a fait chuter considérablement le cours du glycérol ces dernières années. Cela s'est traduit par une augmentation du ratio en glycérol brut/purifié à cause du coût élevé de la distillation. La déshydratation du glycérol en acroléine constitue ainsi l'une des nombreuses réactions dont le développement vise à transformer un produit chimique bon marché en composé valorisé. Provenant de la biomasse, le glycérol a de plus une empreinte carbone plus faible que les hydrocarbures fossiles. La déshydratation du glycérol a déjà été largement étudiée en phase gaz et liquide. Plusieurs classes de catalyseurs incluant des zéolites, des métal-oxydes mixtes et des hétéropolyacides ont ainsi été décrites sous différentes conditions opératoires. Malgré le développement de systèmes catalytiques très efficaces, la désactivation rapide du catalyseur et le faible rendement en acroléine restent les principaux obstacles à la commercialisation d'un procédé de déshydratation du glycérol. La formation de coke ayant un impact décisif sur la longévité du catalyseur, différentes stratégies ont été proposées pour sa régénération. Jusqu'à présent, peu d'études se sont concentrées sur la désactivation du catalyseur au cours d'une réaction en lit fluidisé.

Nous avons évalué la performance catalytique du WO_3-TiO_2 pour la déshydratation du glycérol dans un réacteur à lit fluidisé de 4.6 cm de diamètre. La solution aqueuse de glycérol a été directement pulvérisée sur le lit de catalyseur sous forme liquide. Les conditions optimales de réaction ont été évaluées en vue d'une étude ultérieure sur la formation de coke. Parmi les facteurs testés, la température de réaction, la fraction molaire d'oxygène dans l'influx gazeux et la concentration de glycérol se sont révélées être les plus influents. L'objectif était

de maximiser la production d'acroléine tout en réduisant celle de coproduits. Dépendamment des conditions opératoires employées, les principaux coproduits furent l'acétone, le propionaldéhyde, l'acétaldéhyde et l'hydroxyacétone (acétol), l'acide acétique et l'acide formique. Le catalyseur de WO_3-TiO_2 a conservé toute son activité pendant 6 h continues de réaction au terme desquelles il déshydratait le glycérol en acroléine avec une sélectivité supérieure à 73%. Celle-ci n'était cependant que de 55% après une heure de réaction à une température de 280 °C. Le dépôt de coke sur le catalyseur s'accroit avec le temps : la fraction massique de carbone passe de 2.2% après une heure de réaction au double cinq heures plus tard. Cela améliore graduellement la production d'acroléine tout en réduisant d'autant la sélectivité en coproduits et en coke. Sur la base de la distribution en produits et des intermédiaires détectés, un mécanisme de réaction possible a été proposé pour la déshydratation du glycérol. Un modèle cinétique du premier ordre décrit le taux de réaction de l'oxygène sur les espèces carbonées liées au catalyseur avec une énergie d'activation de 100 kJ mol^{-1} ($R^2 > 0.997$). Le modèle a été validé à différentes températures, en conditions isothermes et avec des rampes de température. L'oxydation partielle de la coke, en tant que nouvelle stratégie de régénération pour le catalyseur, a amélioré la sélectivité pour l'acroléine de 10% à 25% dans les 15 premières minutes suivant l'injection du glycérol. La conversion de glycérol en coke a dans le même temps été réduite de 34% à 6%.

Puisqu'après 6 h de réaction, la production d'acroléine est toujours en régime transitoire, nous avons allongé nos tests jusqu'à atteindre le régime permanent. Celui-ci est atteint pour la conversion en acroléine après 14 h de fonctionnement au terme desquelles la déshydratation du glycérol atteint les 100% de conversion. La sélectivité en acroléine est minimale (5%) en début de réaction et augmente graduellement pour atteindre 73% après 6 h et se maintenir à ce niveau par la suite. Il y a une baisse majeure dans la sélectivité en coproduits (acétone et coke) tout du long des 14 h de réaction. La sélectivité pour la coke passe ainsi de 85% après 5 min à 9% après 14 h. Des échantillons de catalyseur, extraits à une heure d'intervalle, ont été analysés par différentes techniques de caractérisation. Les variations dans la force et le nombre de sites acide/base ont montré une réduction du nombre de sites moyennement ou faiblement acides sur le catalyseur. Le nombre de sites fortement acide n'a en revanche pas varié entre le catalyseur fraichement préparé et celui après 14 h de réaction, ce qui suggère que ces sites sont responsables de l'activité catalytique et de la haute sélectivité en acroléine. Les sites basiques disparaissent après 2 h. Une spectroscopie IFTR-pyridine des catalyseurs frais et usagés ne révèle pas de différence dans l'intensité des bandes d'absorption entre l'échantillon à 6 h et celui à 14 h. La production d'acroléine en régime permanent pourrait donc être attribuée à l'acidité stable (en force et en type) du catalyseur. Le ratio molaire H/C du catalyseur usagé est de 0.26, ce qui suggère que la coke est sous forme polyaromatique.

Finalement la formation de coke réduit la surface spécifique du catalyseur de 30.5 m^2/g à 23 m^2/g après 14 h. Les dépôts de coke n'obstruent donc pas l'orifice des pores du catalyseur mais se déposent plutôt sous forme d'une monocouche le long des parois internes des pores.
Des charges d'acid phosphotungstic (HPW) de 10, 20 et 30 wt% massiques été déposées par imprégnation sur deux types de support d'oxide de titane. Les performances des catalyseurs ont été examinées dans les mêmes conditions opératoires dans un microréacteur à lit fluidisé. Les catalyseurs d'oxide de titane pur ont montré la plus faible sélectivité envers l'acroléine et la plus forte pour l'acétol. La sélectivité pour l'acétol diminue ensuite à mesure que la charge en tungstène augmente. D'un autre côté, pour les deux types de supports, 20% s'est révélé être la charge massique optimale d'acid phosphotungstic pour la production d'acroléine (48% de sélectivité) à 280 °C.
Une diminution des pores du TiO_2 de 17.3 nm à 5.6 nm fait chuter la sélectivité en acroléine de 48% à 35% tout en triplant la formation de coke. Finalement, nous avons examiné les effets de l'addition de promoteurs de coke tels que la tétraline et la décaline sur les catalyseurs de WO_3-TiO_2. La forte formation de coke en début de réaction est attribuée à la présence de sites non sélectifs à la surface du catalyseur frais. Les promoteurs de coke couvrent ces sites et augmentent ainsi la sélectivité en acroléine de 10% à 30% dans les 30 premières minutes de la réaction.

ABSTRACT

Acrolein as an important intermediate for the chemical industry can be produced via dehydration of glycerol. Current process for the commercial production of acrolein is a single step propylene oxidation in multi-tubular fixed-bed reactors. The finite reserves of fossil-fuel feedstocks and environmental issues have encouraged researchers to develop substitutes and/or additives for fuels such as biodiesel, bioethanol or biokerosene. Biodiesel is produced through transesterification of vegetable oil and animal fats. The major (10 wt%) co-product in this process is glycerol which contains impurities such as water, methanol, traces of fatty acids as well as various inorganic and organic compounds. Depending on the type of processes employed for the synthesis of biodiesel, the purity of glycerol could be different. Because of its multifunctional structure, glycerol is used as feedstock or additives in a variety of applications. Prior to any application, however, crude glycerol has to be purified by a distillation step. The value of glycerol has dropped considerably due to a rapid increase in the production of biodiesel and a lack of market for such an enormous production capacity. Regarding the costs of distillation, the ratio of crude/purified glycerol has increased. Therefore, the dehydration of glycerol to acrolein is one of the many reactions under development which aims at converting low cost feedstocks into more value-added products. Moreover, due to its origin from biomass, glycerol exhibits a lower carbon footprint compared to fossil-fuel resources.

Dehydration of glycerol has been widely studied in both liquid and gas-phase. Several classes of catalysts including zeolites, mixed metal oxides and heteropolyacids have been previously examined under various reaction conditions. Although very efficient catalytic systems have been developed for the dehydration of glycerol, rapid deactivation of the catalyst and lack of high acrolein yields, are the main obstacles for commercializing this process. Considering the crucial impact of coke formation, several strategies for catalyst regeneration have been proposed. To date, only few studies have focused on catalyst deactivation nor have performed the reaction in fluidized-bed reactors.

We have evaluated the catalytic performance of WO_3-TiO_2 for the dehydration of glycerol in a 4.6 cm diameter fluidized-bed reactor. The aqueous solution of glycerol was directly sprayed on the catalyst bed in liquid form. The optimal reaction conditions were evaluated for further study on coke formation. Reaction temperature, oxygen molar fraction in the gas feed and glycerol concentration were the most effective parameters. The goal was to maximize acrolein selectivity while reducing the formation of by-products. Depending on the operating conditions, the major by-products were acetone, propionaldehyde, acetaldehyde,

hydroxyacetone (acetol), acetic acid and formic acid.

WO_3-TiO_2 catalyst retained its full activity during the 6 h of the continuous reaction. The catalyst dehydrated glycerol to acrolein at a selectivity exceeding 73% after 6 h time-on-stream. However, after 1 h, the acrolein selectivity was only 55% at the reaction temperature of 280 °C. The mass fraction of carbon was 2.2 wt% at 1 h, which doubled after an additional five hours into the reaction. While the acrolein selectivity increased with reaction time, the selectivity of by-products and coke formation decreased. Based on the product distribution and detected intermediates, a possible mechanism has been suggested for the dehydration of glycerol. A first order kinetic model characterizes the rate of carbon oxidation on the catalyst surface with an activation energy of 100 kJ mol^{-1} ($R^2 > 0.997$). The model was validated at different temperatures, heating ramps and isothermal condition. Partial oxidation of coke, as a new strategy for catalyst regeneration, enhanced the selectivity towards acrolein from 10% to 25% in the first 15 min of reaction. The conversion of glycerol to coke, on the other hand, reduced from 34% down to 6%.

As the 6 h long experiment was not sufficient for the selectivity of acrolein to achieve steady state, the reaction time was extended to 14 h. The selectivity of acrolein was minimal (5%) in the fifth minute of reaction; after 6 h it increased to 70% and remained constant. There was a major drop in the selectivity of by-products from the beginning up to 14 h into the reaction. The selectivity towards coke reduced from 85% at 5 min to 9 % after 14 h. The catalyst samples withdrawn at one hour intervals, were analysed by various characterization techniques. The number of medium and weak acid sites of the catalyst reduced. However, the number of strong acid sites did not vary from fresh to 14 h samples. The basic sites disappeared after 2 h indicating that by-products formation including 1,2-propanediol and acetone is correlated to these sites. FTIR-pyridine of fresh and used catalysts, revealed no difference in the band intensity between 6 h and 14 h samples. Thus the steady-state production of acrolein could be attributed to the stable acid types of the catalyst. The H/C ratio for the used catalyst was 0.26 suggesting that these compounds were in the form of polyaromatic coke. Finally, coke formation reduced the surface area of the fresh catalyst from 30.5 m^2/g to 23 m^2/g after 14 h. Coke deposits entered the pores and established a monolayer on the internal walls of the catalyst pores rather than blocking the entrance.

We synthesized catalysts by impregnating 10, 20 and 30 wt% phosphotungstic acid (HPW) on two types of titania supports. The performance of the catalysts was examined under the same conditions in a micro fluidized-bed reactor. Pure titania catalysts showed the lowest selectivity towards acrolein and the highest towards acetol. As the tungsten loading increased, selectivity of acetol decreased. On the other hand, for both supports, 20 wt% was the optimal loading for the maximum production of acrolein (48%) at 280 °C.

Consequently, the effect of pore size of the titania supports on acrolein selectivity and coke formation was studied. The selectivity of acrolein for the pore sizes of 17.3 nm and 5.6 nm was 48% and 35%, respectively. Coke formation, on the other hand, was three times higher for the smaller pore diameter. At the end, we examined the effect of adding hydrogen rich coke promoters such as tetralin and decalin to the prepared catalysts. Severe coke formation in the first 30 min of reaction is attributed to the presence of non-selective sites on the surface of the fresh catalyst. Coke promoters covered these sites and increased the selectivity of acrolein from 10% to 30% in the first 30 min of reaction.

TABLE OF CONTENTS

LIST OF TABLES

LIST OF FIGURES

LIST OF SYMBOLS AND ABBREVIATIONS

α = Conversion of carbon
BET = Brunauer-Emmett-Teller
BJH = Barret-Joyner-Halenda
d_p = Pore diameter
Δm = Rate of coke build-up
E_a = Activation energy
EC = Electro Conductivity
EDX = Energy Dispersive X-ray
FCC = Fluid Catalytic Cracking
FE-SEM = Field Emission Scanning Electron Microscopy
FTIR = Fourier Transform Infra-red
FCC = Fluid Catalytic Cracking
GC = Gas Chromatography
HKT-1 = Titania, d_p :17.3 nm
HKT-2 = Titania, d_p = 5.6 nm
HPLC = High-Performance Liquid Chromatography
HPW = Phosphotungstic acid
k = Rate constant
k_0 = Rate constant at base temperature
MS = Mass Spectrometer
RT = Residence Time
S = Selectivity
S_{BET} = Surface area
Σm = mass of coke per 100 g of catalyst
TPD = Temperature Programmed Desorption
TGA = Thermo-Gravimetric Analysis
U_{mf} = Minimum fluidization velocity
v_p = Pore volume
WHSV = Weight Hourly Space Velocity
X = Conversion
XRD = X-Ray Diffraction

LIST OF APPENDICES

CHAPTER 1 INTRODUCTION

1.1 Background and problem identification

Acrolein is one of the highest valued commodity chemicals which has wide applications in chemical industries such as the production of acrylic acid, glutaraldehyde, methionine, polyurethanes and poly ester resins. Current commercial process for the production of acrolein involves the single-step oxidation of propylene on Bi/Mo mixed-oxide catalysts to oxidize propylene to acrolein in multi-tubular fixed bed reactors. In this process, a cooling fluid circulates between the tubes to minimize the hot spots and maintain high selectivity and longer catalyst life(Cornils, 2004; Callahan et al., 1970). Most of the acrolein is further oxidized to acrylic acid in a second multi-tubular fixed-bed (William, 2000). Nowadays, replacing propylene with a bio-feedstock has been a priority for the industry due to environmental concerns, high propylene prices, supply shortage and low price of glycerol (Liu et al., 2012; Cornils, 2004; Watanabe et al., 2007; Chai et al., 2007a; Dubois et al., 2006a). Dehydrating glycerol to acrolein would be an alternative to oxidation of propylene, if high yields are attainable and if the price of glycerol relative to propylene remains low.

Biodiesel is a biodegradable and renewable fuel and is derived from vegetable oils and animal fats in the presence of methanol. Glycerol is the main co-product (10 wt%) of biodiesel transesterification (Katryniok et al., 2010a). Due to its multifunctional structure, glycerol can be involved in several reactions leading to the production of value-added products such as acrolein, propylene glycol or 1,2-propanediol, syngas, light olefins and 1,3-propanediol(Posada et al., 2012; Yuan et al., 2010; Xia et al., 2012; Zakaria et al., 2012; Wang et al., 2015; Vasiliadou and Lemonidou, 2013). However, to meet the standards of these industries, crude glycerol requires several purification steps such as distillation to remove salts, non-glyceric organic matter (NGOM) and water. Regarding the high costs of these processes and the abundance of glycerol in the market, many biodiesel manufacturers burn unrefined glycerol, which is a huge waste for such bio-based and cheap feedstock (Katryniok et al., 2010a; Shen et al., 2011; Atia et al., 2008).

Dehydration of glycerol to acrolein is a promising substitute to burning for which many catalysts have been developed in both gas and liquid phase. Gas-phase processes are preferred due to the environmental and technical hurdles of liquid phase processes (e.g. corrosion, waste management and poor catalyst recycling) (Chai et al., 2007a).

Catalysts that dehydrate glycerol to acrolein include MOx-Al_2O_3−PO_4 (M as transition metal), zeolites (ZSM−5, HY, SBA−15, ZSM−23, Hβ), metal mixed oxide catalysts (Nb_2O_5,

WO_3/TiO_2, TiO_2/ZrO_2, WO_3/ZrO_2, CeO_2-ZrO_2), heteropoly acids (phosphotungstic acid, silicotungstic acid supported on activated carbon), $ZrSO_4$ and cerium dopped Fe_3PO_4 (Chai et al., 2007a; Neher et al., 1995; Suprun et al., 2009; Pathak et al., 2010; Callahan et al., 1970; Kim et al., 2010; Cavani et al., 2010; Ning et al., 2008; Dubois et al., 2009a; Patience et al., 2012; Vasconcelos et al., 2011; de Oliveira et al., 2011).

Catalyst deactivation is a crucial issue in commercial processes, due to the costs of process shut-down and catalyst replacement. Depending on the type of the process, time scale of the catalyst deactivation may vary from seconds to years. Catalyst deactivation could be delayed if the mechanism of coke formation is known and the system is well-controlled. Mechanisms of deactivation in heterogeneous catalysis are poisoning, fouling, coking and carbon deposition, thermal degradation and sintering, gas-vapour/solid and solid state reactions, and attrition (Bartholomew, 2000). Although highly efficient catalysts could be synthesized for the dehydration of glycerol, they are prone to rapid deactivation and coke formation. Dubois et al. (2009a) suggested co-feeding oxygen with glycerol in the presence of acid catalysts to maintain the catalyst activity and reduce the formation of by-products. Dubois et al. (2006a), Ulgen and Hoelderich (2009) and Ulgen and Hoelderich (2011) examined WO_3 on TiO_2 and ZrO_2 at various operating conditions and tungsten loadings. They concluded that molecular oxygen not only reduced the catalyst deactivation rate, but also the selectivity to propanal and hydroxyacetone (acetol). The content of molecular oxygen depends on the nature of the catalyst, its acidity and its capacity to form coke.

Most of the works on the gas-phase dehydration of glycerol have been performed in fixed-bed reactors with preheating the liquid feed. Application of fixed-bed reactors is associated with the formation of hot spots specially when the catalyst is regenerated. To avoid this effect, we developed the technology of direct liquid injection into a fluidized-bed of catalyst. A fluidized-bed is an ideal reactor to regenerate the catalyst, minimize the formation of hot spots and achieve a homogeneous distribution of carbon on the catalyst. On the other hand, liquid injection in a fluidized-bed reactor could be an effective method to avoid the decomposition of thermal sensitive materials. A well-designed liquid injection system promotes a complete evaporation of reactants and thus an efficient conversion of glycerol.

1.2 Objectives

The main objective of this project is to develop a fluidized bed process for the dehydration of glycerol to acrolein in the presence of WO_3-TiO_2 catalyst using continuous liquid injection. There is an important number of parameters that have to be considered for an efficient

production of acrolein. One crucial factor is extending the life of the catalyst by understanding the effect of coke formation on the product distribution.
The specific objectives are as followed ;

1. Determine the profile of coke formation and transient production of acrolein as a function of reaction time in the glycerol dehydration process ;
   (a) Identify the performance of WO_3-TiO_2 catalyst in terms of acrolein and by-products selectivity, glycerol conversion and coke formation ;
   (b) Determine the effect of coke formation on the selectivity of acrolein and by-product formation ;
   (c) Propose the most probable reaction mechanism ;
   (d) Establish a kinetic model for the oxidation of coked catalyst ;
   (e) Propose a new strategy for partial re-oxidation of the coked catalyst to increase the selectivity towards acrolein ;
2. Identify the impact of coke build-up on the main characteristics of the catalyst in steady-state production of acrolein from glycerol ;
   (a) Characterize the coked catalyst at different reaction times to identify the type and structure of carbon deposits ;
   (b) Determine the effect of reaction time on acid-base properties of the catalyst ;
3. Investigate the effect of operating conditions on the performance of WO_3-TiO_2 ;
   (a) Evaluate the selectivity of acrolein and by-products as a function of effective parameters (temperature, oxygen concentration, glycerol concentration and residence time)
4. Determine the performance of various HPW-TiO_2 catalysts in the presence of hydrogen-rich coke promoters ;
   (a) Prepare and characterize different types of HPW-TiO_2 catalysts ;
   (b) Examine the prepared catalysts and compare the selectivity of acrolein and by-products for each sample ;
   (c) Modify the surface of the catalysts with hydrogen-rich coke promoters ;
   (d) Examine the effect of tungsten loading, pore diameter and coke promoters on acrolein selectivity and product distribution ;

CHAPTER 2 LITERATURE REVIEW

The finite reserves of fossil fuels and the concerns around GHG (green house gases), have encouraged academic and industrial researchers to study substitutes such as biodiesel, bioethanol or biokerosone. Due to their bio-roots these compounds expose lower carbon footprints compared to the conventional fossil fuels. Moreover, biodiesel reduces the engine emissions such as sulphur oxides (100 %),unburned hydrocarbons (68 %) and poly cyclic aromatic hydrocarbons (80 %–90 %) considerably (Tyson KS, 2006).

2.1 Glycerol as a by-product of biodiesel production

Biodiesel is a biodegradable and renewable fuel. The raw material for biodiesel production are vegetable oil, animal fat and a mono-alcohol (usually methanol). Through the transesterification reaction of fatty acid, this alcohol cleaves the fatty acids leading to the formation of desired fatty acid-esters (biodiesel) and glycerol.
Glycerol is the major co-product in this process representing 10 wt% of the whole product. The increasing capacity of biodiesel all over the world, has led to the over production of glycerol.
The purity of glycerol strongly depends on the process used for the breaking of fatty acid. The purity of glycerol obtained from conventional methods for biodiesel production is around 80 %. The impurities are water, fatty acid, methanol, as well as various non-glyceric organic matter (NGOM). Consequently, crude glycerol requires a distillation step before any application. The high cost of distillation, rapid increase in quantity of glycerol during the biodiesel process and also lack of sufficient market, leads to a considerable decrease in the amount of refined glycerol as compared to the crude form. Furthermore, unrefined glycerol is usually burned, which is a dramatic problem due to the waste of such bio-based raw material. Also, insufficient market to absorb the produced glycerol has reduced the price of glycerol over the past years. For instance, the market price of glycerol was $\$0.43\,\mathrm{kg}^{-1}$ in 2003. This value was dropped to $\$0.18\,\mathrm{kg}^{-1}$ in 2010 for pure glycerol and to only $\$0.02\,\mathrm{kg}^{-1}$ for crude glycerol. Therefore, the conversion of glycerol to different valuable materials through various catalytic processes has been intensively considered for the future scale up .

2.2 Applications of glycerol

Glycerol has three hydroxyl groups in its structure which make it soluble in water and alcohol and insoluble in hydrocarbons. Due to its hydrophilic property, glycerol could be applied in the processes in which the control of water content is needed such as adhesives or glue. Also, glycerol is applied in food industry and pharmaceuticals because of its non-toxicity and sweet taste. Furthermore, plastic industries including resins and lubricants use glycerol due to its high viscosity and high boiling point (290 °C).
Despite all these applications, the market is still not enough for glycerol in comparison to its production capacity. Additionally, before any application, glycerol requires a purification as mentioned before.
Glycerol can be involved in several catalytic reactions to convert into value-added chemicals such as acrolein, syngas and 1,3-propanediol (Figure 2.1).
The industrial applications of glycerol (large scale) are categorized as follows :

- halogenations to epichlorhydrin, applied as an intermediate for epoxy resins (commercialized by Solvay in France, 2007) (Katryniok et al., 2010a) ;
- syngas production in the presence of Pt-Rh catalyst. In addition, alkanes and methanol production by FischerTropsch process (industrialized by BioMCN with 200 kJ/yr capacity Netherland) (Simonetti et al., 2007),(Soares et al., 2006) ;
- production of mono acylglycerol (MAG) and diacylglycerol (DAG) as emulsifiers in cosmetic and food (sauces and margarines) industries by esterification of glycerol (Sonntag, 1982) ;
- selective reduction of glycerol to propylene glycol (commercialized by Syngas Chemicals with capacity of 30 kJ/yr) or 1,3- propanediol (PDO) (Pagliaro and Rossi, 2010) ;

2.3 Acrolein and its applications

Acrolein is the simplest unsaturated aldehyde containing carbonyl and vinyl groups. It is considered as a versatile intermediate for chemical industry in the production of acrylic acid and its esters, glutaraldehyde, methionine, polyurethanes and polyester resins (Figure 2.2).
The majority of crude acrolein is applied in the production of acrylic acid. Methionine, an additive of animal food, is also a major consumer of refined acrolein (80 %(Etzkorn et al., 2000)). The rate of need for methionine has been growing with an annual rate of over 5 % since 1977 (Council, 1981).
The rest of the manufactured acrolein is applied in the production of other chemicals such as : glutaraldehyde, 1,2,6-hexanetriol, quinoline, pentaerythritol, cycloaliphatic epoxy resins, oil-well derivatives, and water treatment chemicals. Acrolein is also directly injected in water

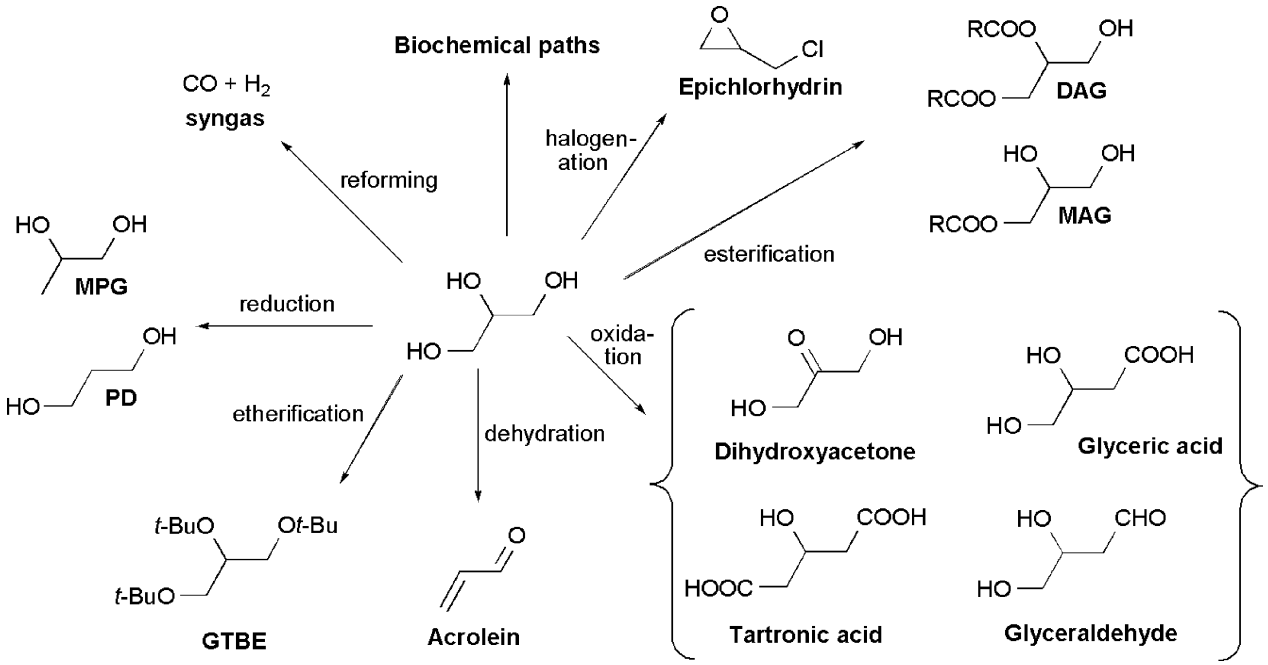

Figure 2.1 Pathways to convert glycerol to value added molecules (Katryniok et al., 2009)

to control the level of the undesired microbials (Bowmer and Smith, 1984).

2.4 Methods for the synthesis of acrolein

Several methods for the production of acrolein are known (Figure 2.3). Considering the importance of acrolein's involvement in chemical industries, these methods are reviewed for more improvements.

The first industrial process for the synthesis of acrolein was catalytic aldol condensation of acetaldehyde and formaldehyde.

Currently, acrolein is produced from a single step oxidation of propylene in multi-tublar fixed-bed reactors. The reaction temperature is usually between 250 °C-400 °C. In general the catalyst applied in this process is a mixed oxide of metals containing Mo, Bi, a divalent (Co,Ni,Mg,Pb) and a trivalent (Fe,Cr,Ce,Al). The major active sites of these catalysts are bismuth and molybdenum. To improve the activity, divalent, trivalent or optionally Sb, Te, W, V, Nb and P or B may be added to the catalyst. The life time of these catalysts in industry is 2-5 years.

Acrolein can further oxidise to form CO_2. The presence of steam in this reaction reduces the formation of CO_2 and enhances the rate of acrolein production. In industry, water is usually

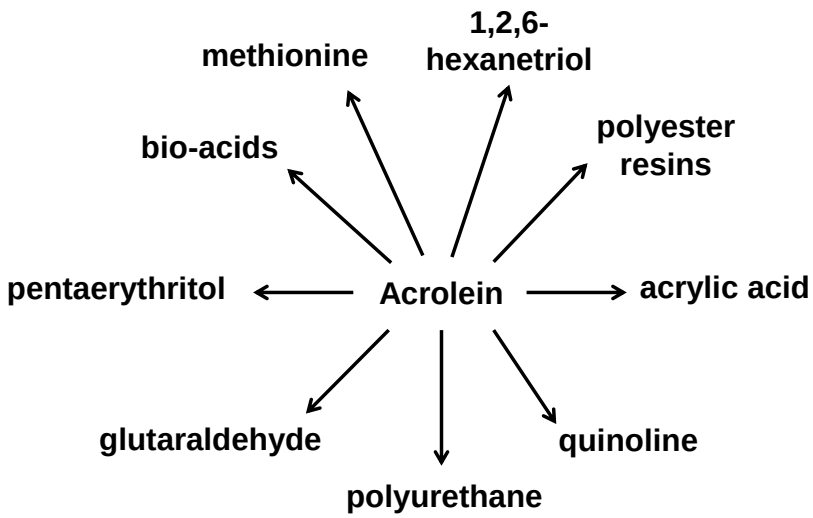

Figure 2.2 Application of acrolein in chemical industries (Liu et al., 2012)

co-fed with the reactants to cover the strong oxidizing sites of the catalyst. Additionally, water can provide new sites on the catalyst for partial oxidation of propylene.
Considering that partial oxidation of propylene to acrolein is exothermic, the management of heat release is crucial in reactor design. Otherwise, the risk of explosion and temperature run-off would be high. One suggestion to solve this problem was using a circulating fluidized bed reactor (Patience and Mills, 1994). This reactor has the advantages of better mass and heat transfer, easier catalyst addition and removal, lower risk of explosion and possibility of using higher propylene concentrations. However, sufficient information on fundamental kinetic and mass and heat transfer is still required to commercialize this process.
Another suggestion to control the heat release in multi-tubular reactor was addition of an inert gas such as CO_2. CO_2 improved the heat transfer during the reaction and the productivity was increased by 14 %.
The application of "wall reactor" and "membrane reactor" were also studied to reduce the effects of high exothermic reaction and improve the yield of acrolein (Redlingshofer et al., 2002), (Redlingshofer et al., 2003),(O'Neil and Wolf, 2006).

2.5 Production of acrolein through dehydration of glycerol

Heating glycerol leads to its decomposition to acrolein, water and by-products. Of course a suitable catalyst is needed to improve the reaction yield under the operating conditions.

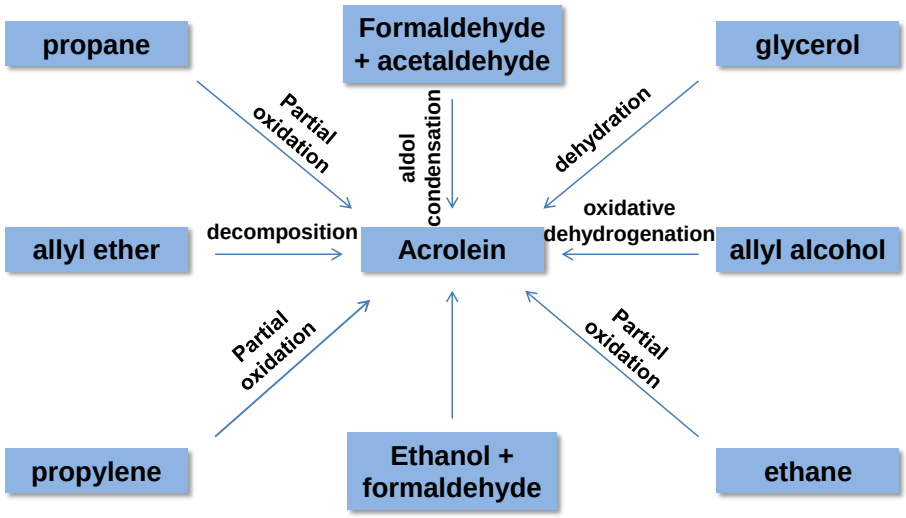

Figure 2.3 Synthesis of acrolein from different routes (Liu et al., 2012)

Due to the availability of glycerol from biodiesel synthesis and its bio-base, dehydration of glycerol to acrolein is a potential alternative to oxidation of propylene.

The early studies of glycerol dehydration were started in 1930. For the first time this subject was patented by Kahlbum (1930). The yield of acrolein for the gas phase reaction over lithium phosphate catalyst was around 75 %.

Later, in 1936, 50 % of acrolein was reported for dehydration of glycerol in liquid phase in the presence of sulfuric acid (as catalyst) (Hearne and A, 1936).

Hoyt and Manninen (1951) further studied this reaction in liquid phase over phosphorous acid catalyst supported on clay. They performed at 300 °C and reached a yield of 70 %.

At the end of 20th century, when biodiesel production process provided cheap glycerol, Neher et al. (1995), continued the experiments over lithium phosphate catalysts and acid catalysts with Hammett acidities (HA) between +3 to -8.2 (e.g. phosphorous acid catalyst supported on alumina). They reported 75 % acrolein yield at full conversion of glycerol for an aqueous solution of glycerol (10 %- 40 %) at 300 °C. Their main by-product was hydroxyacetone (acetol) with a selectivity of 10 %.

2.6 Glycerol dehydration in gas-phase vs. liquid-phase

2.6.1 Liquid-phase reaction

In 1987, liquid-phase dehydration of glycerol was performed with 0.005 molar H_2SO_4 as catalyst. The feed was 0.5 molar solution of glycerol and the reaction was performed under 34.5 MPa pressure. Although the conversion of glycerol was around 50 %, the selectivity towards acrolein was 100 % (Ramayya et al., 1987).

Dehydration of glycerol in sub and super-critical water (SCW) has attracted the interest of few researchers. Buhler et al. (2002) operated the reaction at temperatures between 350 °C - 475 °C under 25, 35 and 45 MPa. The residence time was from 32 s to 165 s. They concluded that longer residence times, lower temperatures and higher pressures favoured the production of acrolein. Nevertheless, without the addition of acid, the maximum conversion and selectivity was 31 % and 37 %, respectively.

Although the addition of mineral acids improves reaction yield, it raises the problem of reactor corrosion. As pure water itself has corrosive effects, the acid intensifies this problem. corrosive-resistant materials (such as inconel) can be applied in building of the plant but due to their high costs, this becomes the main obstacle for commercializing this process.

Ott et al. (2006) used $ZnSO_4$ as catalyst in dehydration of glycerol under SCW condition regarding its less corrosive effects. The addition of zinc sulphate showed a positive effect on selectivity of acrolein. The maximum selectivity obtained (75 %) was for 470 ppm $ZnSO_4$ at 360 °C and25 MPa. The reaction time was shown to be more important when performing under subcritical condition. They also concluded that subcritical condition was more preferable for the production of acrolein as opposed to Watanabe et al. (2007) who reported better results for supercritical conditions.

SCW conditions have several disadvantages.

First : There is a limitation in glycerol feed concentration. If the concentration of glycerol exceeds 5 wt%, the coke will form on reactor wall, pipes and even set-up fittings leading to major security issues specially at high pressures.

Secondly : The corrosion caused by addition of a mineral acid or even pure water is a limiting factor. For this reason and also blockage of the lines, the entire set-up might need to be replaced after a while.

Third : Separation of the homogeneous catalyst from the reaction mixture is a concern.

Fourth : After separation, waste management or poor recycling of the acid catalyst is an issue.

These drawbacks and also the complexity of the process stand in the way of scale-up and commercialization for the liquid-phase reactions (Liu et al., 2012).

Shen et al. (2014a) performed the glycerol dehydration reaction in liquid phase over Brønsted acidic ionic liquid catalysts (BAILs). They synthesized various types of BAILs for liquid phase dehydration of glycerol and reported that the catalysts prepared with 1-butyl-3-methylimidazolium (Bmim) cation and moderate acidity enhanced the formation of acrolein in liquid phase glycerol dehydration.

2.6.2 Gas-phase reaction

Glycerol dehydration in gas-phase is more popular due to its simplicity and advantages over liquid-phase reaction. The reaction may even occur in a regular set-up with minimal adjustments. Since usually the reaction is operated under atmospheric pressure, there's no need for pressure controlling system which reduces the process costs. Also, the effect of corrosion is minimized in this case.
Additionally, packed-bed reactors (PBR) and heterogeneous catalysts are utilized for the gas-phase dehydration of glycerol. So, the issue of the acid catalyst separation in reactor downstream is no longer considered (Liu et al., 2012).
Solid and specially acid catalysts are proper candidates for gas-phase dehydration. The catalyst performance is evaluated by several factors including the surface area, pore size, acid type and acid strength.

2.7 Catalysts for dehydration of glycerol

Various classes of catalysts have been applied for dehydration of glycerol in gas-phase.

2.7.1 Zeolites

Zeolites are well known for their thermal stability, controllable pore size distribution and also adjustable distribution of Brønsted and Lewis acid sites. The general formula of zeolites is represented as $Mx/n[(AlO_2)x\text{-}(SiO_2)y]$. They have been considered as catalysts or supports, for many reactions.
Beside Dubois et al. (2006a) who patented the application of ZSM−5 and H-Beta zeolites for dehydration of glycerol in the gas-phase, other researchers also studied catalytic performance of zeolites in this process.
Li et al. (2007) patented the application of zeolites for glycerol dehydration in fixed-bed reactor. They tested several zeolite structures such as MCM−49, MCM−22, MCM−56 and ZSM−11. The maximum selectivity of 82 % was reported for ZSM−11 at 320 °C.

Corma et al. (2008) studied the application of ZSM−5 catalyst for glycerol dehydration in moving and fixed-bed reactors. They obtained 62 % acrolein yield in this system at 350 °C and 100 % glycerol conversion. The advantage of moving-bed reactors is continuous and easy separation of catalyst for regeneration purpose.
HZSM−5 catalyst was applied for liquid-phase dehydration of glycerol. Under the reaction conditions (300 °C and 7 MPa), although the glycerol conversion was 15 %, selectivity of acrolein was 75 % (Neher et al., 1995).
Chun-Jiao et al. (2006) synthesized micro- and mesoporous ZSM−5 composites by changing factors such as crystallization temperature, crystallization time and pH to tune SiO_2/Al_2O_3 (25-360). They examined the produced samples for gas-phase dehydration of glycerol and claimed a full conversion of glycerol for 72 % selectivity towards acrolein.
Pathak et al. (2010) followed their work by investigating the impact of textural properties such as pore size of ZSM−5 on the selectivity of acrolein.They showed that the selectivity for acrolein increases with the pore size, while the selectivities to acetaldehyde, formaldehyde and acetol decrease in the same time.
Kim et al. (2010) used NaZSM−5 and HZSM−5 catalysts with SiO_2/Al_2O_3 ranging from 23 to 1000. The highest selectivity of acrolein was achieved for HZSM−5 at 350 °C. Base on TPD-NH_3 and FTIR-pyridine techniques, the authors concluded that density of acid sites of the catalysts were decreased when SiO_2/Al_2O_3 ratio increased. However, although low Si/Al showed highest acidity, the activity of catalyst was lowest for that.
Non-crystalline ZSM−5 catalysed the dehydration of glycerol to acrolein. According to Jia et al. (2010) small-sized particles enhanced the catalytic performance of ZSM−5. However, the best results were obtained for small-sized catalysts with more Brønsted acid sites (higher Al content).
Zeolites are offering another interesting mean for dehydration of glycerol in both gas and liquid-phases. This is provided by tailoring their acid properties by tuning the bulk composition (SiO_2/Al_2O_3).

2.7.2 Supported mineral acids

Several mineral acids including boronic acid, sulfuric acid and phosphoric acid have been studied for dehydration of glycerol. Since mineral acids are soluble in water, first they are supported on a material such as alumina, silica, zeolite, activated carbon or activated bentonite. So far, phosphoric acid supported on Al_2O_3 have shown the best selectivity to acrolein (89 %) (Hoyt and Manninen, 1951),(Yan and Suppes, 2009), (Haas et al., 1993). Haas et al. (1993) described a method for conversion of glycerol to 1,2- and 1,3- propandiol. The first step involving the dehydration of glycerol to acrolein was performed over alumina-supported

phosphoric acid and yielded in the production of 70.5 % acrolein. Li et al. (2007), applied the same catalyst for glycerol dehydration in a semi-batch reactor. The authors added the droplets of glycerol to the reactor and obtained 42 % conversion and 89 % selectivity.

2.7.3 Mixed metal oxides

Table 2.1 summarises the reaction conditions and the obtained results for different metal oxides, phosphates and pyrophosphates.
For some metal oxides (e.g. niobium oxide, tungsten oxide and pyrophosphates), the catalyst preparation condition, particularly calcination temperature and pH value of precipitation, has an impact on the reaction products. These factors can allow tuning the acid-base properties of the catalyst and improve the production of acrolein in gas-phase dehydration of glycerol. Thermal treatment of the catalyst affects the specific surface area and pore size by sintering.

Table 2.1 Gas phase dehydration of glycerol over mixed-metal oxides

Catalyst	$T_{reac.}$ (°C)	$T_{calc.}$ (°C)	Co-feed	Conv.(%)	$S_{acrolein}$ (%)	S_{acetol} (%)	ref.
Nb_2O_5	315	350	-	75	47	10	(Chai et al., 2007b)
Nb_2O_5	315	400	-	88	51	12	(Chai et al., 2007b)
Nb_2O_5	315	500	-	91	35	14	(Chai et al., 2007b)
TiAl	315	600	-	86	46	17	(Tao et al., 2010)
SAPO-11	280	-	-	66	62	10	(Suprun et al., 2009)
SAPO-34	280	-	-	59	72	7	(Suprun et al., 2009)
VPO	300	700	O_2	81	95	9	(Wang et al., 2009)
VPO	300	800	O_2	100	80	6	(Wang et al., 2009)
VPO	300	900	O_2	97	58	15	(Wang et al., 2009)
Fex-PO_4y	280	-	-	100	92	0	(Deleplanque et al., 2010)
9%WO_3-ZrO_2	300	-	-	100	74	11	(Dubois et al., 2006b)
19%WO_3-ZrO_2	280	-	-	83	69	10	(Ulgen and Hoelderich, 2009)
19%WO_3-TiO_2	280	600	-	85.7	76.5	11	(Ulgen and Hoelderich, 2011)
19%WO_3-TiO_2	280	600	-	85.7	76.5	11	(Ulgen and Hoelderich, 2011)
19%WO_3-TiO_2	280	600	O_2	91	68	2	(Ulgen and Hoelderich, 2011)
La_4-$(P_2O_7)_3$	320	-	-	76	78	7	(Liu et al., 2009)
Ce_4-$(P_2O_7)_3$	320	-	-	45	43	10	(Liu et al., 2009)
Nd_4-$(P_2O_7)_3$	320	-	-	87	80	4	(Liu et al., 2009)
Sm_4-$(P_2O_7)_3$	320	-	-	90	78	6	(Liu et al., 2009)
Eu_4-$(P_2O_7)_3$	320	-	-	83	78	6	(Liu et al., 2009)
Gd_4-$(P_2O_7)_3$	320	-	-	88	79	7	(Liu et al., 2009)
Tb_4-$(P_2O_7)_3$	320	-	-	88	79	6	(Liu et al., 2009)
Ho_4-$(P_2O_7)_3$	320	-	-	84	77	7	(Liu et al., 2009)
Er_4-$(P_2O_7)_3$	320	-	-	87	80	7	(Liu et al., 2009)
Tm_4-$(P_2O_7)_3$	320	-	-	87	78	8	(Liu et al., 2009)
Yb_4-$(P_2O_7)_3$	320	-	-	49	64	4	(Liu et al., 2009)
Lu_4-$(P_2O_7)_3$	320	-	-	58	64	7	(Liu et al., 2009)
20%VPO-ZrO_2	300	550	-	100	60	4	(Pethan Rajan et al., 2014)
20%VPO-ZrO_2	300	550	O_2	100	66	-	(Pethan Rajan et al., 2014)

2.7.4 Heteropoly acids

Heteropoly acids (HPAs) are considered as good candidates for glycerol dehydration, due to their high Brønsted acidity which approaches superacid region (stronger acidity than pure H_2SO_4(Timofeeva, 2003)). HPAs are economical, environment friendly, and feature well-defined structures and tunable acidity levels. The most common HPAs are HPW ($H_3PW_{12}O_{40}$), $H_4PW_{11}VO_{40}$, HSiW ($H_4SiW_{12}O_{40}$), H_4SiMoO_{40} and H_3PMo_{12} (Timofeeva, 2003), (Wu et al., 1996), (Kozhevnikov, 2007).

For catalytic applications, HPAs are usually loaded on supported materials due to their low specific surface area (Chu et al., 1996), (Izumi et al., 1983), (Verhoef et al., 1999). The addition of support improves the surface area of HPAs while their acidity remains high enough for the desired reaction. However, several factors must be carefully considered when preparing supported catalysts. For instance an optimum loading of HPA on the support is critical as low loadings lead to less acidity of the catalyst and high loadings will affect the uniform dispersion of the HPA.

Several groups have examined different HPAs on different supports. Tsukuda et al. (2007) used silica-supported heteropoly acids for gas-phase dehydration of glycerol. The activity of their catalysts depended on the type of the heteropoly acid and the pore size of the support. The maximum selectivity (85 %) was reported for HSiW supported on silica with mesopores of 10 nm. The size of the mesopores in the silica support influenced the performance of the catalyst as small mesopores (3 nm) led to the fast deactivation of catalyst and the selectivity of acrolein was 67 %.

Different loadings of HSiW on activated carbon was examined by Ning et al. (2008). The results showed that 10 wt% loaded catalyst was the most active (93 %) and selective to acrolein (75 %). This promising yield is related to 1 : good dispersion of silicotungstic acid on activated carbon and 2 : relatively high density of the catalysts acid sites. The authors also observed that acid strength of 5 wt% HSiW loadings on activated carbon reduced whilst at higher loadings HSiW molecules agglomerated and caused smaller pore size and severe deactivation of the catalyst.

Katryniok et al. (2010b) prepared HSiW supported on silica samples for dehydration of glycerol. Prior to the preparation they loaded the support with 10- 40 wt% zirconia. The long term performance of the catalyst was enhanced by addition of ZrO_2 to support due to the decrease in Brønsted acidity. The selectivity of acrolein was 69 % and 24 % for treated and bare silica, respectively. However, a careful balancing between the HPA and ZrO_2 is required to reach a high selectivity for acrolein.

Dubois et al. (2009a) patented the application of supported HPAs for gas-phase dehydration of glycerol. The reaction yield to acrolein was between 50- 93% for 79- 100% conversion of

glycerol (Dubois et al., 2009b), (Dubois et al., 2009a).
Atia et al. (2008) confirmed the results of Tsukuda et al. (2007) for the effect of the type of support and pore size distribution on acrolein production. Different types of HPAs were loaded on several supports and tested. HSiW was better catalyst than $H_3PMo_{12}O_4$, $H_3PW_{12}O_{40}$ (HPW), or $(NH_4)_3PMo_{12}O_{40}$ due to their higher acidity. Alumina and aluminosilicate-supported catalysts were also more stable. Although they reported that either 10 wt% or 20 wt% loading of HSiW did not cause a significant difference in acrolein selectivity, the size of mesopores of alumina showed the same effect on the catalyst performance ; larger mesopores (12 nm vs. 5 nm) resulted in better catalytic production of acrolein (85 % vs. 65 %).
Anti sintering zirconia nano-crystals was used as support for HPW by Chai et al. (2007a). The use of zirconia as support enhanced the thermal stability of the catalyst due to its interaction with HPW. The optimum loading of HPW was 10- 20 wt%.
Alhanash et al. (2010) prepared caesium salts of HPAs as catalysts for dehydration of glycerol. Although all the catalysts were active and selective, HPW-Cs salt performed better performance than HSiW-Cs salt. The authors also doped the samples with platinum group metals (PGM) (0.3–0.5%). The PGM improved the acrolein production in the order : Ru < Pt < Pd. The best performance was for 0.5%Pd/CsPW catalyst when it gave 96 % acrolein selectivity at 79 % glycerol conversion.

2.8 Acidity of the catalyst in dehydration of glycerol

The choice of acid catalyst can greatly influence the yield of acrolein in dehydration reaction as well as catalyst stability. Dubois et al. (2006a) for the first time studied the effect of solid acidity quantitatively. They tested various types of catalysts including zeolites, heteropolyacids (HPA), Nafion and acid impregnated metal oxides. The authors concluded that the selectivity of acrolein depended on the acidity of the catalyst and the best selectivity for acrolein was obtained for the catalysts with HA between -10 to -16. The highest selectivity (near 70 %) at full conversion of glycerol was reported for tungsten oxide on zirconia (HA= -14.5) and Nafion (HA= -12) catalysts. For the zeolites (HA< +2), on the other hand, the selectivity roughly reached 60 %.
Chai et al. (2007b) examined niobium oxide catalyst for dehydration of glycerol. Since the calcination temperature reversely affects the catalyst acidity and surface area, the catalysts calcined at rather low temperatures (250 °C - 300 °C) showed better performances. However, the selectivity of acrolein at 90 % conversion of glycerol was 50 %. The main observation was the catalyst fast deactivation for lower calcination temperatures.

The authors followed their study by screening different classes of catalysts in terms of their acidities (Chai et al., 2007a). They measured the Hammett acidity and basicity of the catalysts by n-butylamine and benzoic acid titration methods using Hammett indicators. These catalysts and their performance in production of acrolein are listed below ;

1. Basic catalysts (HA > +7) such as cerium, magnesium and lanthanum oxides. These catalysts showed low selectivity towards acrolein (less than 10 %) ;
2. Weak and medium strong acid catalyst (-3 < HA < +6.8) such as SiO_2 (SBA-15), ZrO_2 and Nb_2O_5 (calcined at 700 °C). The selectivity of acrolein for this class did not exceed 30 % ;
3. Strong acid catalysts (-8.2 < HA < -3). This group includes H_3PO_4-Al_2O_3, WO_3-ZrO_2, $H_3PW_{12}O_{40}$-Al_2O_3, $NiSO_4$-Al_2O_3, HZSM−5, SAPO−34, Nb_2O_5 (calcined at 500 °C)and pure alumina. The reaction yields were more promising than group 2 and the selectivity of 70 % was obtained for WO_3-ZrO_2 and HPW-Al_2O_3 catalysts at 70 % conversion of glycerol. These results showed good agreement with those of Dubois et al. (2006a). Despite the acceptable performance obtained by this group, the catalysts were poor in stability. For both catalysts, the conversion of glycerol dropped from 70 % to less than 25 % after 10 h of reaction time, while the selectivity remained unaffected ;
4. Very strong acid catalysts (HA < -8.2) such as SO_4-ZrO_2, SiO_2-Al_2O_3, Nb_2O_5 (calcined at 350 °C) and Hβ. In general, selectivity to acrolein was not as much as group 3, but time-on-stream had less effect on the performance of catalyst. This group also suffered from coke deposition and catalyst deactivation.

The type of the acid sites (Brønsted and Lewis) influences the reaction pathway. Brønsted acids donate proton and Lewis acids accept electron pairs. Chai et al. (2007a) did not separate the acid types when they were studying different classes of catalysts. According to their results, Brønsted acids (e.g. silicotungstic acid, protonated zeolites or phosphorous acid) revealed better selectivity towards acrolein than Lewis acids (niobium oxide or pure alumina). Alhanash et al. (2010) proposed reaction mechanisms over Lewis and Brønsted sites for glycerol dehydration (Figures2.4 and 2.5). They compared the catalytic performance of acidic caesium salts of phosphotungstic acid (pure Brønsted) and tin-chromium mixed oxide (pure Lewis). In the presence of Lewis acids, higher selectivity to hydroxyacetone (acetol), which is the main by-product in glycerol dehydration, was obtained. However, strong Brønsted acid sites were highly active (100 %) and selective to acrolein (98 %) initially, but conversion dropped quickly due to the fast catalyst deactivation.

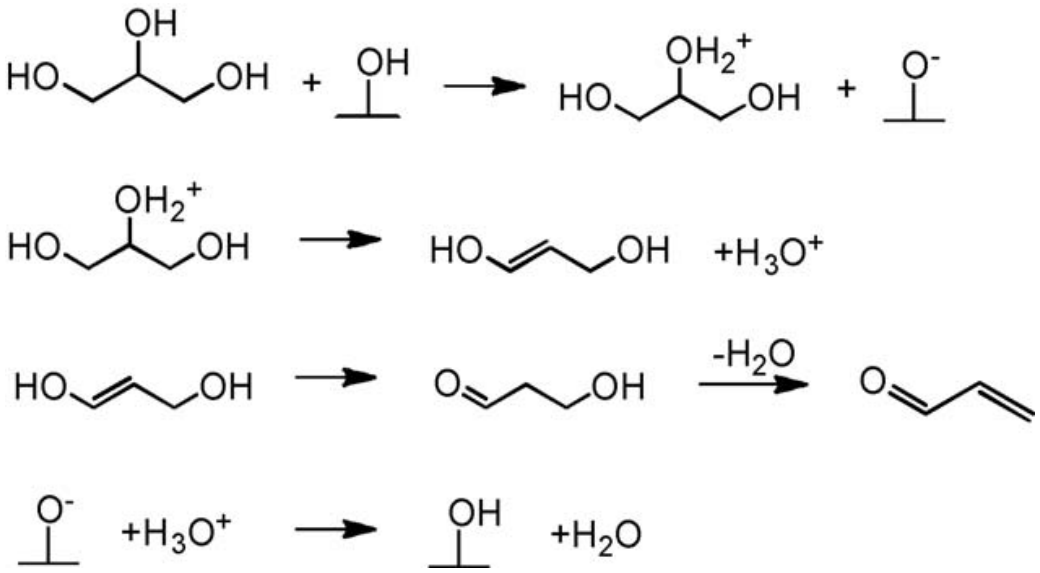

Figure 2.4 Glycerol dehydration mechanism over Brønsted acid sites (Alhanash et al., 2010)

These results were confirmed by examining HZSM−5 catalyst for dehydration of glycerol (Kim et al., 2010). The authors changed the ratio of SiO_2/Al_2O_3 in the synthesized catalysts. The strength and type of the acid sites were measured by TPD-NH_3 and FTIR techniques. They found that increasing the ratio of SiO_2/Al_2O_3 decreased the number and density of the acid sites. They also observed the lowest reaction yield was obtained for NaZSM−5 catalyst which is a moderate Lewis acid.

In a recent work by Wang et al. (2015), tuning the properties of Brønsted and Lewis acids individually did not improve the production of acrolein. The authors considered a new route in which, the Lewis sites cooperated with Brønsted sites to promote acrolein production.

Chai et al. (2007a) had already reported higher acetol production of acetol over basic catalysts. Inspired by their study, Kinage et al. (2010) studied selective dehydration of glycerol to acetol to understand the effect of basic sites of the catalyst on reaction pathway. In their proposed mechanism, initially 2,3- dihydroxypropanal is produced through dehydrogenation of glycerol over basic catalyst. Further dehydration and hydrogenation of 2,3-dihydroxypropanal results in the production of acetol. Another pathway is retro-aldol reaction leading to the formation of formaldehyde and hydroxyacetaldehyde which can be hydrogenated and make ethylene glycol (Figure2.6).

The effect of acidic-basic features of calcium phosphate catalyst -with different Ca/P ratio-

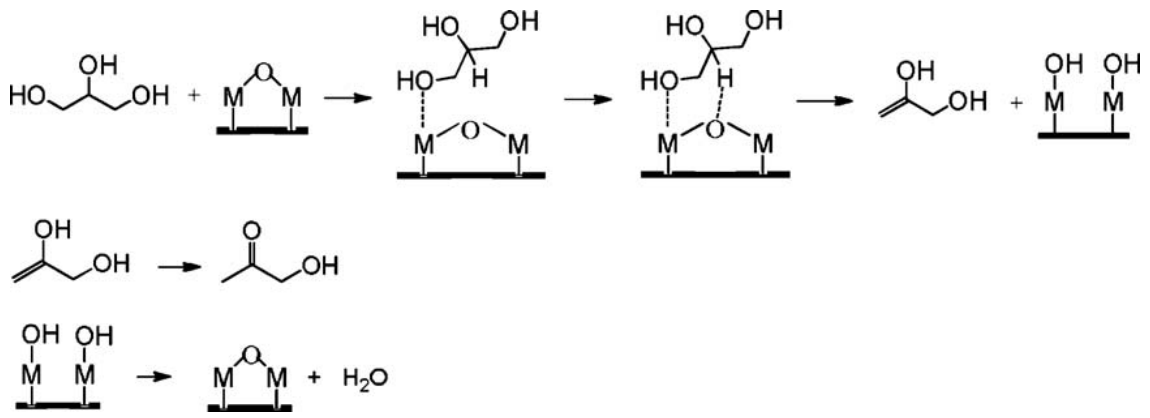

Figure 2.5 Glycerol dehydration mechanism over Lewis acid sites (Alhanash et al., 2010)

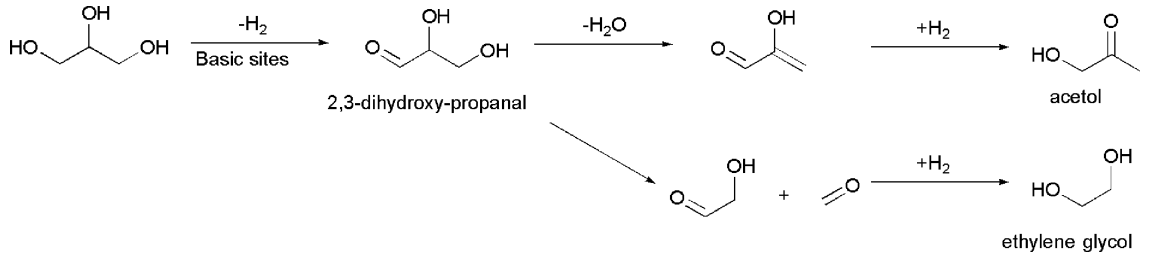

Figure 2.6 Glycerol dehydration mechanism over basic sites (Kinage et al., 2010)

was studied for glycerol dehydration (Stosic et al., 2012). Beside the acidity, the authors also measured the basicity of the samples by TPD-SO_2. Basic sites directly affect the production of acrolein and acetol. Higher yields of acrolein are obtained not only by the acidity of the catalyst but also by hindering the basic sites.

Although the role of strong Brønsted sites in production of acrolein is confirmed, the state of Lewis sites is not clear under the reaction conditions. Considering the availability of steam in the reaction media, Lewis sites could react with steam and generate more Brønsted sites (Alhanash et al., 2010) and (Katryniok et al., 2010b).

As the catalyst usually contains both acidic and basic sites, the effect of basicity should also be considered.Chai et al. (2007a) have reported that over basic sites, acetol was the major product in glycerol dehydration.

2.9 Catalyst deactivation

Catalyst deactivation, defined as the loss of catalytic activity and/or selectivity with time, is problematic in industrial catalytic reactions because of the expenses of process shut-down and replacement of the catalyst. Time scale of the catalyst deactivation vary from seconds to years ; for instance, chemical cracking catalysts deactivate in order of seconds while the catalyst of ammonia synthesis may last for 5-10 years.
Although catalyst deactivation is unavoidable, it could be delayed in a well-controlled system. For example, in steam reforming of methane or naphta, if the reaction temperature increases excessively or the ratio of steam/hydrocarbon passes a critical value, large quantities of carbon filaments will block the catalyst pores resulting in process shutdown in a matter of hours.

2.9.1 Mechanism of deactivation of heterogeneous catalysts

There might be many different pathways for deactivation of the catalyst. For example it could happen because of the presence of contaminants in the reaction media, blockage or fouling of the catalyst surface or voids by carbon or coke especially for the reactions that involve hydrocarbons and high operating temperatures which cause thermal degradation of the catalyst. Thus the causes of catalyst deactivation, are thermal, mechanical and chemical. The mechanisms of solid catalyst deactivation are categorized in 6 groups (see Table 2.2).

Table 2.2 Mechanism of catalyst deactivation (Bartholomew, 2000)

Mechanism	Type	Description
poisoning	chemical	chemisorption of contaminants on catalytic sites resulting in blockage of active sites
fouling	mechanical	physical desorption of species from fluid phase on catalyst surface and pores
thermal degradation	thermal	loss of catalytic surface area and active phase-support reaction due to the thermal effects
vapour formation	chemical	Formation of volatile compounds by reaction of gas-phase with catalyst
vapour-solid and solid-solid reactions	chemical	reaction of gas-phase, support or promoter to produce inactive phase
attrition/crushing	mechanical	loss of catalytic material due to erosion of internal surface area caused by mechanical crushing of the catalyst

2.9.2 Poisoning

Poisoning (Jacque and Henry, 1985), is strong chemisorption of impurities or even reactants or products on the catalytic active sites. Blockage of the adsorption sites and changes in the electronic and geometric structure of the catalyst surface could be consequences of the poisoning. There are different classes of catalyst poisons based on their chemical structure, selectivity for active sites, and the type of the reaction. For example, there are 4 types of common poisons classified based on their chemical structure ;

— Groups VA and VIA : N, P, As, Sb, O, S, Se, Te.
— Group VIIA : F, Cl, Br, I.
— Toxic heavy metals and ions : As, Pb, Hg, Bi, Sn, Zn, Cd, Cu, Fe.
— Molecules that adsorb with multiple bonds : CO, NO, HCN, benzene, acetylene, unsaturated hydrocarbons.

Examples of common poisons for known catalytic reactions over specific catalysts are given in Table 2.3.

Table 2.3 Common poisons for specific catalytic reactions over selected catalysts (Bartholomew, 2000)

Reaction	Catalyst	Poisons
cracking	silica-alumina, zeolites	organic bases, hydrocarbons, heavy metals
hydrogenation/dehydrogenation	Ni, Pt, Pd	compounds of S, P, As, Zn, Hg, halides, Pb, NH_3, C_2H_2
steam reforming of methane, naphta	nickel	H_2S, As
ammonia synthesis	Fe, Rh	O_2, H_2O, CO, S, C_2H_2,
Fisher-Tropsch synthesis	Fe, Co	rH_2S, COS, As, NH_3, metal carbonyls
hydrocracking	noble metals on zeolites	NH_3, S, Se, Te, P
ethylene oxidation	Ag	C_2H_2
oxidation/selective catalytic reduction	vanadium oxide	As/Fe, K, Na from fly ash
oxidation of CO and hydrocarbons	Pt, Pd	Pb, P, Zn, SO_2, Fe
hydrotreating of residues	Co and Mo sulphides	asphaltenes ; N, Ni, V compounds

2.9.3 Fouling, coking and carbon deposition

In contrary to poisoning, fouling is the physical adsorption of species from the fluid phase on the catalyst surface and blockage of active sites or pores. Famous examples of this class of deactivation are deposition of coke and carbon in porous catalysts. Regarding the origin of the carbon and coke, their definition differs ; carbon is sourced from disproportionation of CO while coke is formed by decomposition and/or condensation of carbonaceous compounds on catalyst surface. Coke could be in form of a polymerized heavy hydrocarbon to simple carbons, namely graphite.

Menon (1990) classified the catalytic reactions which are accompanied by carbon or coke formation to coke-sensitive and coke-insensitive. In coke-sensitive reactions, the catalyst losses its activity due to the deposition of unreactive coke on active sites. Catalytic cracking and hydrogenolysis are examples of this classification. In coke-insensitive reactions, on the other hand, reactive coke is removed by a gasifying agent (O_2, H_2...). Fisher-Tropsch synthesis and catalytic reforming are examples of coke-insensitive reactions. Based on this classification, the structure and location of the coke formation as well the mechanism under which the coke forms has a great impact on catalyst activity. Fortunately, some forms of poisoning and many forms of fouling are reversible and regeneration of these systems are easier (Bartholomew, 2000).

2.9.4 Thermal degradation and sintering

Loss of catalytic surface area due to crystalline growth, loss of support porosity and conversion of catalytic phases to non-catalytic phases are responsible for thermal deactivation of catalyst. The first two processes are also considered as "sintering" which typically happen at reaction temperatures higher than 500 °C.
The rate of sintering depends on temperature, atmosphere, metal type, metal dispersion promoters, support surface area, texture, and the porosity (Bartholomew, 2000), (Farrauto R. J., 1997). Baker et al. (1991) studied the effects of sintering on catalyst activity. Depending on the type of the reaction, specific activity of the catalyst could increase, decrease or remain constant with increasing metal crystallite size.
The principal mechanisms of metal crystallite growth are (1) crystallite migration, (2) atomic migration and (3) vapour transport. However, there is disagreement regarding which mechanism of sintering occurs at a certain condition. In some cases, all the mechanisms may occur simultaneously or be coupled with each other. Thermal degradation is generally slow process and its rarely reversible. So, in many cases regeneration of catalyst is not possible (Bartholomew, 2000).

2.9.5 Gas-vapour/solid and solid state reactions

Beside poisoning, there are several chemical routes in chemical deactivation of catalysts. The reaction of vapour phase with catalyst surface, catalytic surface solid-support or solid-promoter reaction and solid-state transformation of catalytic phases under reaction condition (Bartholomew, 2000).
Gas/solid reactions could either form inactive bulk and surface phases or volatile compounds. For example, Fe and Ru are active phases in ammonia synthesis while oxides of this reagents

are inactive. If any of these metals is oxidized, sulfided or carbided, the activity will be reduced.

2.9.6 Attrition

Attrition is an indication of catalysts mechanical failure and commonly occurs in slurry or fluidized-bed reactors. Reduction of particle size, rounding or smoothing of catalyst particles are signs of catalyst attrition. High increases in pressure drop of the process could indicate the blockage of the lines by accumulation of attrited catalyst. Generally, commercial catalysts are subject to mechanical failure because of their preparation method. Fine particles ranging from 10 nm to 100 nm, agglomerate to form catalyst granules, extrudates and pellets. Precipitation and sol-gel methods followed by spray drying, extrusion or compaction are the most common steps for this method. As a result, these catalysts exhibit lower strength than primary particles making them vulnerable to mechanical failure.
Other types of mechanical failure of catalyst are : crushing of granular or monolithic catalyst and erosion of catalyst coating caused by high gas velocities (Bartholomew, 2000).

From our discussion around types of catalyst deactivation, we can conclude that it is easier to prevent catalyst deactivation than regenerating deactivated catalyst. For instance, to avoid fouling and poisoning of fresh catalyst, some contaminants could be removed from reaction feed. Lowering the reaction temperature could reduce the sintering rate and minimize the thermal degradation of catalysts. Careful choice of gas velocity, carrier material and catalyst preparation method could prevent mechanical degradation of catalyst. Finally, addition of regenerating reagents such as steam, oxygen and hydrogen to gasify coke precursors and lower the deactivation rate Bartholomew (2000).

2.10 Catalyst deactivation and regeneration in glycerol dehydration

The most probable mechanism for the deactivation of catalysts in glycerol dehydration is coke formation. Parameters such as type of catalyst, time-on-stream and operating conditions could affect the carbon composition. According to the literature, efficient catalysts for this process can be prepared, but not all of them are applicable in industrial plants. Strong Brønsted acids could efficiently dehydrate glycerol to acrolein but in most cases coke formation is severe and the catalyst deactivates rapidly. Erfle et al. (2011) analysed used vanadium based catalysts by FTIR spectroscopy and concluded that Brønsted sites are responsible for coke formation. The conclusion was confirmed by Suprun et al. (2009) who evaluated the

formation of carbon deposits on phosphate catalysts. They also observed that higher reaction temperatures and small pore diameter of the catalyst lead to further carbon formation (Table 2.4).
Elemental analysis of used catalysts exhibited a decrease in the H/C ratio as the reaction temperature increased meaning that coke deposits become richer in carbon.

Table 2.4 Correlation between acidity and coke formation for phosphate catalysts (Suprun et al., 2009)

Catalyst	Acidity $\mu molNH_3/g$	D_P Å	S_{BET} m^2/g	Coke (at 280 °C) wt%	Coke (at 300 °C) wt%	Coke (at 320 °C) wt%
Al_2O_3	295	111	118	2.4	3.9	5.8
TiO_2-PO_4	258	101	38	3.1	6.8	8.9
SAPO-11	1330	6	172	4.6	7.4	9.5
SAPO-34	498	5	49	9.6	12.7	16.2

Pethan Rajan et al. (2014) characterized the spent VPO by TPD-NH_3 and FTIR-pyridine. The results showed that the acidity and Brønsted acidic sites of the catalyst decreased after 40 h of reaction. Consequently, the conversion and selectivity of the catalyst decreased.
It is critical to find a solution to avoid or to decrease coke deposition on the catalyst surface or at least to define an effective method to regenerate the spent catalyst. Generally, oxygen and hydrogen are used in order to eliminate the formed carbon on the catalyst surface. Three kinds of solutions have been proposed for the continuous regeneration of the catalyst :

— In-situ regeneration : co-injection of oxygen or hydrogen with the gas feed (Dubois et al., 2006a).
— Periodic regeneration : periodic regeneration of the used catalyst by injection of a flow or pulses of oxygen or hydrogen (Oconnor et al., 2008).
— External regeneration : circulation of the catalyst in a moving-bed reactor and parallel regeneration in a separate reactor (e.g. FCC process) (Corma et al., 2008).

First method could cause the explosion and/or oxidation of the reaction products. For this reason, the concentration of co-fed oxygen must be kept below 7 mol% (Dubois et al., 2006b). The second option has the disadvantage of productivity loss, while the third alternative, on the contrary, doesn't have these drawbacks. However, it is associated to high cost and technical difficulties of construction and operation of a separate reactor.

2.10.1 In situ regeneration of catalyst : effect of oxygen

The idea of co-injection of air first was proposed by Dubois et al. (2006a). The authors studied the effect of molecular oxygen on catalyst deactivation and product distribution for different catalytic systems such as zeolites, sulphated zirconia, tungsten zirconia and phosphate zirconia. The authors observed that addition of oxygen reduced the formation of coke on the catalyst. Aromatic compounds such as phenol, and of by-products originating from a hydrogenation of dehydrated products such as propanaldehyde and acetone, but also from hydroxypropanone, were formed to lesser extents. Supplying oxygen resulted in maintaining the conversion and selectivity of the catalyst while the formation of by-products decreased or eliminated.

Application of oxygen was extended to other catalysts such as vanadium pyrophosphate (Wang et al., 2010), boron phosphate (Dubois, 2010), iron phosphate (Deleplanque et al., 2010), tungsten oxide on zirconia and titania (Ulgen and Hoelderich, 2009)(Ulgen and Hoelderich, 2011) and caesium salts of phosphotungstic acid Dubois et al. (2009b). For all systems, the selectivity of by-products such as acetaldehyde, acetol and formaldehyde decreased whereas oxidation products such as acrylic acid, acetic acid and formic acid increased. Selectivity of acrolein for zeolites, vanadium oxophosphates and tungsten oxide on zirconia did not improve noticeably. For caesium salt of phosphotungstic acid selectivity of acrolein doubled when oxygen was supplied. For boron and iron phosphates, co-feeding of oxygen affected the selectivity of acrolein negatively due to the redox character of these catalysts which enhances over-oxidation to carbon oxides. However, an optimal concentration of oxygen needs to be defined for each system. Dubois et al. (2009a) suggested doping the catalyst with metal oxides such as caesium, potassium, strontium, silver and platinum to help splitting molecular oxygen. The authors were able to reach a selectivity of 70% by this approach.

Okuno et al. (2007) followed the same technique as Dubois et al. (2009a), but the injection of air did not improve acrolein selectivity for MFI (protonated zeolite) catalyst. They doped the catalyst with Pt, Pd, Au, Ir, Cu and Ru to facilitate oxygen activation. The maximum acrolein yield, 80.7%, was obtained for 0.1 wt% Pt at 100% conversion of glycerol.

2.10.2 Other approaches for catalyst regeneration

(Alhanash et al., 2010) applied hydrogen instead of oxygen to reduce the coke formation. They also modified the catalyst (caesium salts of phosphotungstic acid) by addition of noble metals. Catalyst activity was doubled while the selectivity of acrolein remained unaffected.

Dubois (2009) examined the addition of SO_2 to the feed solution to decrease the deactivation

of WO_3/ZrO_2. Formation of acetol was eliminated while the selectivity of acrolein was not changed by the presence of SO_2. After 24 h of reaction, the conversion was still high (87%) whereas it was 69% without SO_2. Although this method is effective, it might not be compatible with some catalytic systems because of the catalyst poisoning and toxicity of SO_2.
Arita et al. (2008) applied cyclic regeneration method for HZSM-5 catalyst. The primary performance of the catalyst was achieved after regeneration but the formation of hot-spots raised the temperature to 100 °C higher than dehydration temperature. So, the thermal degradation of catalyst must be considered in this technique.
Corma et al. (2008) and Oconnor et al. (2008) injected crude glycerol into FCC plant to regenerate the catalyst in circulating bed reactor. Dubois had already proposed to inject glycerol in an existing propylene oxidation plant to obtain acrolein from both sources (Dubois, 2007). However, in FCC plants the heat released from coke burning could provide the required energy for evaporation of glycerol. The authors even studied the possibility of glycerol reforming at 500 °C- 600 °C to produce ethylene and propylene.
Okuno et al. (2007) proposed an original technique for pretreatment of MFI catalyst. The treatments were :

— 1. a flow of acetol, water and nitrogen.
— 2. a flow of acrolein, water and nitrogen.
— 3. a flow of acetol, water and air.

All these treatments enhanced acrolein selectivity in early minutes of reaction, but after 150 min, the catalytic performance returned to untreated catalyst.

2.11 Industrial applications of fluidized-bed reactors

In a fluidized-bed reactor, an upwards stream of fluid suspends the solid particles. The advantages of this type of reactor are :

— ease of solids handling ;
— providing an efficient iso-thermal condition due to high heat transfer rate ;
— homogenous distribution of reactants due to high mass transfer rate ;
— avoiding hot spot formation in exothermic reactions ;
— excellent gas-solid contact ;

The fluidization behaviour depends on operating conditions such as gas velocity, as well as solid and gas properties. Different fluidization regimes are defined based on the following parameters : fixed-bed, homogeneous, bubbling, slugging, turbulent, fast-fluidization and lean phase fluidization with pneumatic transport (Figure 2.7) (Kuni Daizo, 1991).

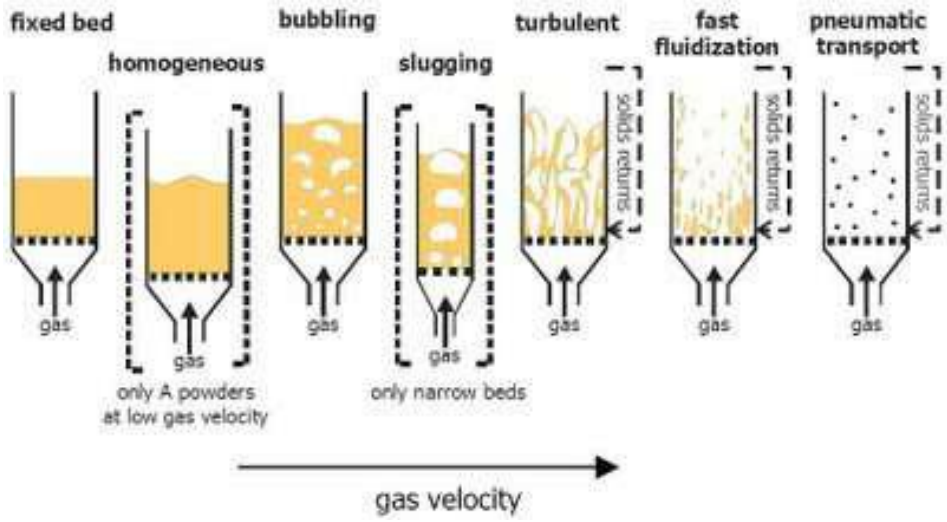

Figure 2.7 Fluidization regimes (Kuni Daizo, 1991)

In 1941 fluidized beds were developed to crack oil to gasoline/diesel/jet fuel. Application of fluidized-bed reactors in commercial scale has been growing since then. Catalytic/non-catalytic reactions, acrylonitrile, Fischer-Tropsch and phthalic anhydride synthesis, conversion of methanol to gasoline and olefins, cracking of hydrocarbons (FCC), coal combustion, coal gasification, cement clinker production, titanium dioxide production, calcination of $Al(OH)_3$, granulation drying of yeast, absorption and nuclear energy including uranium processing, nuclear fuel fabrication and reprocessing of fuel and waste disposal (Yang, 2003). Table 2.5 shows some commercial processes applying catalytic fluidized-bed reactors (Yang, 2003) and (Bi et al., 2000).

2.12 Liquid injection in fluidized bed reactors

Fluidized bed reactors have many industrial applications (from particle coating and agglomeration to gas phase heterogeneous catalysis) and offer several advantages compared to other reactor types. The major advantage of fluidized bed reactors is a better solid mixing and homogeneity in comparison with the fixed bed reactors (Kuni Daizo, 1991). However, this characteristic could be affected by liquid injection in the vicinity of the injector.
Liquid injection in fluidized bed reactors is emphasized in some commercial scale reactors.

Table 2.5 Commercial fluidized-bed reactors (Patience et al., 2012)

Product/Reaction	Process
Phthalic anhydride	Sherwin-Williams-Badger
Fisher-Tropsch Synthesis	Kellog, Sasol
Vinyl acetate	Nihon Gosei
Acrylonitrile	Sohio
Ethylene dichloride	BASF, ICI, Goodrich
Chlorometahne	Asahi Chemical
Maleic Anhydride	Mistubishi, Dupont, Lonza
Polyethylene	Union Carbide
O-cresol and 2,6-xylenol	Ashai Chemical

Fluid catalytic cracker (FCC) processes inject liquid into the catalytic bed to produce gasoline, LPG and diesel (Fan et al., 2010). Other processes such as production of aniline by BASF and also polyethylene synthesis in super-condensed mode are using this technology. In all of these processes, as soon as the liquid is injected into the reactor, it vaporizes inside the fluidized bed and the generated gas phase participates in the catalytic reaction.

In comparison to gas injection of reactants, liquid injection provides some advantages. Since the reactants are injected in liquid form, they don't need to evaporate outside of the reactor. So, avoiding an external heat exchanger would help reduce the expenses of the process. Additionally, the formation of hot spots close to the feed entrance is minimized by liquid injection because of the efficient cooling, which is provided by the latent heat of evaporation (especially for exothermic reactions). This could also be an efficient method for thermally sensitive compounds. Liquid injection may also provide a uniform distribution of reactants inside the reactor (Bruhns and Werther, 2005).

There are several models for liquid injection in a fluidized bed reactor. An initial model assumes that the liquid instantly evaporates at the injector exit and the liquid feed is treated as a gas stream entering the bed (Theologos and Markatos, 1993). In another model, it is assumed that penetration of the gas phase follows the same pattern as that of gas jets. In other words, the droplets that are continuously formed during the liquid injection are distributed and vaporized individually through the gas phase, and reactants interact with the solid phase in gaseous form (Theologos et al., 1999),(Gao et al., 2001),(Gupta and Rao, 2003). The granulation model in the fluidized bed considers that liquid drops emerging from the injector are deposited on the catalyst surface forming a liquid layer that will subsequently evaporate. The reaction occurs in gas and liquid phases at the liquid / solid interface (Heinrich and Mörl, 1999). By using a tracer technique for the injection of atomized bitumen on solid coke

particles, Maronga and Wnukowski (1997) and Fan et al. (2001) have defined three zones for liquid spraying by measuring the humidity and temperature changes caused by liquid injection. These three zones are :

— A spraying zone near the injector : where the drops are formed and they wet the solid particles ;

— A drying zone : where the liquid evaporates from the surface of the solid particles ;

— A heat transfer zone : where particles are heated-up in order to start the reaction.

Traditionally, there are two injector models for the injection of liquid in industrial fluidized beds ; external mixing in which the liquid and spraying gas are premixed in the exterior of the injector and internal mixing in which the liquid and spraying gas are mixed inside the injector (Figure 2.8) (Bruhns and Werther, 2005). The internal injector model is preferred to the other type because of the ease in manufacture and its smaller outside diameter.

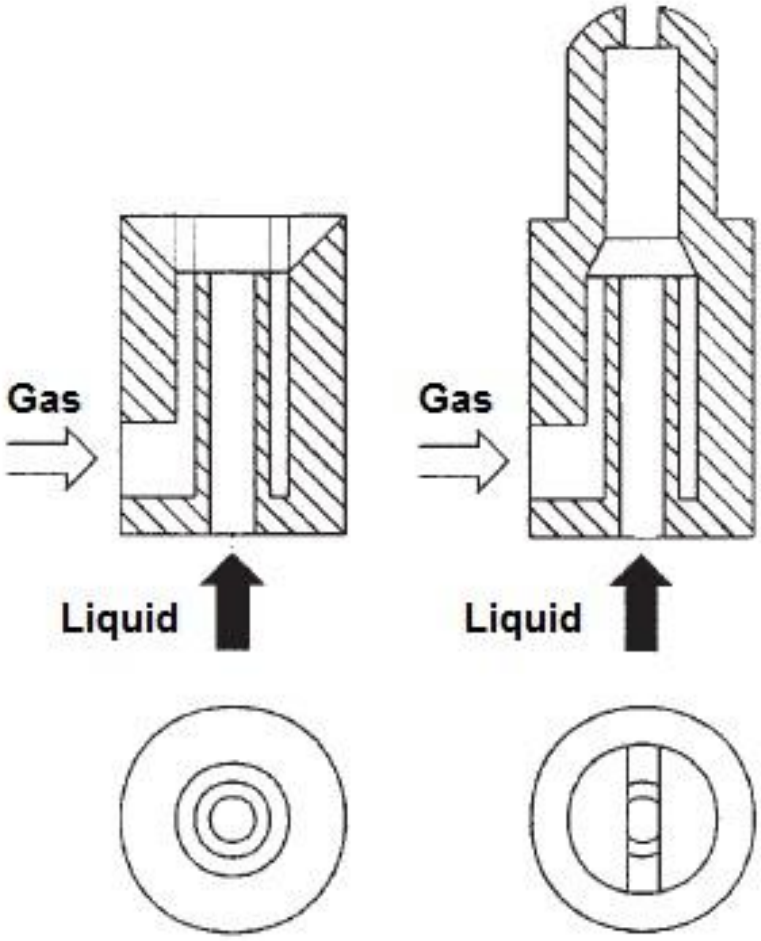

Figure 2.8 Types of fluid injectors.left : externally, right : internally mixed (Bruhns and Werther, 2005)

CHAPTER 3 ORGANIZATION OF ARTICLES

This section is dedicated to the scientific contribution of this thesis in the form of three original journal articles.

The first part of this study involves a 6 h glycerol dehydration reaction performed at 280 °C in the fluidized-bed of WO_3-TiO_2 catalyst (ID : 4.6 cm, quartz reactor). The mole ratio of feed in the gas phase was glycerol/O_2/H_2O/Ar : 0.1/0.1/1.3/5.3, respectively. The reaction products (gas and liquid) and catalyst samples were collected and analysed in 1 h intervals during the reaction time. The evolution of acrolein selectivity, by-products selectivity and coke formation was established with reaction time. According to the product distribution and detected intermediates, the possible mechanism of the reaction was proposed. The interesting results of this experiment led us to suggest a new method for the catalyst regeneration. Then, we validated our method with complementary experiments and proved that it was effective. Understanding the re-oxidation kinetics is critical to identify the amount of carbon on the surface. The model necessarily relates the carbon coverage with time and temperature. We developed a first order kinetic model for oxidation of coked catalyst at various oxidation temperatures and heating ramps. The results obtained from 6 h long experiment guides this thesis toward extending the reaction time in order to characterize and study the behaviour of coked catalyst. This paper entitled "Transient acrolein selectivity and carbon deposition study of glycerol dehydration over WO_3/TiO_2 catalyst", has been published in the "Chemical Engineering Journal" (Dalil et al., 2015).

In the second article, first we have extended the 6 h experiment to 14 h to reach steady-state selectivity for acrolein. The analysis of the gas, liquid and catalyst samples suggested that as the coke forms on the surface with reaction time, the properties of the catalyst is affected, resulting in a different pattern for product distribution. Fresh and coked catalysts were thoroughly characterized by various techniques to understand the effect of reaction time on catalyst behaviour. Acid/base properties of fresh, 2 h, 6 h and 14 h catalyst samples were analysed by calorimetric technique for the adsorption of NH_3 and SO_2. Subsequently, the FTIR-pyridine analysis identified the types of the acid sites remaining on the catalyst surface at different reaction times. Textural properties of fresh and coked catalyst such as surface area, pore volume and pore diameter was obtained by BET and BJH methods. We also performed the elemental analysis (CHNS/O) of the coked catalyst in order to obtain the type of carbon deposits. Finally, the SEM and TEM images were recorded for the fresh and used catalyst. We also studied the effect of reaction conditions such as temperature, oxygen concentration, glycerol concentration and residence time on the selectivity of acrolein and

by-products. This paper entitled "Effect of coke formation on behaviour of WO_3-TiO_2 catalyst in steady-state gas-phase dehydration of glycerol" has been submitted to the "Journal of Catalysis Science and Technology".

In the third paper, we have synthesized 10, 20 and 30 wt% loadings of phosphotungstic acid on two types of titania supports by impregnation method. The pore size of two supports were different ; HKT-1 : 17.3 nm and HKT-2 : 5.6 nm. The prepared catalysts were characterized and tested in fluidized-bed reactor in order to monitor the effect of tungsten loading and pore diameter of titania on products selectivity and coke build-up. At the end, 20 wt% HPW impregnated on HKT-1 and HKT-2 titania as well as WO_3-TiO_2 (ARKEMA) were treated by hydrogen rich coke promoters. Tetralin and decalin were used to coat the catalysts in order to increase the selectivity of acrolein in the initial phase of reaction. The performances of the catalysts were compared with and without the addition of coke promoters under the same reaction conditions. The effect of coke promoters on selectivity of acrolein and hydrogenated by-products (acetone and propionaldehyde) was studied and the reaction mechanism proposed in the second paper was confirmed by these results. This paper entitled "Improved acrolein selectivity by coke promoters for catalytic gas-phase dehydration of glycerol in a fluidized-bed reactor" has been submitted to the "Journal of Applied Catalysis : A".

CHAPTER 4 ARTICLE 1 : TRANSIENT ACROLEIN SELECTIVITY AND CARBON DEPOSITION STUDY OF GLYCEROL DEHYDRATION OVER WO_3/TiO_2 CATALYST

Marjan D, Davide Carnevali, Jean-Luc Dubois and Gregory S. Patience

4.1 Abstract

Acrolein is one of the highest valued commodity chemicals for which glycerol is an attractive feedstock. Glycerol is derived from transesterification of vegetable oils and animal fats. WO_3/TiO_2 catalyst dehydrated glycerol to acrolein at a selectivity exceeding 73 % after 6 h time-on-stream. However, after 1 hour, the acrolein selectivity was only 55 %. All the glycerol reacted at reaction temperature (280 °C) and the by-products were predominantly propanal, acetaldehyde, formic and acetic acids. The weight gain of carbon on the catalyst increased with time and after one hour, the mass fraction of carbon was 2.2 % ; after an additional five hours, it doubled. A first order kinetic model characterizes the rate at which oxygen reacts the carbon on the catalyst with an activation energy of 100 kJ mol^{-1}(R^2>0.997).
Partial oxidation of coke, as a new strategy for catalyst regeneration, enhanced the selectivity toward acrolein from 10 % to 25 % in the first 15 minutes of glycerol injection. Glycerol conversion to coke was reduced from 34 % to 6 %.
This article has been published in the Chemical Engineering Journal.

4.2 Introduction

Bi/Mo-mixed oxide catalysts partially oxidize propylene to acrolein in a single step process. Commercial processes rely on multi-tubular fixed bed reactors in which a cooling fluid circulates between the tubes to minimize hot spots, thereby maintaining high selectivity and longer catalyst life (Cornils, 2004; Callahan et al., 1970). Most of the acrolein is further oxidized to acrylic acid in a second multi-tubular fixed bed in series (William, 2000). Over the last decade, replacing propylene with a bio-feedstock has been a priority for many industries due to a concern for the environment, high propylene prices and supply uncertainty as well as the low price of glycerol (Liu et al., 2012; Cornils, 2004; Watanabe et al., 2007; Chai et al., 2007a; Dubois et al., 2006a). Dehydrating glycerol to acrolein is an attractive alternative to partial oxidation of propylene if high yields can be achieved and the glycerol price relative to proylene remains low.

Biodiesel is a biodegradable and renewable fuel and is derived from vegetable oils/animal fats and methanol. Glycerol is a product of the biodiesel transesterification or oleochemicals and represents a mass fraction of about 10 % (Katryniok et al., 2010a). Due to its multifunctional structure, glycerol can go through various routes leading to the production of value-added products such as acrolein, propylene glycol or 1,2 propanediol, syn-gas and light olefins (Posada et al., 2012; Yuan et al., 2010; Xia et al., 2012; Zakaria et al., 2012; Wang et al., 2015; Vasiliadou and Lemonidou, 2013). Oxidehydration of glycerol is a process that leads to a direct production of acrylic acid. The catalyst with both oxidative and acidic sites such as Mo-V and W-V should be applied for this process (Shen et al., 2014b). Glycerol is also applied as a raw material for pharmaceuticals and cosmetics. However, these applications are highly regulated and the purity standards are difficult to reach economically with crude glycerol. Crude glycerol requires several separation steps, including distillation, to remove salts, non-glyceric organic matter and water to meet the standards of these industries. For lack of a market, many biodiesel manufacturers burn unrefined glycerol (Katryniok et al., 2010a; Shen et al., 2011; Atia et al., 2008).

Dehydrating glycerol to acrolein is a promising alternative to burning. Many catalysts and processes have been examined to dehydrate glycerol in both the gas phase and liquid phase. Considering environmental and technical hurdles of liquid phase processes — corrosion, waste management and poor catalyst recycling — gas phase processes appear to be better suited (Chai et al., 2007a).

Catalysts that dehydrate glycerol include MOx-Al_2O_3−PO_4 (M as transition metal), zeolites (ZSM−5, HY, SBA−15, ZSM−23, HB), metal mixed oxide catalysts (Nb_2O_5, WO_3/TiO_2, TiO_2/ZrO_2, WO_3/ZrO_2, CeO_2-ZrO_2), heteropoly acids (phosphotungstic acid, silicotungstic acid supported on activated carbon), $ZrSO_4$ and cerium dopped Fe_3PO_4 (Chai et al., 2007a; Neher et al., 1995; Suprun et al., 2009; Pathak et al., 2010; Callahan et al., 1970; Kim et al., 2010; Cavani et al., 2010; Ning et al., 2008; Dubois et al., 2009a; Patience et al., 2012; Vasconcelos et al., 2011; de Oliveira et al., 2011).
Although the acid catalysts are efficient in terms of activity and selectivity, they coke and deactivate with time-on-stream. de Sousa et al. (2013) synthesized and examined nanoparticles of several metal oxides such as Ru, Cu, Zn and Co on SBA-15 for dehydration of glycerol. They observed more catalyst deactivation for ZnSBA-15 and CuSBA-15 samples, which had been prepared under more acidic conditions.

Chai et al. (2007a) claimed that strong acid catalysts are selective for acrolein but, on the other hand, they form coke quickly. Dubois et al. (2009a) suggested co-feeding oxygen with glycerol to acidic type catalysts to maintain catalyst activity and reduce by-products. Dubois

et al. (2006a) and Ulgen and Hoelderich (2009, 2011) examined WO_3 on TiO_2 and ZrO_2 at various operating conditions and tungsten loadings. They (Dubois et al., 2006a) concluded that molecular oxygen not only reduced the catalyst deactivation rate, it also reduced the selectivity to propanal and hydroxyacetone (acetol). However, in some catalytic systems, molecular oxygen increases acrolein yield but in others, yield is lower and by-products are higher (acetol or acetic acid, for example) (Katryniok et al., 2010a). Acrolein selectivity for zeolites, vanadium oxophosphates and tungsten oxide on zirconia catalysts changed slightly or was the same. In the case of caesium salt of phosphotungstic acid, the selectivity of acrolein doubled (93 % vs. 47 %) and for boron or iron phosphates, co-injecting oxygen decreased acrolein selectivity (Ulgen and Hoelderich, 2009; Deleplanque et al., 2010; Dubois et al., 2009a; Wang et al., 2010; Devaux and Dubois, 2013; Ulgen and Hoelderich, 2011).

4.3 Materials and Methods

4.3.1 Experimental Set-up and Analytics

WO_3/TiO_2 catalyst from ARKEMA dehydrated glycerol in 46 mm ID quartz fluid bed reactor with a straight section that was 700 mm long. The reactor flanged out to 300 mm in order to reduce catalyst carryover to the quench. A 6-point thermocouple monitored the temperature of each zone and an electrical furnace controlled the temperature of the reactor. A ceramic frit (20 µm) placed 50 mm from the bottom of the reactor, uniformly distributed the gas across the diameter. An HPLC pump injected the glycerol/water solution through a 1.6 mm diameter nozzle protruding through the distributor from the bottom into the bed by 20 mm. Argon at a flow rate of 200 mL min^{-1} helped to atomize the liquid.The effluent gas passed through a quench to trap all condensables as well as the mist (Figure 4.1).
Atomizing the liquid into uniform drops is important to operate the fluidized bed : large droplets agglomerate the catalyst and block the injector and/or accumulate on top of the grid. We examined several gas and liquid flow rates and glycerol concentrations to identify the optimum conditions. Qualitatively, the best droplets uniformity was at a liquid feed rate of 0.5 mL min^{-1}, 200 mL min^{-1} of argon and a mass fraction of 30 % glycerol in water. The pressure drop in the injector at this condition was 40 kPa.
A Bruker GC equipped with Hyesep Q, Molsieve 5A and FFAP columns analyzed the CO, CO_2 and O_2 as well as acrolein and other light products. In addition, a Pfeiffer mass spectrometer monitored the permanent gases that exited the second quench. A Varian HPLC measured the condensables trapped in in the liquid phase (Metacarb 87H column).

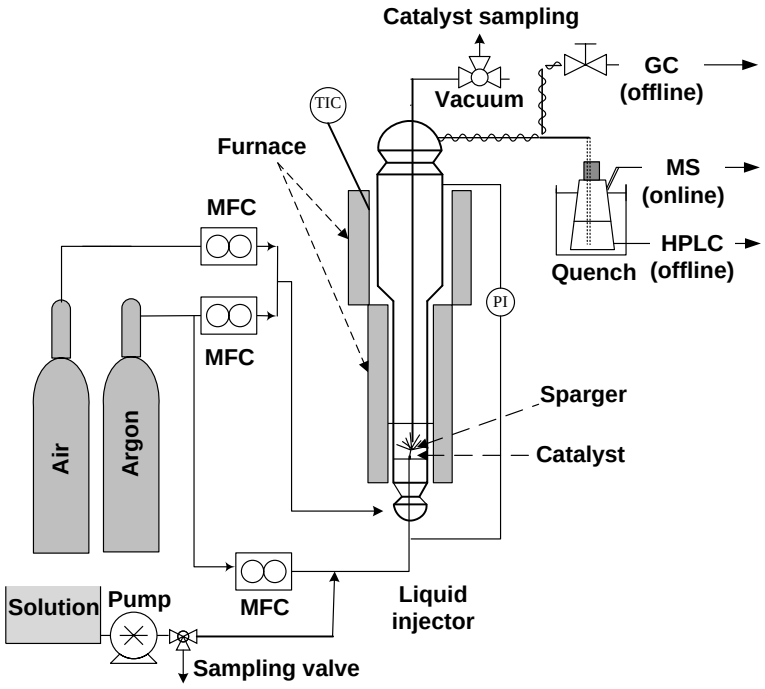

Figure 4.1 Schematic of the experimental set-up

4.3.2 Methods and Techniques

For the extended glycerol dehydration run, we loaded the reactor with 100 g of catalyst and heated up to 400 °C for 30 min with argon. After setting the flows of oxygen (10 mol% O_2/Ar) and argon at desired values, the catalyst bed reached 280 °C which was the reaction temperature. 28 wt% glycerol in water solution entered the reactor. The mole ratio of feed in the gas phase was glycerol/O_2/H_2O/Ar : 0.1/0.1/1.3/5.3, respectively. The gas, liquid and catalyst samples were collected every one hour during the reaction.

We carried out 7 point BET (Brunauer, Emmett and Teller) analysis in an Autosorb-1 machine by adsorption and desorption of liquid nitrogen at 77 K to obtain the specific surface area of the samples.

A TA-Q50 instrument recorded the thermogravimetric curves for 20 mg of catalyst -sampled at 1 h cycles- from 20 °C to a desired temperature at a rate of 10 °C min^{-1}. The samples were loaded to a 10 µm aluminum crucible. In order to assure that no light components (adsorbed during the reaction) retains on the catalyst, a flow of 40 mL min^{-1} of nitrogen purged the sample while heating up to 300 °C. For carbon mass measurement, after 15 min isothermal hold, oxygen replaced the nitrogen with the same flow rate and the furnace reached 500 °C. A Platinel II thermocouple placed 2 mm above the sample pan measured the temperature.

The balance mechanism had a resolution of 0.1 µg and accuracy > ±0.1 %.
We also conducted a kinetic analysis of a catalyst sample that was collected from the reactor after 6 h of continuous operation. The TGA heated the samples to 300 °C at a rate of 10 °C min^{-1} under nitrogen flow. After 15 min at 300 °C, we switched the gas from nitrogen to air and then ramped up to the desired temperature at a rate of either 5 °C min^{-1} or 10 °C min^{-1} (Table 4.1). In the last experiment, the TGA ramped up the sample temperature to 400 °C and then switched to air after 15 min. We maintained the temperature at 400 °C for 1 h in air.

Table 4.1 Thermogravimetic analysis conditions for kinetic study

Exp.	$T_{N_2 \rightarrow O_2}$ (°C)	T_{final} (°C)	ramp (°C min^{-1})
1	300	375	10
2	300	400	10
3	300	425	10
4	300	450	10
5	300	400	5
6	400	400	isothermal

The conversion of glycerol ($X_{gly.}$) as well as selectivities towards products (S_p) and coke (S_{coke}) were calculated as follows ;

$$X_{gly.}(mol\%) = \frac{n^{in}_{gly.} - n^{out}_{gly.}}{n^{in}_{gly.}} \times 100 \tag{4.1}$$

$$S_p(mol\%) = \frac{n_p}{n^{in}_{gly.} - n^{out}_{gly.}} \times \frac{z_p}{z_{gly.}} \times 100 \tag{4.2}$$

$$S_{coke}(mol\%) = \frac{n_{coke}}{n^{in}_{gly.} - n^{out}_{gly.}} \times \frac{1}{3} \times 100 \tag{4.3}$$

Where : $n^{in}_{gly.}$ and $n^{out}_{gly.}$ are the molar flow rates of glycerol at reactor entrance and exit. In equation 6.2, n_p is the molar stream of each product. z_p and $z_{gly.}$ represent the number of carbon atoms of the products and glycerol. Equation 4.3 is a simplified form of equation 6.2 in which the values of z have been replaced as 1 and 3 for coke and glycerol. We obtained the molar flow rate of coke by TGA data.

4.4 Results and Discussion

4.4.1 Product analysis

The mass fraction of glycerol in water was 28 wt% and this solution was atomized into the catalyst bed that was maintained at 280 °C. This temperature is optimal for WO_3/TiO_2 and WO_3/ZrO_2 catalysts since carbon oxides form at higher temperatures as well as acetaldehyde and propionaldehyde (propanal). On the other hand, at lower temperatures glycerol converts to oligomers (Ulgen and Hoelderich, 2011, 2009).
During the six hours test, neither the GC nor the HPLC detected any glycerol in liquid product which confirms that the catalyst remained very active over the entire test and converted 100 % of the glycerol. The co-injection of oxygen reduced the catalyst deactivation and maintained the glycerol conversion. Several researchers reported the same behaviour. (Dubois et al., 2006a; Ulgen and Hoelderich, 2011, 2009). For a long-term experiment with 13.9 wt% WO_3/TiO_2, Ulgen and Hoelderich (2011) observed that the conversion of glycerol dropped only 50 % after 4 days of time on stream. They also compared the conversion of glycerol with and without oxygen and observed that it increased between 5% and 18% in the case of oxygen co-feeding. Dubois et al. (2006a) also, concluded that addition of molecular oxygen improved or maintained the conversion of glycerol. In the case of WO_3-ZrO_2, the presence of oxygen slightly dropped the conversion of glycerol due to the blockage of the active sites by molecular oxygen (Ulgen and Hoelderich, 2009).

During the injection of glycerol in the first hour, the GC traces showed a very small quantity of acrolein which could be related to the formation of coke on the catalyst surface. By time on stream, carbon builds up on the catalyst surface continually and coincidentally acrolein selectivity increases as the by-product selectivity decreases (Figure 5.5). After 6 h, the selectivity to acrolein exceeded 73 % whereas it was less than 55 % after one hour time-on-stream (Table 5.2).

The main by-products were acetaldehyde and propanal and their selectivities decreased by over 40 % during the six hour run. The concentrations of formic acid and acetic acid were much lower than acetaldehyde and propanal. The HPLC and GC detected traces of acrylic acid, propionic acid, formaldehyde and 3-hydroxypropanal (selectivity < 0.5 %). Both CO and CO_2 remained constant during the six hours at about 12 % and 4 %, respectively. This would indicate alternative pathways for the carbon oxides versus acrolein and the aldehydes (and perhaps coke).
Conversion of glycerol to hydroxyacetone (acetol) is a possible side reaction in acidic environment but it was absent in our product quench. This is consistent with Deleplanque et al.

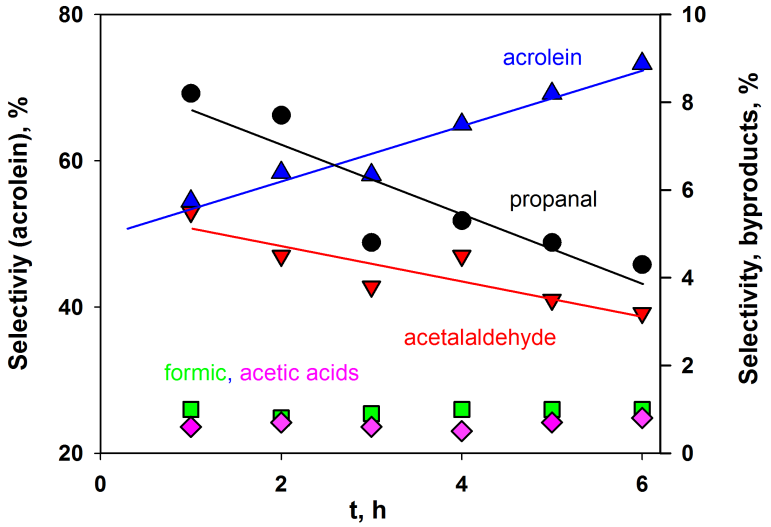

Figure 4.2 Selectivity of acrolein and by-products vs. time for glycerol dehydration over WO_3-TiO2 catalyst at 280 °C and molar feed composition of : glycerol/O_2/H_2O/Ar= 0.1/0.1/1.3/5.3

(2010) observations. Dubois et al. (2006a) and Ulgen and Hoelderich (2009) reported that oxygen reduced the selectivity of side products. Additionally, we didn't observe any traces of other common by-products such as phenol or acetone. This phenomenon was related to the presence of oxygen in our system. According to Dubois et al. (2006a), for HZSM−5, sulfate zirconia, tungsten zirconia and H-beta catalysts, supplying oxygen decreased the formation of by-products. It also enhanced the selectivity towards acrolein. For WO_3-TiO_2 catalyst, the presence of oxygen considerably reduced the selectivity of acetol and propanaldehyde while the selectivity towards acrolein slightly decreased (Ulgen and Hoelderich, 2011). Similar positive effects of oxygen on glycerol conversion and selectivities were reported by Wang et al. (2010) for VPO catalyst. Ulgen and Hoelderich (2009) also observed a decrease in the by-products and an increase in acrolein selectivity for WO_3-ZrO_2.

The first step in glycerol dehydration is to form either 3-hydroxypropanal, or acetol (Fig. 4.3). 3-hydroxypropanal further reacts through retroaldol reaction and forms acetaldehyde and fromaldehyde which are also the source of acetic acid and formic acid. Formaldehyde is very unstable and could be easily hydrogenated. Since the drop in the selectivity of both propanal and acetaldehyde are similar, 3-hydroxypropanal is the likely precursor to these compounds. Acrolein and propanal can be converted to propionic and acrylic acid in the presence of oxygen. Chai et al. (2007a) fed an acrolein solution to a reactor at glycerol dehydration

Table 4.2 Product distribution for glycerol dehydration reaction over WO_3/TiO_2 catalyst

TOS	1 h	2 h	3 h	4 h	5 h	6 h
$S_{acrolein}$	55	58	58	65	69	73
$S_{propanal}$	8	8	5	5	5	4
$S_{acetaldehyde}$	5	4	4	4	3	3
$S_{formic\ acid}$	1	1	1	1	1	1
$S_{acetic\ acid}$	1	1	1	1	1	1
S_{CO}	12	9	13	11	12	12
S_{CO_2}	3	3	5	3	4	4

condition and observed that acrolein formed coke during the first hours of injection. After 6 h the conversion of acrolein dropped to 40 % and no other products were condensed in the liquid trap at reactor exit.

4.4.2 Mass of carbon

Time-on-stream

The catalyst maintains activity for six hours, but coke accumulates on the surface which requires a frequent regeneration step. The level of coke as a function of time was measured by withdrawing the catalyst every hour then running the samples in a TGA. We loaded a crucible with 20 mg of coked catalyst and purged the TGA at (40 mL min^{-1}) of N_2. At the same time, the TGA ramped the temperature to 300 °C at a rate of 10 °C min^{-1} . After 15 min at 300 °C, we substituted the nitrogen for air and then ramped the temperature to 500 °C at 10 °C min^{-1}.

Table 4.3 Mass of carbon on the catalyst withdrawn at one hour intervals based on TGA analysis. (Δm : rate of coke build-up, Σm : mass of coke per 100 g of fresh catalyst and X_{O_2} : oxygen conversion).

time (h)	Δm(%)	Σm(g)	X_{02}
0	0.0	0.0	0.0
1	2.2	2.2	67
2	0.9	3.1	50
3	0.3	3.4	43
4	0.5	3.9	43
5	0.4	4.2	40
6	0.2	4.4	42

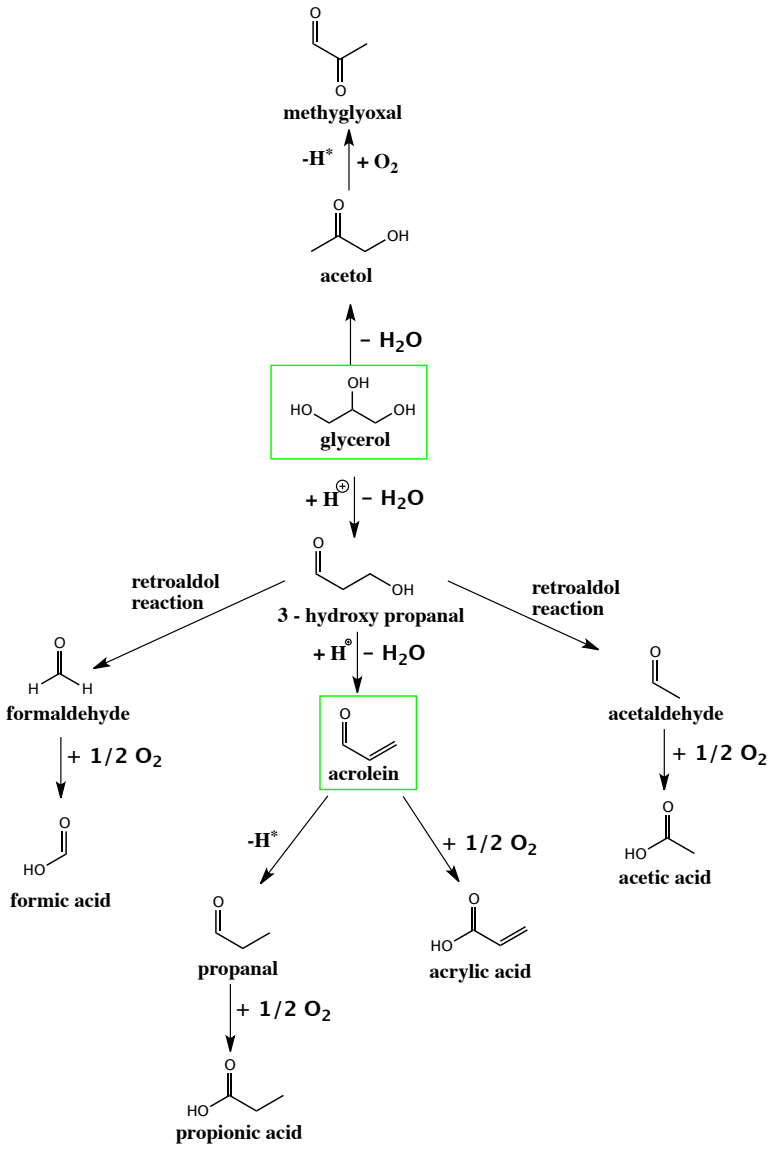

Figure 4.3 Possible pathway for dehydration of glycerol in the presence of WO_3-TiO_2 catalyst for 6 h time-on-stream

After one hour, the mass fraction of coke on the catalyst was 2.2 % (Fig. 4.4a). It increased at a slower rate and reached a mass fraction of 4.4 % after 6 h. Oxygen conversion dropped proportionately.

Coke deposition slightly decreased the surface area of the catalyst. According to BET analysis, the surface area of fresh catalyst was 30.5 m^2/g.

In the first hour of reaction, when the amount of coke increased to 2.2 g, the surface area was reduced to 26.5 m^2/g and after 6 h, it was 25 m^2/g for 4.4 g of coke formation.

Concurrently while less coke forms on the surface, acrolein yield increases (Table 5.2) and the by-product aldehydes decrease. The decrease in by-product aldehydes accounts for some of the increased acrolein. The major part in the increase in acrolein selectivity is likely due to lower coke formation.

The molar balance of carbon atoms for the streams of feed and products (including coke) showed that at the first hour of reaction, 84% of carbon in the feed stream was recovered in the form of products and coke. This difference could be explained by the unknown by-products which were formed in the early stages of the reaction and appeared as minor peaks in GC chromatogram. Additionally, some of the missing products might be decomposed in the GC injector before we analyze them. As the reaction continued, carbon mass balance increased and after 6 hours, we were able to recover 96% of injected carbon in the form of products and coke deposition (Table 4.4).

Table 4.4 Carbon balance between the feed and product streams (including coke)

TOS (h)	1	2	3	4	5	6
Carbon balance (%)	84	85	86	89	93	96

Temperature effect

During the first hour with glycerol in the feed, coke builds up on the catalyst at a higher rate than at 6 h, oxygen conversion decreases and selectivity to acrolein increases. Coke appears to modulate the surface activity of the catalyst and cover the sites that are responsible for by-products.

An incomplete regeneration could leave some coke on the surface. Presumably this coke would remain on the non-selective sites and when we feed glycerol afterwards, the initial acrolein selectivity would be higher than if we thoroughly reoxidize the catalyst. Understanding the re-oxidation kinetics is critical to identify the amount of carbon on the surface. The model necessarily relates the carbon coverage with time and temperature.

We applied the same methodology in which the TGA heated the sample to 300 °C, switched to air after holding that temperature for 15 min and then ramped it up to the set point. The weight loss in the initial stages for each temperature is identical and begins to deviate after about 10 min (Fig. 4.4b). After one hour, 50 % of the carbon reacts at 350 °C. In 20 min almost all of the carbon reacts above 425 °C. The total amount of carbon adsorbed is 1.2 mg for 20 mg of coked catalyst, which represents 4.6 % of the total weight. The selectivity to acrolein increases as the coke begins to build-up but eventually, activity and selectivity will decrease.

Oxidizing the carbon is necessary to re-establish the catalytic performance. However, keeping a certain level of carbon with a partial regeneration could maintain a higher level of selectivity (versus oxidizing all of the carbon).

Table 4.5 Below 400 °C, a one hour regeneration is insufficient to oxidize all the coke on the catalyst. Catalyst weight loss obtained by TGA at different temperatures for 6 h sample

T (°C)	weight loss (%)
350	2.9
375	4.2
400	4.6
425	4.6
450	4.6
500	4.6
550	4.6

4.4.3 Glycerol injection over partially regenerated catalyst

We compared the acrolein selectivity and glycerol conversion of experiments performed over fresh and partially regenerated catalysts. The operating conditions for both tests were similar to the 6 h experiment. After 3 h of glycerol injection on fresh catalyst, 21 mole% oxygen in helium regenerated the catalyst. We interrupted the oxidation of the coke when the quantity of CO and CO_2 reached almost 50 % of their total. TGA analysis of the catalyst samples withdrawn before and after the partial oxidation showed that 44 % of the coke remained on the catalyst.

The second experiment was to inject glycerol over partially regenerated catalyst for 3 h under the same conditions. After 3 h, the mass of the carbon on the fresh catalyst was 3.6 g while for the partially regenerated catalyst, only 0.6 g of coke was deposited on the catalyst. In other words, the selectivity toward the production of coke was reduced from 34 % to 6 %

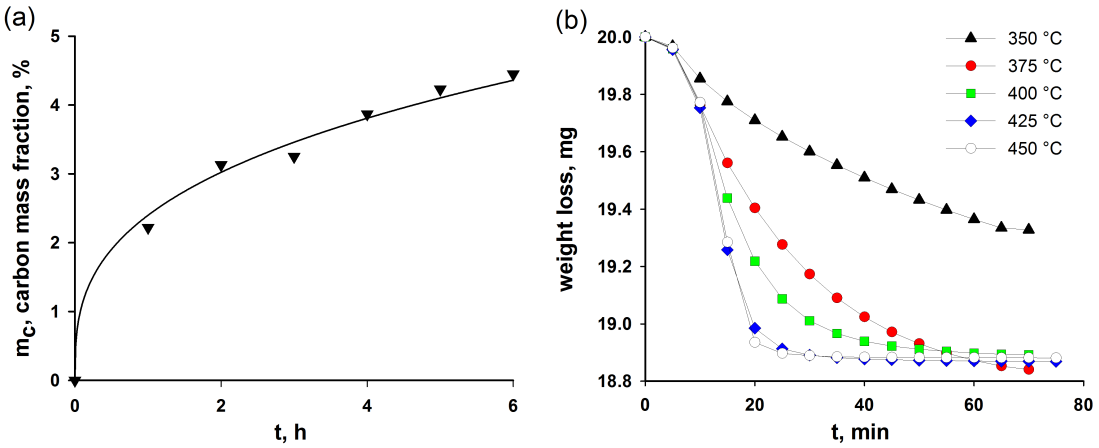

Figure 4.4 (a) Carbon deposition on WO_3-TiO_2 catalyst at 280 °C and molar feed composition of : glycerol/O_2/H_2O/Ar= 0.1/0.1/1.3/5.3 (m_c is the mass of coke per 100 g of fresh catalyst obtained by TGA). (b) Carbon combustion at various temperatures from coked catalyst after 6 h of reaction (TGA ramp : 10 °C min^{-1})

(Table 4.6).

Table 4.6 The mass of carbon on the catalyst after 3 h of reaction for fresh and partially oxidized catalyst measured by TGA

Catalyst	Mass of carbon (g)
Fresh (after 3 h)	3.6
Partially oxidized (before reaction)	2
Partially oxidized (after 3 h)	2.6

The intervals of sampling was 15 min in the first hour of reaction and after that every 30 min. For fresh catalyst, the selectivity of acrolein was 11 % after 15 min and it reached up to 56 % in 3 h. The conversion of glycerol in this case increased from 95 % to 100 % after 45 min of glycerol injection. Partial oxidation of coke between the dehydration cycles increased the selectivity of acrolein to 25 % after 15 min and to 61 % after 3 h. Meanwhile, the glycerol conversion dropped to 95 % after 30 min.

On the other hand, propanal and acetaldehyde production followed a decreasing trend in both experiments but the level of selectivities for these by-products were reduced almost to half when the catalyst was not fully regenerated (Fig. 4.5).

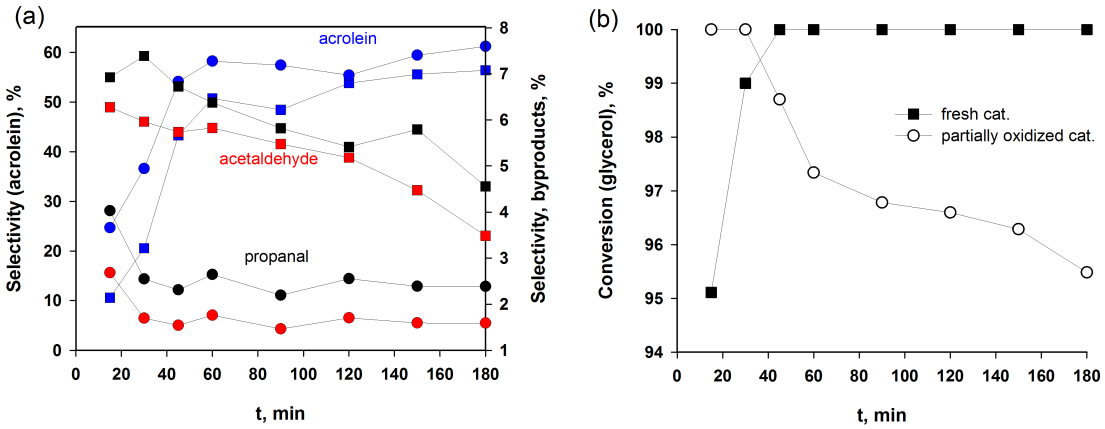

Figure 4.5 (a) Selectivity towards acrolein and by-products for glycerol dehydration over fresh (■) and partially oxidized (●) WO_3-TiO_2. (b) Conversion of glycerol vs. time-on-stream (T=280 °C, molar feed composition : glycerol/O_2/H_2O/Ar= 0.1/0.1/1.3/5.3)

4.4.4 Kinetic modelling

The reaction rate depends on temperature, mass of carbon and partial pressure of the gases :

$$\frac{d\alpha}{dt} = k(T)f(\alpha)g(P) \tag{4.4}$$

During oxidation, oxygen conversion was less than 5 % and the pressure was constant, so we assume that the carbon conversion, α, depends solely on temperature and mass of carbon :

$$\frac{d\alpha}{dt} = k(T)f(\alpha) \tag{4.5}$$

k obeys to the Arrhenius law :

$$k = k_0 \exp\left(\frac{-E_a}{R}\right)\left(\frac{1}{T} - \frac{1}{T_0}\right) \tag{4.6}$$

where k_0 is the reaction rate at the reference temperature (T_0 = 300 °C), R and E_a are the gas constant and activation energy, respectively.
$f(\alpha)$ is a function of the degree of conversion.

$$\alpha = \frac{m_0 - m_i}{m_0 - m_f} \tag{4.7}$$

m_0, m_i and m_f are the initial, instantaneous and final mass of coked catalyst.

The shape of the isothermal TGA curve indicates the type of reaction that predominates ; the curve of accelerating, decelerating and sigmoidal reaction types each have distinctive profile shapes (Vyazovkin et al., 2011). In this process, the carbon loss rate is highest at the beginning and decreases as the conversion increases, which corresponds to a decelerating reaction type :

$$f(\alpha) = (1 - \alpha)^n \tag{4.8}$$

where n is a constant.
For the case of a first order reaction $n = 1$ and the equation 4.8 becomes :

$$\frac{d\alpha}{dt} = k(1 - \alpha) \tag{4.9}$$

$$\frac{d\alpha}{1 - \alpha} = kdt \tag{4.10}$$

$$t = 0, \alpha = 0 \tag{4.11}$$

$$\alpha = 1 - \exp(-kt) \tag{4.12}$$

We coupled the differential equation 4.9 to equations 4.6 and 4.7 and solved it with a Runge-Kutta fourth-order iteration scheme with a step size of 0.5 s. The best fit parameters, k_0 and E_a, were estimated by minimizing the sum of the squares of the error with the Maquardt-Levenberg algorithm (Marquardt, 1963).

$$SSE = \sum_{i=1}^{n} (y_i - f_i)^2 = min \tag{4.13}$$

where y_i is the experimentally measured value and f_i is the estimate.
The agreement between the experimental data and the first order model is excellent and accounts for 99.7 % of the variance in the data (Figure 4.4.4a).
To substantiate the model, we ran two additional experiments and compared the predicted mass loss versus the experimentally measured values. In the first experiment, we changed the TGA ramp from 10 °C min^{-1} to 5 °C min^{-1}. In the second test, the TGA ramped the temperature to 400 °C in nitrogen and then it switched to air while maintaining the temperature

constant (isothermal operation) (Table 4.1).
The model predicts the trends for both tests remarkably well (Figure 4.4.4b), which validates the model.

The activation energy of the carbon oxidation for the 6 h sample is $100\,\mathrm{kJ\,mol^{-1}}$ while the oxidation rate is slow ($k_0 = 8.2 \times 10^{-5}\,\mathrm{s^{-1}}$).

4.5 Conclusions

The selectivity to acrolein increases with an increase in coke formation over a WO_3/TiO_2 catalyst. During a 6 hour time-on-stream, the it increased from 55 % to 73 %. The main by-products, propanal and acetaldehyde, dropped proportionately. The reaction kinetics are first order with respect to the carbon on surface with an activation energy of $100\,\mathrm{kJ\,mol^{-1}}$. Partially regenerated catalyst improved the selectivity of acrolein. A fluidized-bed would be an ideal reactor to regenerate the catalyst (Compared to a multi-tubular fixed bed) to minimize hot spots and to achieve a homogeneous distribution of carbon on the catalyst.

4.6 Acknowledgements

The authors would like to thank NSERC and Canadian Foundation for Innovation (CFI) for their financial support of this study. Also, the assistance of Dr. Mahesh Edake at École Polytechnique de Montréal for the presentation of this work and great efforts of Dr. Cristian Neagoe at École Polytechnique de Montréal for set-up preparation and analytics development are greatly appreciated.

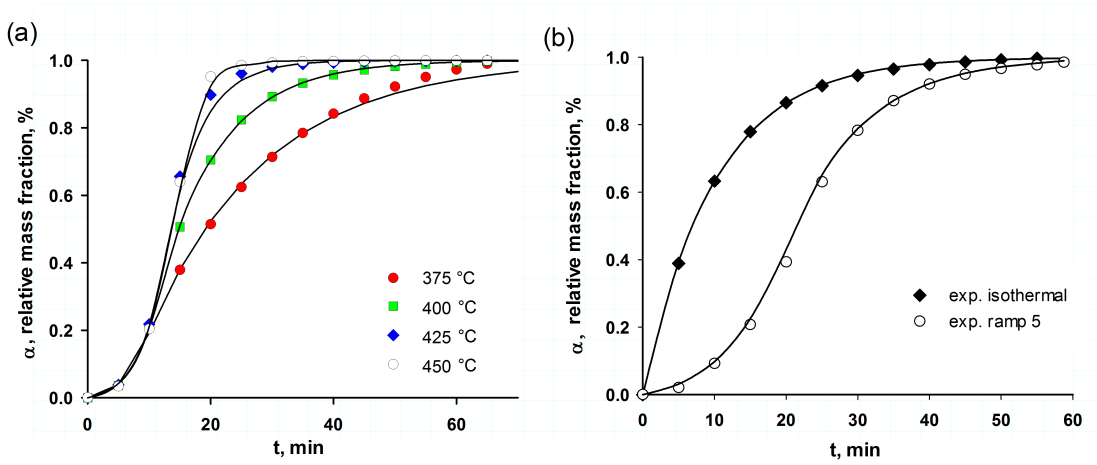

Figure 4.6 (a) Experimental (scatter) vs. model calculated (solid line) data for carbon combustion from WO_3-TiO_2 catalyst after 6 h of continuos glycerol dehydration. (TGA ramp : 10 °C min^{-1}) (b) Experimental (scatter) vs. model calculated (solid line) data for 6 h sample at isothermal (400 °C) and 5 °C min^{-1} ramp

CHAPTER 5 ARTICLE 2 : GAS PHASE DEHYDRATION OF GLYCEROL TO ACROLEIN : COKE ON WO_3/TiO_2 REDUCES BY-PRODUCTS

Marjan Dalil, Davide Carnevali, Mahesh Edake, Aline Auroux, Jean-Luc Dubois and Gregory S. Patience

5.1 Abstract

Glycerol is a renewable feedstock for specialty chemicals that is co-produced when oil and fats are transesterified to biodiesel or hydrolysed to fatty acids. Acrolein is a target specialty chemical but catalysts deactivate with time due to coke and thus require frequent regeneration cycles to maintain activity. WO_3/TiO_2 catalyst dehydrated glycerol for 14 h while the acrolein selectivity increased as coke formed on the catalyst. After the first hour of reaction the acrolein selectivity was 36 % and it reached steady state after 6 h at a selectivity of 73 %. The major by-products were acetone, propanaldehyde, acetaldehyde, acetol and formic acid. Coke selectivity dropped from 50 % in the first hour to 9 % after 14 h. Elemental analysis (CHNS/O) of the catalyst withdrawn from the reactor during the experiments confirmed that polyaromatics formed on the surface. Based on NH_3 and SO_2 adsorption calorimetry the number of strong acid sites remained constant during 14 h, while the number of the weak and medium acid sites dropped. The basic sites disappeared after 2 h ; coincidentally, less by-products (acetone) formed. Samples treated with pyridine, were analysed by FTIR and they had fewer Brønsted sites but no Lewis acid sites. Carbon deposits on walls of the cylindrical pores (based on Barret-Joyner-Halenda method) and reduced the pore diameter.

This article has been submitted to the Catalysis Science and Technology Journal.

5.2 Introduction

Substitution of petroleum based feedstocks and chemicals with bio-sustainable sources is a global priority. Biodiesel from vegetable oils, animal fats or cultured algae complement petrodiesel transportation fuels (An et al., 2011; Aransiola et al., 2014; Nasrin et al., 2012). Glycerol is a co-product of triglyceride transesterification (biodiesel synthesis) and represents a mass fraction of 10 % of the total biodiesel produced. It is also is an oleochemical co-product of fatty acids obtained by hydrolysis of oils and fats. As a consequence of the large scale production of biodiesel, the price of crude glycerol has dropped since there was insufficient demand to absorb the additional capacity.

The low glycerol price makes it an attractive feedstock for many specialty chemicals including acrolein. It is a large volume intermediate for acrylic acid and has several other industrial applications : D,L-methionine, fragrances, polymers and detergents. Currently, the commercial process for production of acrolein is selective oxidation of propylene in the gas phase over Bi/Mo-mixed oxide catalysts (Eley et al., 1979).

Schering Kahlbum AG dehydrated glycerol to acrolein in the gas phase over over lithium-phosphate and copper-phosphate catalysts in 1933 (Kahlbum, 1930). The acrolein yield reached 75 % between 300 °C– 600 °C. Zeolites, heteropolyacids, metal oxides and supported mineral acids, dehydrate glycerol to acrolein in either the gas phase or the liquid-phase. The selection of the best catalyst depends on the surface area, pore size, acid strength and the nature of the acid sites for a catalytic system. Acidity is the key factor to determine whether the catalyst is a suitable to dehydrate glycerol. (Dubois et al., 2006a; Chai et al., 2007a; Tsukuda et al., 2007; Atia et al., 2008; Benjamin et al., 2010; Alhanash et al., 2010; Dubois et al., 2006b). For the first time, Neher et al. (1995) demonstrated the effect of acidity on the catalyst performance for glycerol dehydration. Dubois et al. for the first time examined the effect of molecular oxygen on acrolein selectivity over acidic catalysts. They tested zeolites, Nafion, heteropolyacids and acid-impregnated metal oxides and observed an improved acrolein selectivity when oxygen added (Dubois et al., 2006a,b).

Stosic et al. (2012) studied the influence of acid/base properties of zirconia and titania based catalysts on the the selectivity of acrolein and by-products. They observed that beside the acid sites, the number of basic sites had a direct impact on acrolein selectivity in the gas-phase dehydration of glycerol in the absence of oxygen. Therefore, in order to increase the selectivity of acrolein, it is necessary to control not only the strength and the amount of the acidic sites, but also to hinder the number/strength/action of the basic sites. However, the selectivity of acetol was not correlated to the acid-base properties.

The main disadvantage of current best catalysts is that they deactivate within 24 h. Erfle et al. (2011) and Suprun et al. (2009) reported that high reaction temperature, small catalyst pore size and high acidity of the catalyst led to severe catalyst deactivation. Erfle et al. (2011) analyzed the spent catalyst by FTIR-pyridine and detected cyclic anhydride compounds. They also stated that Brønsted sites deactivated the catalyst.

In this study, WO_3/TiO_2 dehydrated glycerol in a fluidized-bed reactor continually for 14 h. We withdrew catalyst samples at 1 h intervals and measured the by-product distribution to assess the rate of carbon deposition and its effect on performance.

5.3 Methodology

5.3.1 Catalytic reaction

The fluidized bed reactor was a 46 mm ID quartz tube with a straight section (700 mm long) flanging out to 70 mm ID 300 mm long (to reduce catalyst carried by the gas to the quench). The reactor set-up has been described in detail in our previous publication (Dalil et al., 2015). A 20 µm ceramic frit, 50 mm from the bottom of the reactor, distributed the feed gases. A 1.6 mm diameter nozzle passed through the distributor and atomized the glycerol/water solution directly into the WO_3/TiO_2 bed. The injector was 20 mm higher than the distributor. The quality of the spraying is crucial to prevent catalyst from agglomerating, blocking the injector and liquid accumulating at the bottom of reactor. A gas assisted feed nozzle atomized the liquid. The ratio of argon to glycerol solution (G/L) was 400. The pressure drop in the injector at this condition reached 0.4 bar. Although the spray quality was better at higher gas to liquid ratios more catalyst attrited.
An electrical furnace heated the reactor and a 6-point thermocouple monitored the temperature of the catalyst bed and each zone of the reactor. Condensable products of the reaction were trapped in two quenches in series. A Varian HPLC (Metacarb 87H column) measured the concentration of the condensables whilst a Bruker GC equipped with Hyesep Q, Molsieve 5A and FFAP columns analyzed the acrolein and other light products e.g. acetaldehyde in the gas phase. A Pfeiffer mass spectrometer monitored the permanent gases (Figure 5.1).
We preheated the catalyst bed (180 g) to 400 °C for 30 min under a flow of argon. The reactor operated at 280 °C for 14 hour and we withdrew catalyst, liquid and gas samples at 1 hour intervals. but more frequently during the first hour. The molar composition of the feed in the gas phase was glycerol/oxygen/water/argon : 0.06/0.05/1.3/8.9.
The conversion of glycerol (X_{gly}) and selectivities towards products (S_p) were calculated as Equation 6.1 and 6.2.

$$X_{\text{gly}} = \frac{n_{\text{gly}}^{\text{in}} - n_{\text{gly.}}^{\text{out}}}{n_{\text{gly.}}^{\text{in}}} \times 100 \tag{5.1}$$

$$S_p = \frac{n_p}{n_{\text{gly}}^{\text{in}} - n_{\text{gly}}^{\text{out}}} \times \frac{m_p}{m_{\text{gly}}} \times 100 \tag{5.2}$$

Where : $n_{\text{gly}}^{\text{in}}$ and $n_{\text{gly}}^{\text{out}}$ are the molar flow rates of glycerol at the reactor entrance and exit. In equation 6.2, n_p is the molar stream of each product while m_p and m_{gly} represent the number of carbon atoms of the products and glycerol.

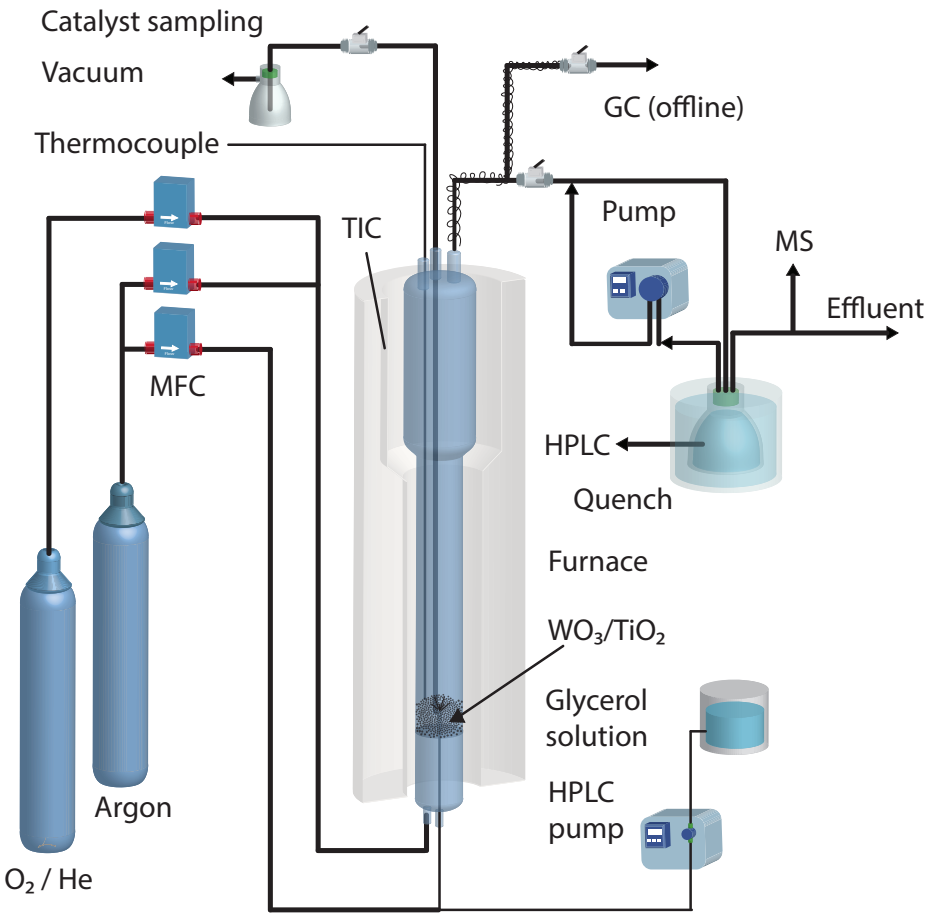

Figure 5.1 Schematic of the 46 mm ID fluidized bed, inlet gas manifold, quenches and analytical

5.3.2 Characterization techniques

We compared the catalyst samples collected during the reaction with fresh WO_3/TiO_2. A TA-Q50 thermogravimetric analyzer (TGA) measured the weight loss of catalyst as a function of temperature. We loaded 20 mg of catalyst to a 10 µm aluminium crucible A Platinel II thermocouple placed 2 mm above the sample pan monitored temperature. The resolution and accuracy of the balance was 0.1 µg and $> \pm 0.1$ %. To assure that the recorded weight loss was only related to the carbon, a stream of 40 mL min^{-1} nitrogen first purged the sample at 300 °C. After a 15 min isothermal hold, air substituted the nitrogen at the same flow rate and the furnace ramped to 500 °C and held the temperature for 60 min.

A JEOL JSM-7600TFE Field Emission Scanning Electron Microscopy imaged the samples. Graphite adhesive tape held the powder on the sample holder. We used both a LEI (lower secondary electron image) and LABE (Low-Angle Backscattered Electron) detectors.

An Autosorb-1 porosimeter (Quantochrome) measured the N_2 adsorption/desorption isotherms at 77 K. We calculated the surface area based on the multi-point BET (Brunauer, Emmett and Teller) method and the pore size and pore volume by the BJH (Barrett-Joyner-Halenda) method.

We treated the catalyst samples with pyridine then measured the acidity by Fourier transform infrared spectroscopy (FT-IR) with a Spotlight 400- PerkinElmer FTIR spectrometer. The IR range of the analysis was 600 cm^{-1} to 4000 cm^{-1} with resolution of 16 cm^{-1}.

A heat flow calorimeter (Setaram C80) linked to a conventional volumetric apparatus measured the acidity and basicity of the catalyst at 150 °C. The instrument was equipped with a Barocel capacitance manometer to monitor pressure. The probes (ammonia for acidity and sulphur dioxide for basicity) were purified by successive freeze-pump-thaw cycles. Prior to the test, a 100 mg sample was pre-treated overnight at 250 °C under vacuum. To record the differential heats of adsorption, small doses of the adsorbate were introduced repeatedly onto the catalyst the pressure reached 66 Pa. The samples outgassed for 30 min at the same temperature, and the procedure was repeated at 150 °C and 27 Pa. The difference between the amounts adsorbed in the first and second steps represents the irreversibly adsorbed quantity (Virr) of a respective gas from which we estimate the number of acidic/basic sites.

A EURO EA instrument measured the H/C content of the fresh and used catalyst (CHNS/O). The instrument combusted C, H, S and N at 600 °C. A carrier gas -He- swept the products out of the combustion chamber. The gases passed over heated copper to remove unreacted oxygen during in the initial combustion and a thermal conductivity detection (TCD) measured their concentration. We calibrated the instrument with acetanilide.

Transmission electron microscopy micrographs of fresh and coked WO_3/TiO_2 were recorded by a JOEL JEM-2100F field emission electron microscope. We supported the samples on a

copper grid for the experiment.

5.4 Results and Discussion

5.4.1 Effect of reaction conditions

To determine the optimal reaction condition for glycerol dehydration, we executed a 2^4 by full factorial experimental design. In process optimization, selectivity of the catalyst for acrolein was the response variable. The factors were temperature, gas phase O_2 concentration, mass fraction of glycerol in the solution, and residence time. All tests were at ambient pressure and lasted 2 h.

Reaction temperature

The operating tempearatures were 280 °C and 300 °C. The catalyst was very active at high temperature (conversion > 95) and selectivity dropped as conversion increased ; acrolein selectivity was higher 280 °C and fewer by-products formed including acetaldehyde, propanaldehyde and acetone. The HPLC detected traces of hydroxyacetone (less than 2 % in the samples from the liquid trap (experiments at 280 °C). Acrolein decomposes at higher temperature to acetaldehyde and formaldehyde. Moreover, at high temperatures, more carbon deposits on the catalyst and it deactivates more rapidly. Even at 280 °C, the conversion of glycerol was nearly complete.

Oxygen concentration

The aim of applying molecular oxygen in gas-phase dehydration of glycerol is to decrease the formation of aromatic by-products (phenol) and also the by-products originating from hydrogenation of dehydrated products such as propanal and acetone. The presence of molecular oxygen also reduces coke and thereby maintaining the catalyst active (Dubois et al., 2006b).
We fed a mole fraction of 0.5 % and 1.5 % oxygen to the reactor. The glycerol conversion was the same at both conditions, however, acrolein selectivity was higher at the higher oxygen concentration while the selectivity of acetone, acetaldehyde and propanaldehyde was lower. Whereas the effect of oxygen was much higher for acetone than for acetaldehyde or propanaldehyde (Table 5.1). Acetone may form via the hydrogenolysis of hydroxyacetone (acetol)

which is a product of single-step glycerol dehydration when the primary OH is released (Dubois et al., 2006b; Ulgen and Hoelderich, 2011).

Glycerol concentration

The solid catalyst should be insoluble in water and hydrothermally stable when water vapour is present during reaction. In the screening experiments, we tested glycerol solution mass fractions of 14 % and 28 %. The selectivity of acrolein was higher for the reactions performed with a mass fraction of 14 % glycerol (Figure 5.2 and 5.3). The selectivity was higher with the higher water concentration and there was less coke : some Lewis acid sites converted to Brønsted sites, which favour acrolein production.

Residence time

In the range of conditions we tested, residence time (RT) had no effect on glycerol conversion, nor on acrolein selectivity.

Table 5.1 Effect of operating conditions on product distribution for glycerol dehydration over WO_3/TiO_2 after 2 h time-on-stream.

T °C	y_{O_2} mol%	Gly. con. wt%	RT s	$S_{acrolein}$ %	$S_{acetaldehyde}$ %	$S_{popanal}$ %	$S_{acetone}$ %
300	1.5	28	1.5	43	8	7	4
300	1.5	28	1.2	40	8	9	5
300	1.5	14	1.5	50	6	4	3
300	1.5	14	1.2	41	9	6	3
300	0.5	28	1.5	30	6	8	12
300	0.5	28	1.2	36	7	9	12
300	0.5	14	1.5	48	5	5	6
300	0.5	14	1.2	35	8	7	9
280	1.5	28	1.5	58	5	4	4
280	1.5	28	1.2	55	6	6	6
280	1.5	14	1.5	60	3	5	4
280	1.5	14	1.2	60	5	6	7
280	0.5	28	1.5	45	3	8	10
280	0.5	28	1.2	40	7	8	11
280	0.5	14	1.5	50	3	5	7
280	0.5	14	1.2	48	5	7	9

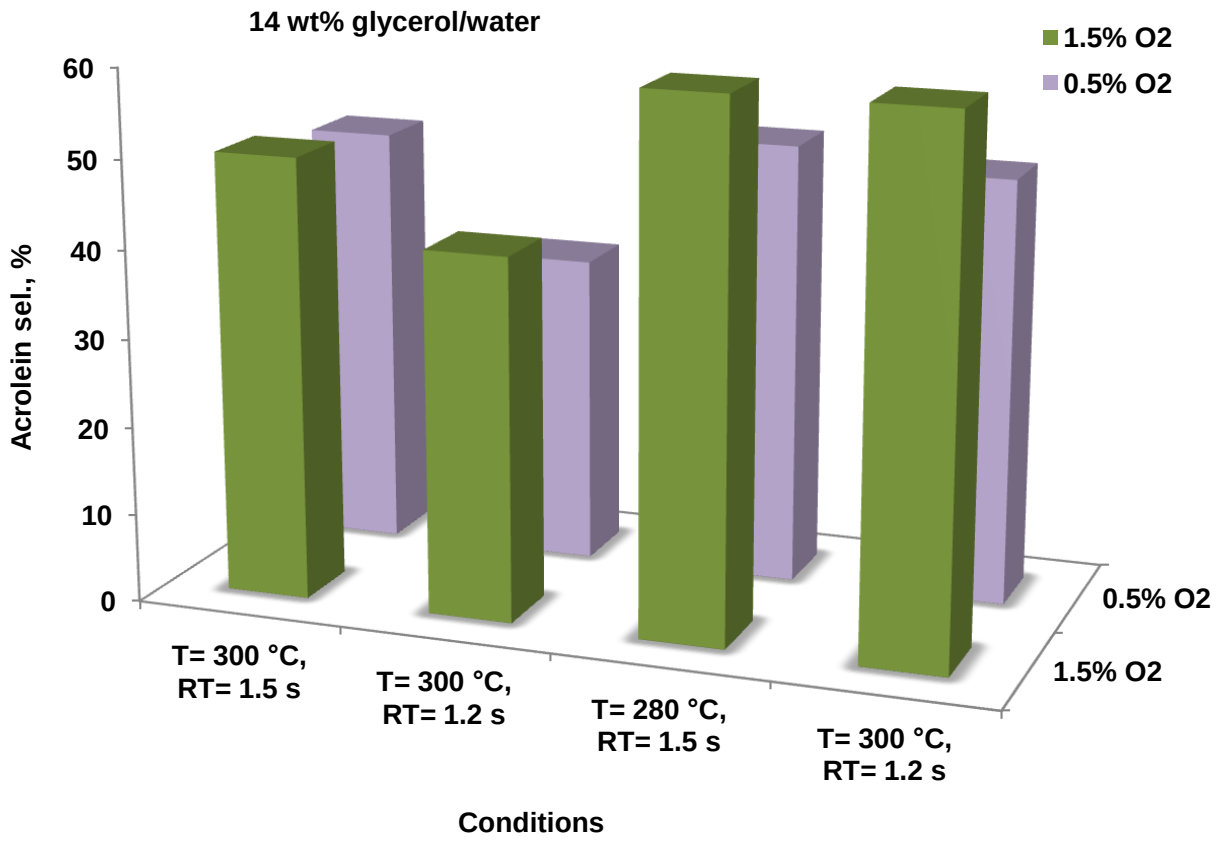

Figure 5.2 Acrolein selectivity versus reaction conditions for 14 wt% glycerol/water solution

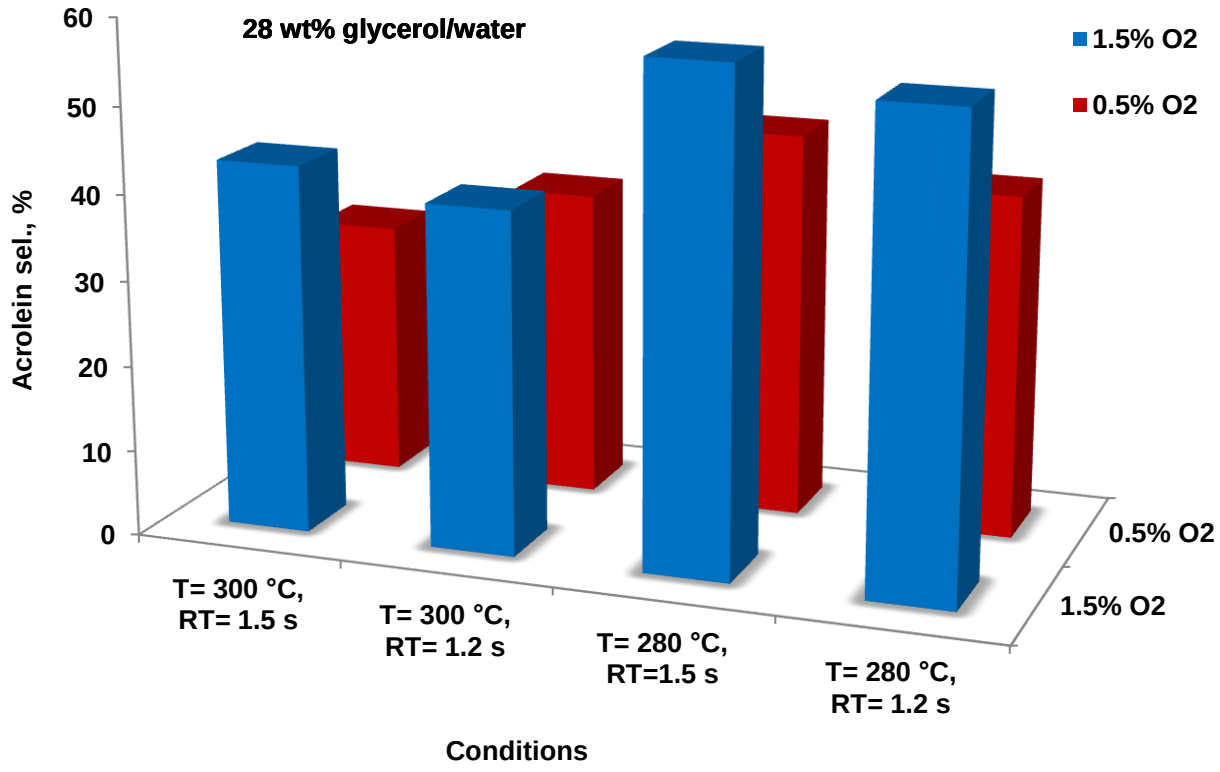

Figure 5.3 Acrolein selectivity versus reaction conditions with a mass fraction of 28 % glycerol/water solution

5.4.2 14 h Catalytic test

WO_3/TiO_2 catalyst remained fully active during 14 h of reaction and converted 97 % of glycerol during the first 2 h of injection ; after 3 h all of the gylcerol reacted. Co-feeding oxygen improves glycerol conversion. Furthermore, it maintains catalyst active (Dubois et al., 2006a; Ulgen and Hoelderich, 2009, 2011). Based on our liquid and gas phase analysis of reaction products, propanaldehyde (propanal), hydroxyacetone (acetol), acetaldehyde, acetone and formic acid were the major by-products. Glycerol dehydrates by first losing −OH from the secondary carbon atom. During the first 5 min of reaction, the acrolein selectivity was 3 % and the selectivity towards by-products and coke were high. The acrolein selectivity increased as coke accumulated on the catalyst ; its selectivity was constant after 6 h (Figure 5.6b) while coke continued to accumulate with time-on-stream.
Another reaction pathway involves removal of OH group from primary carbons to give 1-hydroxyacetone (acetol). We observed minor peaks of methylglyoxal in the first hour samples but it disappeared with reaction time. Oxidation of 1-hydroxyacetone gives methylglyoxal.
Acetone was the dominant by-product during the first hour of reaction and its selectivity was 10 %. It dropped to 4 % after 2 h and to below 1 % after 11 h. Acetone was likely produced through the hydrogenation (or hydrogen transfer) of hydroxyacetone forming 1,2-propanediol (traces observed). Another possible route to acetone is the hydrogenolysis of hydroxyacetone.
Acetaldehyde forms from the retroaldol reaction of 3-hydroxypropanal (a glycerol dehydration intermediate). The selectivity of acetaldehyde decreased by 50 % during the 14 h test.
The selectivity of formic acid was constant during the reaction and it is produced via the oxidation of formaldehyde. Formaldehyde is formed through the retroaldol reaction of 3-hydroxypropanal. We didn't detect any traces of formaldehyde in our product analysis as it is very unstable (boiling point : −19 °C) and perhaps quickly oxidizes to formic acid or degrades to CO and H_2. CO, CO_2 and H_2 were present in our gas phase analysis. CO can be the product of side reactions or in-situ coke combustion. The concentration of H_2 as an intermediate increased slightly with time. Some acrolein oxidized to make acrylic acid but it was less than 1 %. Propanal selectivity was 2 % throughout the entire reaction (Figure 5.4).

With reaction time, acrolein selectivity increased, which suggests that either glycerol or acrolein tend to convert to coke and by-products. As coke grew, the non-selective sites were destroyed and the catalyst became more selective to acrolein. Consistent with our kinetic experiments, acrolein selectivity increases while in addition to coke selectivity, by-product selectivity of acetaldehyde, formic acid, propanal and acetone decreases (Figure 5.5a).
During the first hour, we sampled the catalyst, gas and liquid products at shorter intervals (5–10 min). The formation of coke was severe in this period and even only after 5 min. The

catalyst colour changed from light green to grey. It produced coke rather than acrolein ; its selectivity was only 3 % in the 5 min sample.

5.4.3 Characterization of fresh and coked WO_3/TiO_2

TGA

TGA analysis of the samples withdrawn at 1 h intervals established a profile for coke formation. Fluidized beds are ideal mixers so there are no axial or radial concentration gradients and the coke on the catalyst represents the average of the bed. After 5 min the mass fraction of coke on the catalyst was 0.2 % and it reached 1 % after 1 h. At the end of reaction (14 h), the coke fraction reached 2.5 %, which represents 4.5 g on the 180 g of catalyst (Figure 5.5b). During the first hour, the coke selectivity was 87 %. It dropped to 50 % after 1 h and the acrolein selectivity increased to 36 %. The coke selectivity continued to drop after 6 h but it reached a steady state thereafter (Figure 5.6b). After 14 h, the coke selectivity was 9 %. The acrolein selectivity plateaued at 73 % after 6 h, which confirms that it is related to the coke.

The carbon balance closed to better than 88 % based on summing the moles of detected products, unreacted glycerol and the coke. The carbon loss could be related to the minor unknown peaks in the GC chromatogram or decomposition of some products at the time of injection to GC. Measuring the coke during the entire experiment allowed us to achieve a better mass balance, particularly during the early stages when the coking rate was highest (Figure 5.7).

Elemental analysis (CHNS/O)

The mass fraction of carbon based on the CHNS/O analysis for the 1 h sample was 0.8 % and it increased to 2.2 % after 14 h. The TGA results were similar for carbon content (Table 5.3). Although the amount of carbon and hydrogen increased continuously, the H/C ratio of carbonaceous compounds formed on the catalyst increased from zero to 0.26 after 1 h and remained constant up to 14 h. The H/C ratio suggests that these compounds were polyaromatic coke. However, the type of coke was the same throughout the reaction (Table 5.3).

FE-SEM

The surface of the fresh catalyst was rough and the particle size distribution was heterogeneous (Figure 5.8a), which was do to crushing the pellets. However, the particle shape was

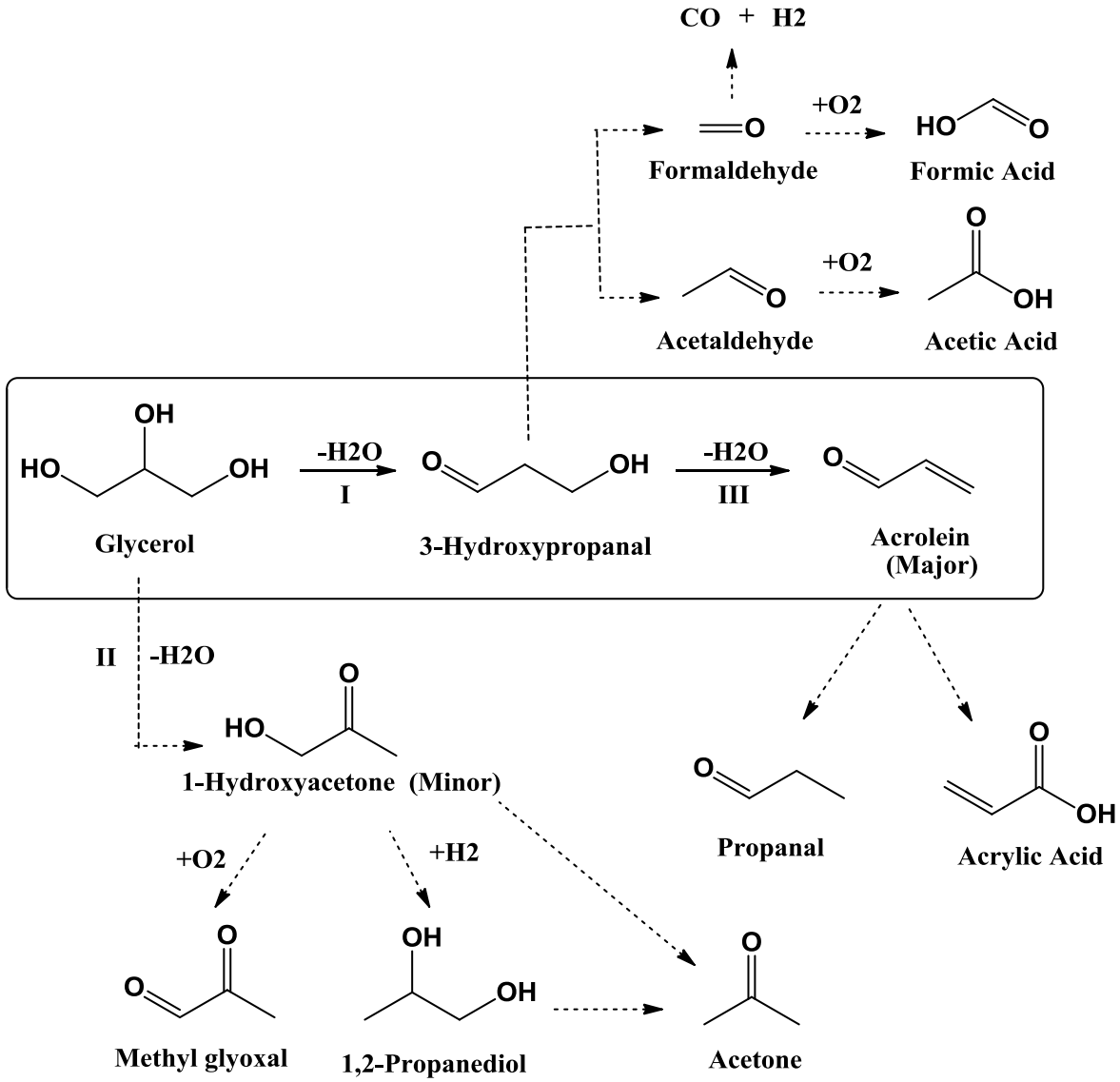

Figure 5.4 Reaction mechanism for steady-state dehydration of glycerol to acrolein and by-products

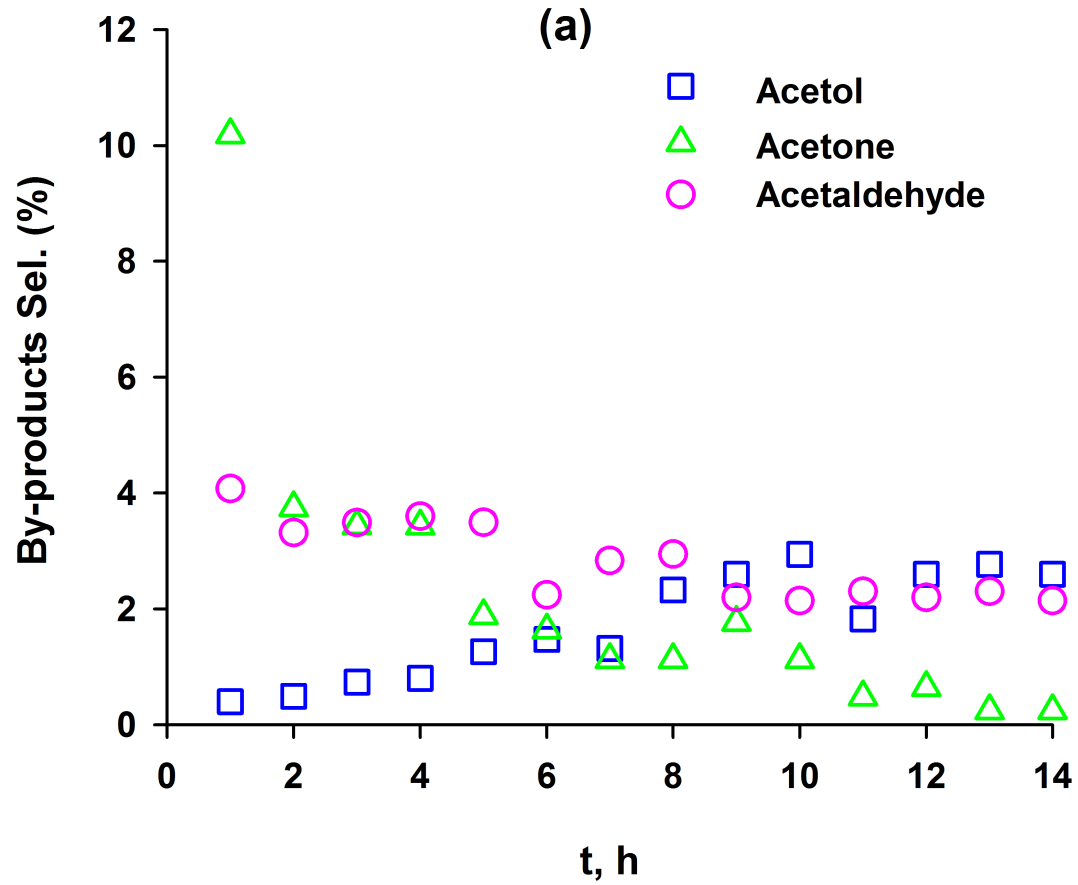
(a)
Acetol
Acetone
Acetaldehyde
By-products Sel. (%)
t, h
0
2
4
6
8
10
12
14

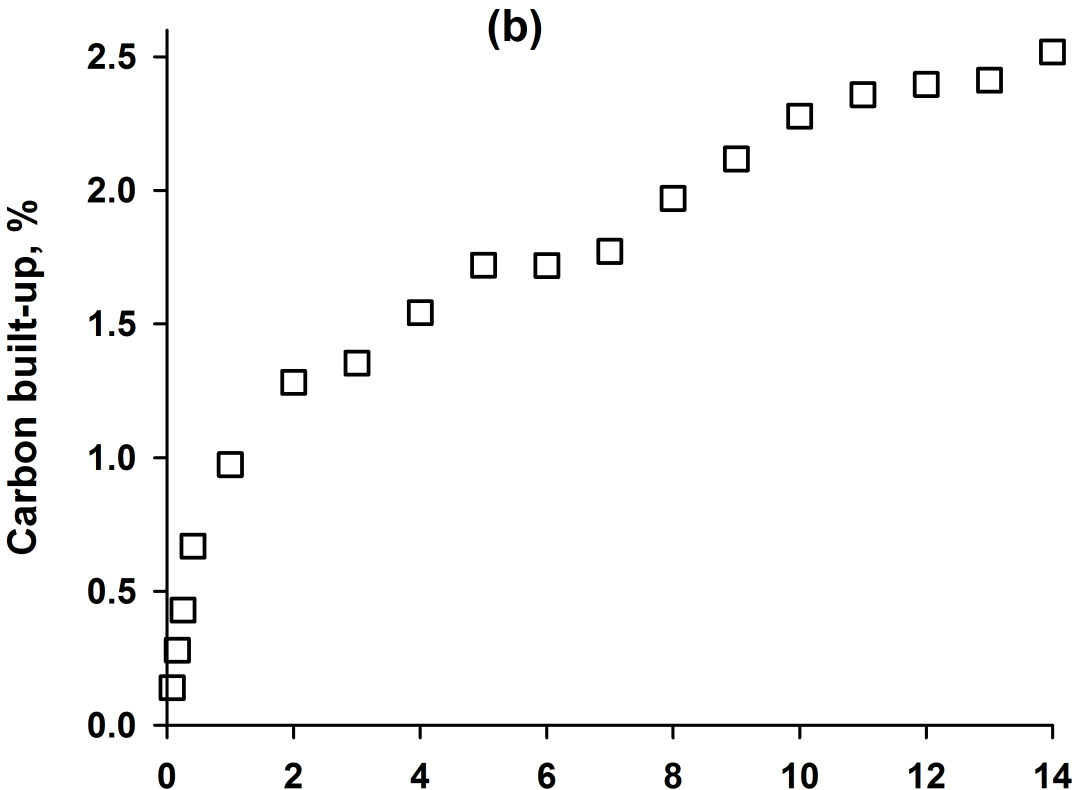
(b)
Carbon built-up, %
0.0
0.5
1.0
1.5
2.0
2.5
0
2
4
6
8
10
12
14

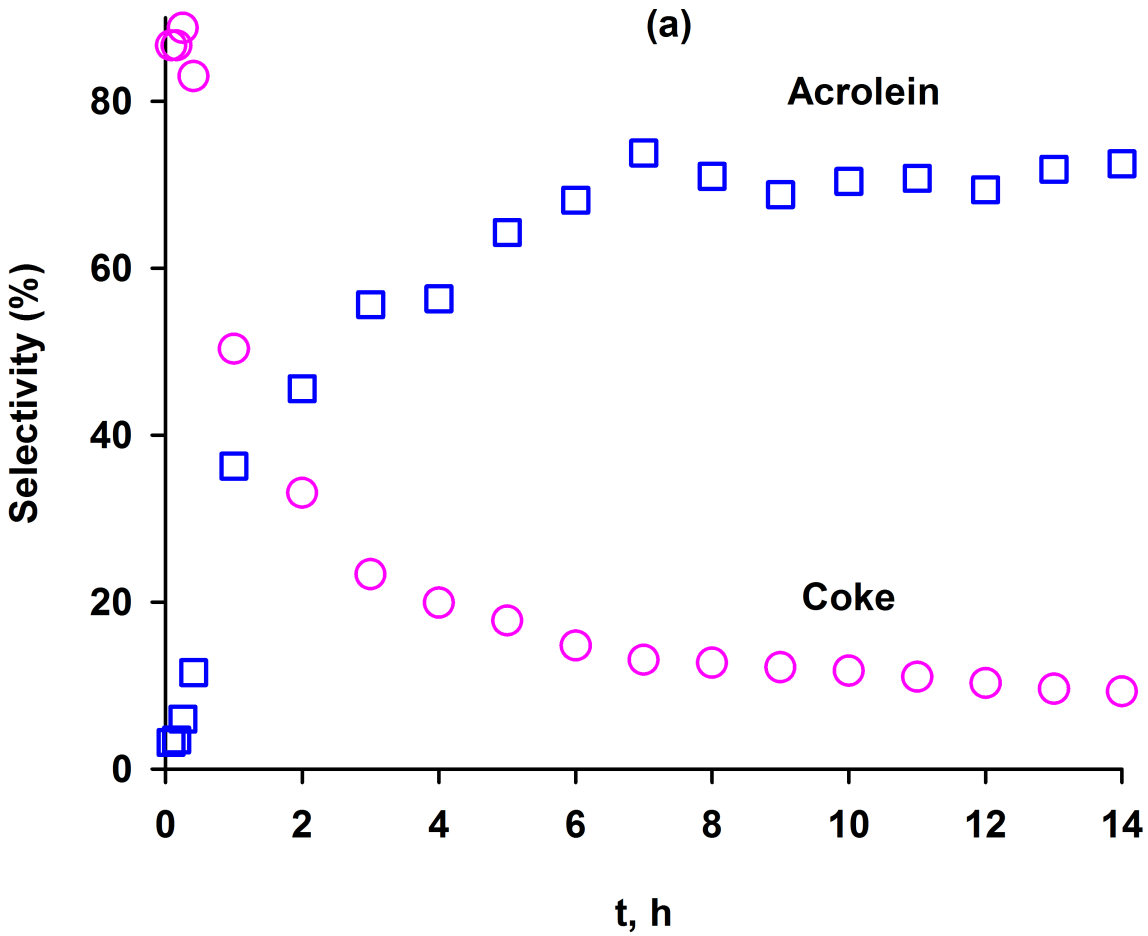
(a)
Acrolein
Coke
Selectivity (%)
t, h
0
20
40
60
80
0
2
4
6
8
10
12
14

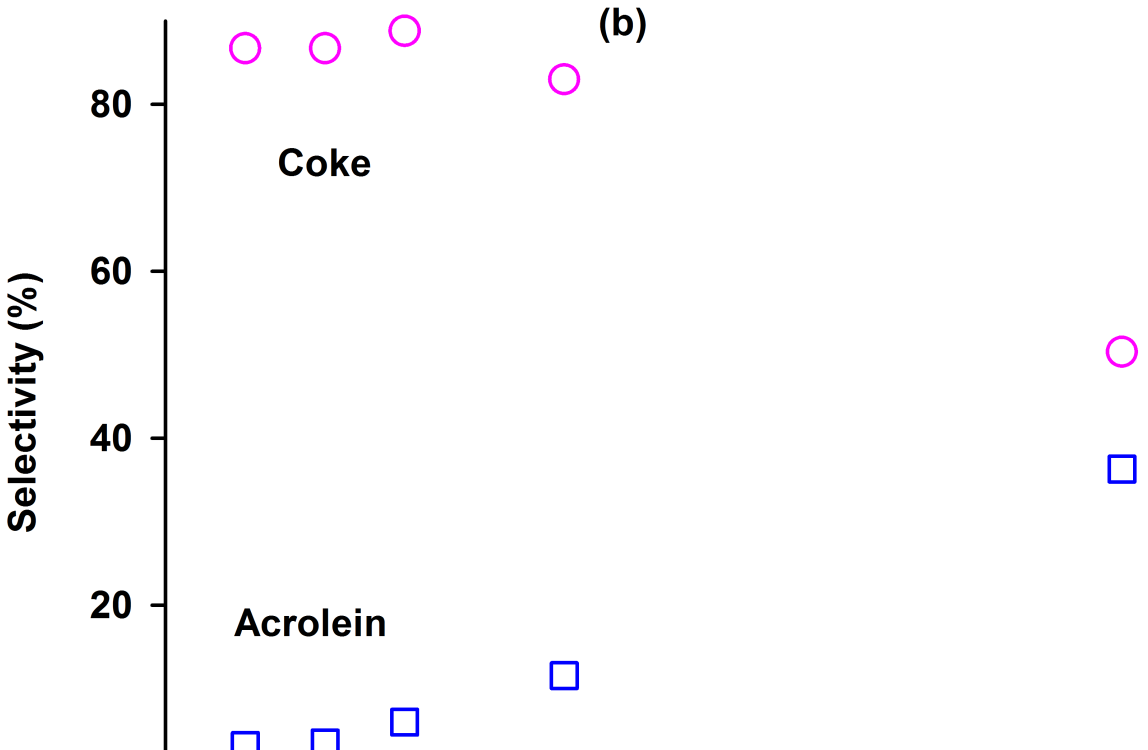
(b)
Coke
Acrolein
Selectivity (%)
20
40
60
80

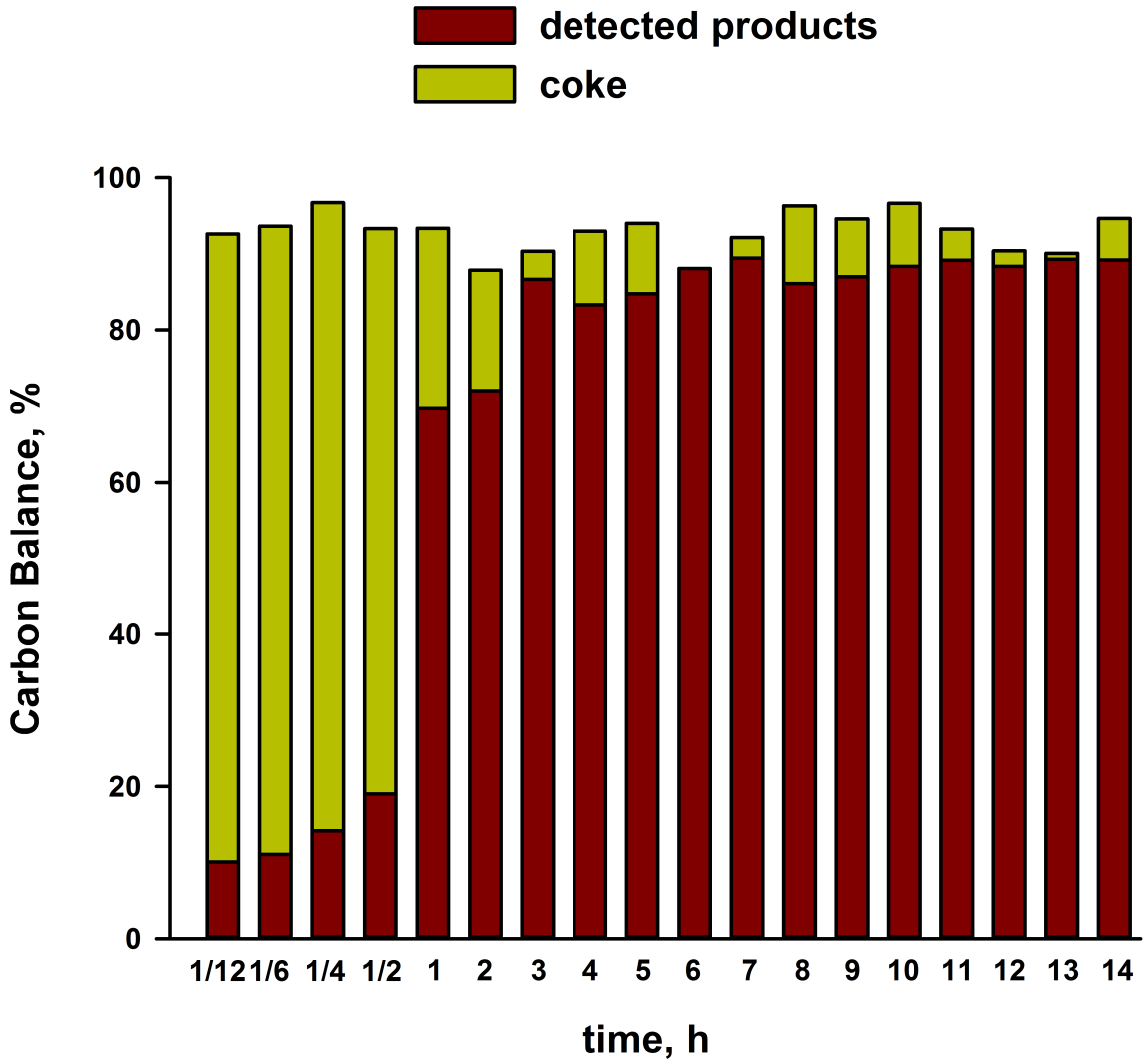

Figure 5.7 Carbon balance versus time

Table 5.2 Product distribution for 14 h glycerol dehydration over WO_3/TiO_2 catalyst

TOS (h)	S_{acrolein}	$S_{\text{acetaldehyde}}$	S_{acetol}	$S_{\text{formic acid}}$	S_{popanal}	S_{acetone}
1/12	3	3	1	-	-	7
1/6	3	3	3	-	1	9
1/4	4	3	2	2	1	9
1/2	11	4	3	3	1	10
1	36	4	1	1	2	10
2	45	3	1	1	3	4
3	55	3	1	1	2	3
4	55	3	1	1	1	3
5	63	3	1	1	1	2
6	67	2	1	1	2	2
7	74	3	1	1	1	1
8	71	3	2	1	1	1
9	70	2	2	1	1	2
10	71	2	3	-	1	1
11	71	2	2	-	1	1
12	70	2	2	-	1	1
13	72	2	2	-	1	-
14	73	2	2	-	1	-

Table 5.3 Elemental analysis data revealing H/C ratio

Time (hour)	H	C	H/C	C (TGA)
1	0.21	0.82	0.26	0.97
14	0.58	2.2	0.27	2.4

the same after 14 h (Figure 5.8c) and it did not agglomerate. However, for both fresh and used samples, a fine powder ($d_p < 1\,\mu m$) covered the surface, which was due to crushing it (Figure 5.8b and d).

TEM

TEM micrographs exhibited agglomeration of fine particles in the structure of WO_3/TiO_2 (Figure 5.9a). We observed a representative lattice fringe pattern for fresh catalyst indicating that of WO_3/TiO_2 particles were crystalline (Figure 5.9c). The crystalline structure was confirmed by the selected-area electron diffraction (SAED) pattern (Figure 5.9d).

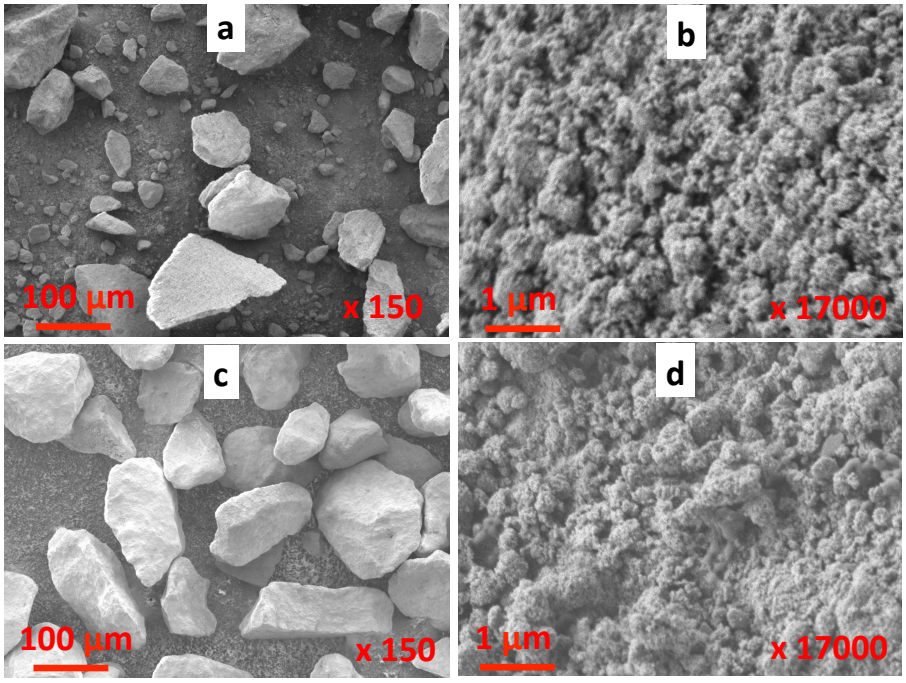

Figure 5.8 FE-SEM images of : (a) and (b) fresh catalyst, (c) and (d) used catalyst.

N_2 adsorption

The hysteresis loops for the N_2 adsorption/desorption isotherms are type H_1 as defined by IUPAC. In H_1 type hysteresis, two of the branches are almost vertical and nearly parallel in the range of the gas uptake (Sing et al., 1985). The shape of the hysteresis loop is associated with the structure of the pores. Type H_1 represents cylindrical shaped pores. This type of hysteresis has been reported for pure titania by Bavykin and Walsh (2010) and Bing et al. (2009). The pore volume of fresh catalyst was $0.22\,cm^3\,g^{-1}$ and it reduced to $0.18\,cm^3\,g^{-1}$ after 2 h and remained constant. Thereafter, the coke reduced the mean pore diameter of the catalyst from 17.3 nm to 12.4 nm at 6 h. The decrease in pore volume and diameter was related to the coverage of the catalyst pores by coke (Table 6.1). The adsorption/desorption isotherms of the 14 h sample was the same as the fresh sample indicating that the pores remained cylindrical. This data suggests that the coke forms in the pores and covers the internal walls of the cylinders rather than plugging the entrance (Figure 5.10).

The nitrogen adsorption/desorption isotherms exhibited an inflection at $0.6 < P/P_0 < 0.9$ indicating that the fresh catalyst was mesoporous. The surface area of fresh catalyst was

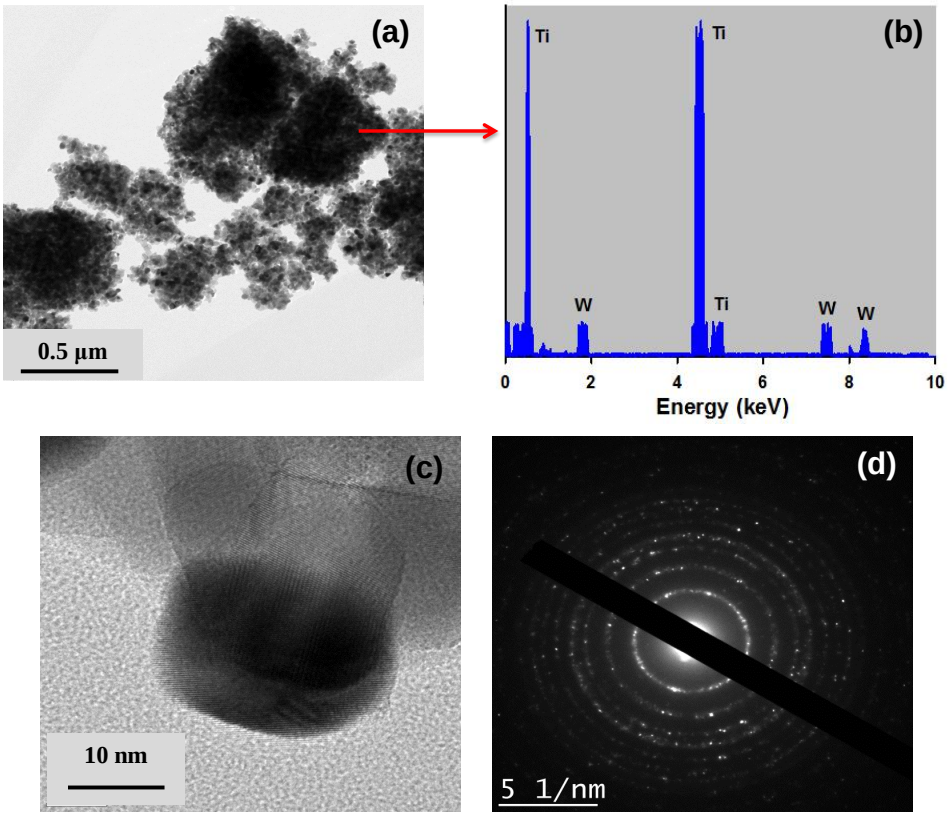

Figure 5.9 TEM images of fresh catalyst : (a) 0.5 µm, (b) EDAX, (c) 10 nm and (d) SAED. The crystalline structure of WO_3/TiO_2 is observed in (c) and (d).

$30.5\,m^2\,g^{-1}$ and it decreased with time (coke loading) (Dalil et al., 2015). After 1 h, when the mass fraction of coke was 1 % (1.8 g of carbon), the surface area dropped to $27\,m^2\,g^{-1}$ and after 14 h it was $23\,m^2\,g^{-1}$ with 2.5 % coke (4.5 g) (Table 6.1).

Table 5.4 Textural properties of WO_3/TiO_2 catalyst

Time (h)	SA ($m^2\,g^{-1}$)	υ_p ($cm^3\,g^{-1}$)	d_p (nm)
0	30.5	0.22	17.3
1	27.1	0.20	17.5
2	26.3	0.18	17.3
6	25.5	0.17	12.4
14	23.0	0.18	12.4

To calculate the number of the carbon layers on surface, we considered the formation of a graphite type carbon. Graphite with hexagonal structure, has cell dimensions of a= 2.461 Å and c= 6.708 Å. So, there are 2 carbon atoms per basal plane or 3.8×10^{19} atoms m^{-2}. The number of C layers for 2.5 % carbon deposition on $30.5\,m^2\,g^{-1}$ of catalyst, is equivalent to a monolayer after 14 h.

Acid/base properties (TPD-NH_3 and SO_2)

The adsorption of probe molecules by micro-calorimetery indicates catalyst acid/base features. NH_3 was used as a basic molecule to determine the acidity while SO_2 titrated the basic sites (Air Liquide > 99.9 %). The initial sharp rise in the volume of NH_3 adsorbed corresponds to irreversible adsorption, whereas the rising slope after 0.05 torr relates to reversible adsorption (Figure 5.12).

Fresh WO_3/TiO_2 adsorbed the most ammonia because it has most acid sites and the highest strength (high heats of adsorption). As coke forms, the catalyst adsorbs fewer probe molecules. The number of acid sites decreased in the order : fresh WO_3/TiO_2 > 2 h > 6 h $\simeq$ 14 h. The greatest drop was from the fresh catalyst to the 2 h sample. The volume adsorbed by the 6 h and 14 h samples were the same indicating that the number of acid sites remained constant after 6 h (Table 5.5). The NH_3 adsorption isotherms of 6 h and 14 h samples are identical in Figure 5.12. Initially, the acrolein selectivity was negligible ; it increased with time to reach a steady rate and was constant after 6 h, which is the identical trend for NH_3 and SO_2 adsorption. Thus the change in selectivity relates to the change in acidity and basicity of the catalyst.

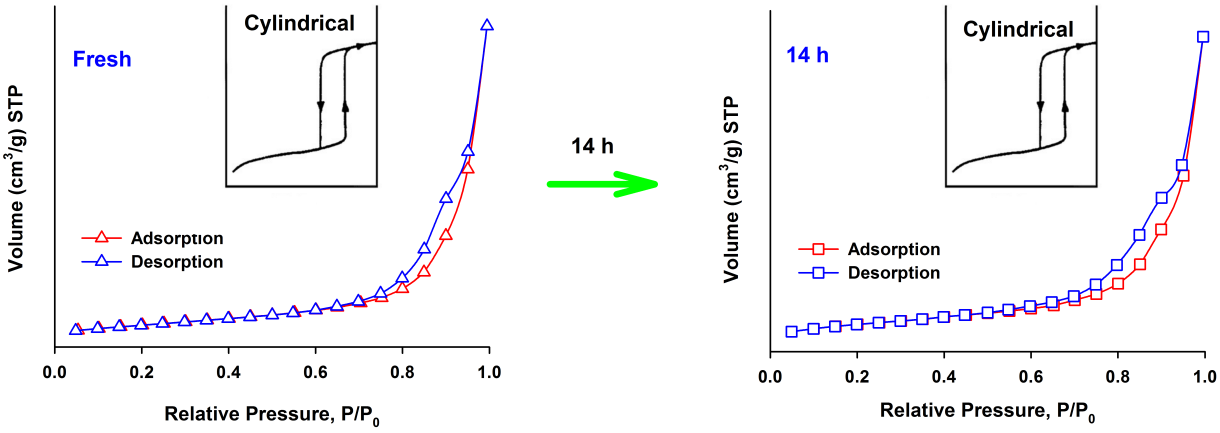

Figure 5.10 N_2 adsorption/desorption isotherms for fresh and used WO_3/TiO_2

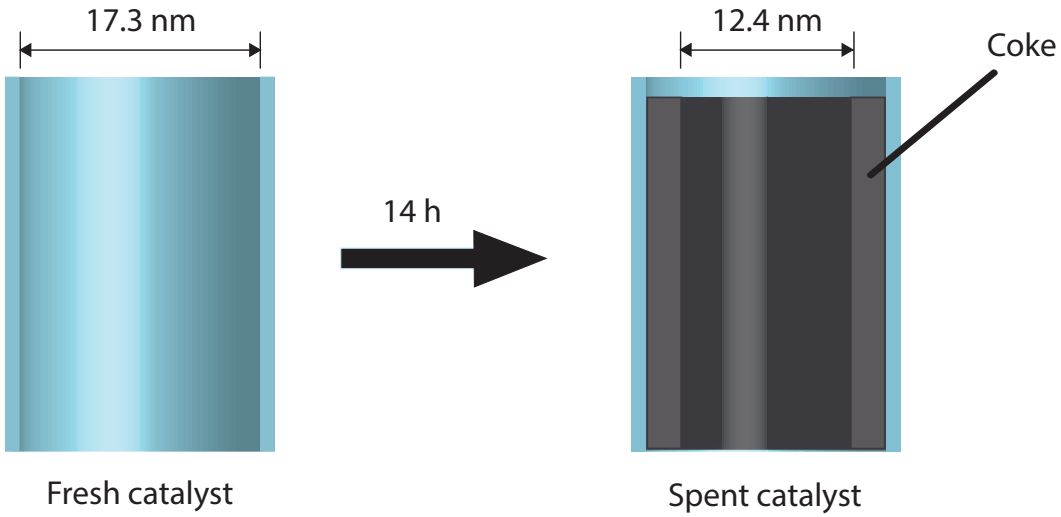

Figure 5.11 Carbon deposited on the wall of the pores of WO_3/TiO_2, reducing the pore diameter

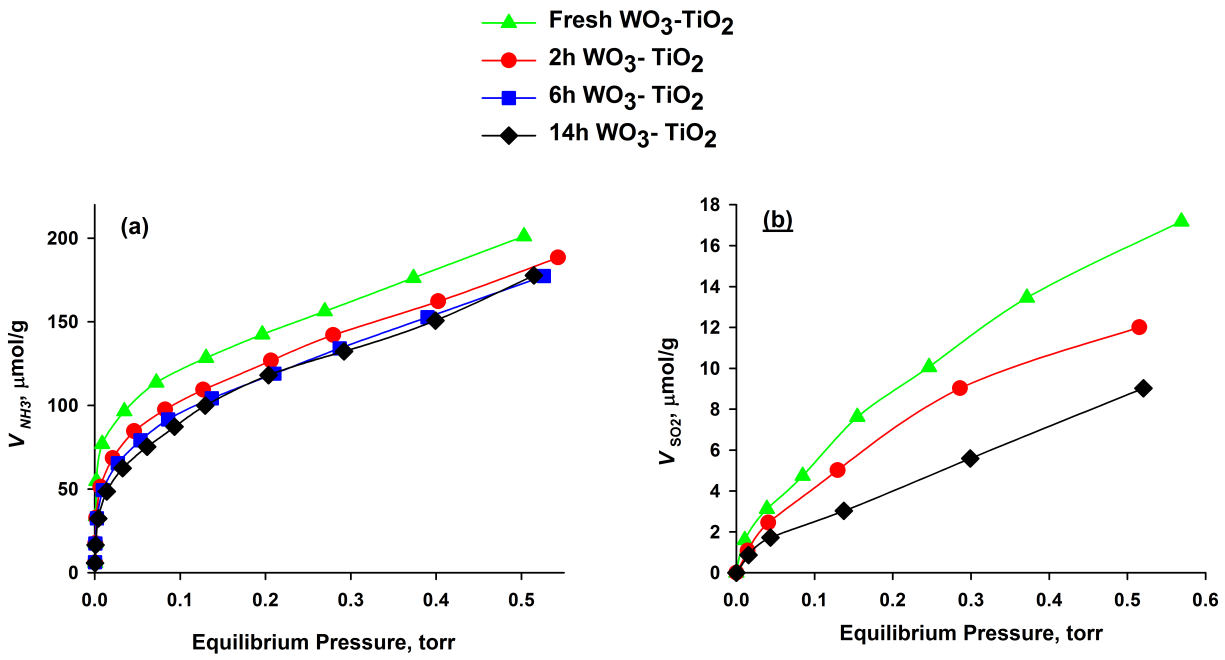

Figure 5.12 Volumetric isotherms of (a) NH_3 and (b) SO_2 adsorption on fresh and spent WO_3-TiO_2 catalyst

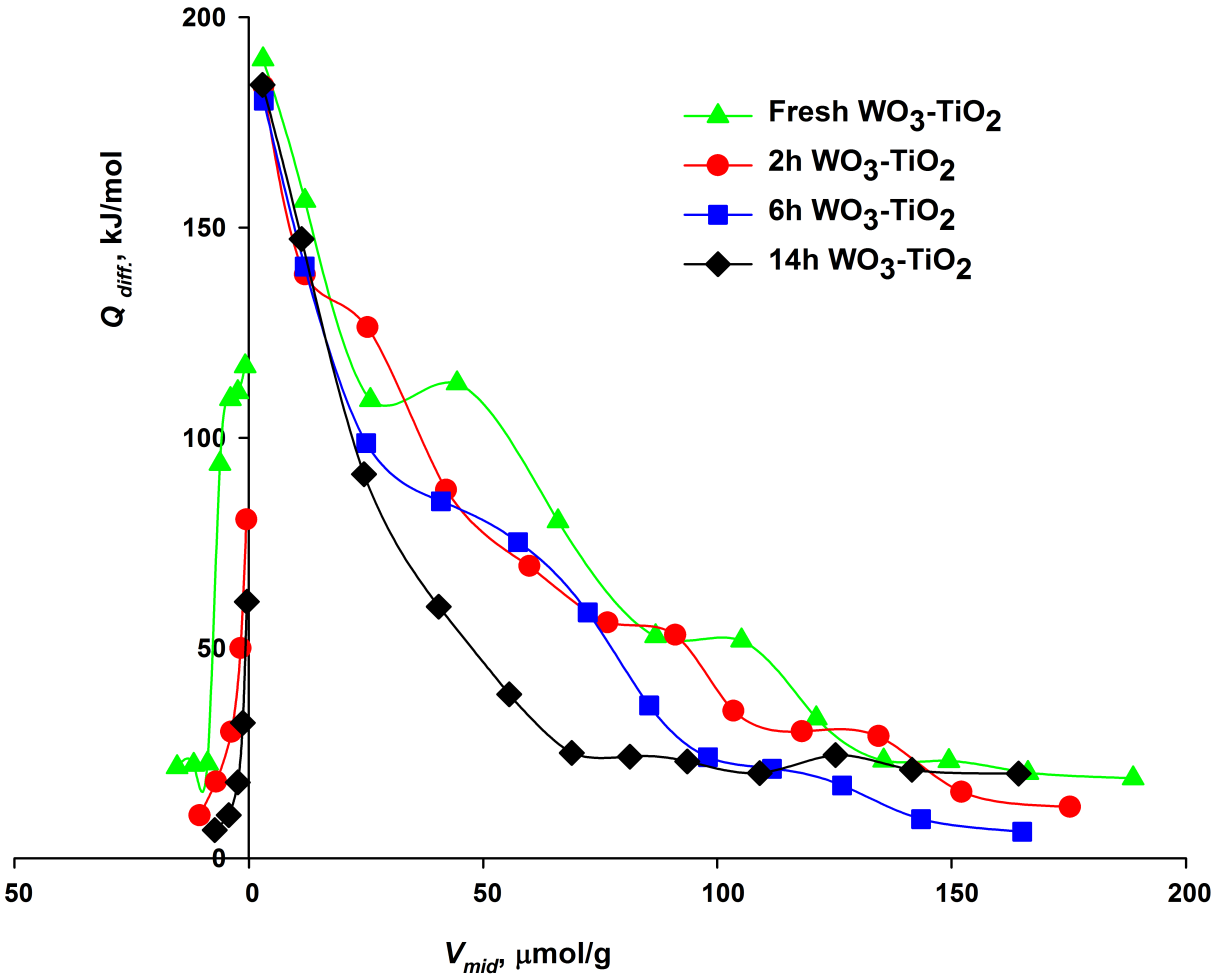

Figure 5.13 Differential heats of NH_3 and SO_2 adsorption as a function of surface coverage for fresh and spent WO_3/TiO_2 catalyst

The fresh catalyst has few basic sites (medium to weak strength) compared to the acid sites according the SO_2 adsorption measurements (Table 5.5 , Figure 5.12). The basic sites disappear quickly, as coke accumulates and less acetone forms as well as 1,2-propanediol (Figure 5.5). The differential heats of adsorption confirm the presence of strong, medium and weak acid sites on the fresh catalyst (Figure 5.13). We derived the number of acid and basic sites from Figure 5.13. The three domains of acid sites for Q_{diff} are defined as weak, medium and strong (Auroux, 2013) :

— $90 < Q < 120$: weak
— $120 < Q < 150$: medium
— $150 < Q$: strong

Coke formation reduced the number of medium and weak acid sites of the catalyst (Figure 5.14), while after 14 h, and still producing acrolein selectively. Because of the presence of the strong sites, the catalyst remained fully active after 14 h producing acrolein.

Table 5.5 Virr. and Vtot. calculated from adsorption isotherms of SO_2 and NH_3 on fresh and used WO_3/TiO_2

Sample	NH_3 adsorbed amount		SO_2 adsorbed amount	
	$V_{\text{tot.}}$ µmol g^{-1}	$V_{\text{irr.}}$ µmol g^{-1}	$V_{\text{tot.}}$ µmol g^{-1}	$V_{\text{irr.}}$ µmol g^{-1}
fresh	143.2	86.5	8.8	3.8
2 h	125.4	64.3	6.8	2.2
6 h	116.9	61.3	-	-
14 h	117.2	60.2	3.1	0.8

FTIR-pyridine

Although TPD-NH_3 measures the strength of the acid sites but not the type (Brønsted or Lewis acid). The FT-IR pyridine spectra of WO_3/TiO_2 differentiates between the Brønsted and Lewis acid sites (Figure 5.15). Lewis acid sites may react with steam to generate Brønsted sites (Alhanash et al., 2010). Brønsted sites dehydrate glycerol to acrolein by protonating its secondary hydroxyl (Alhanash et al., 2010).

We recorded the the background spectra of samples before analysing any samples. Then we treated the samples with pyridine at room temperature and desorbed the excess pyridine at 100 °C for 1 h. After cooling to room temperature, the instrument recorded the spectra. The bands of the spectra relate to pyridinium cations (PyH^+) and Brønsted sites appear at 1640 cm^{-1}, 1620 cm^{-1} and 1540 cm^{-1}. The band at 1490 cm^{-1} corresponds to a mixture

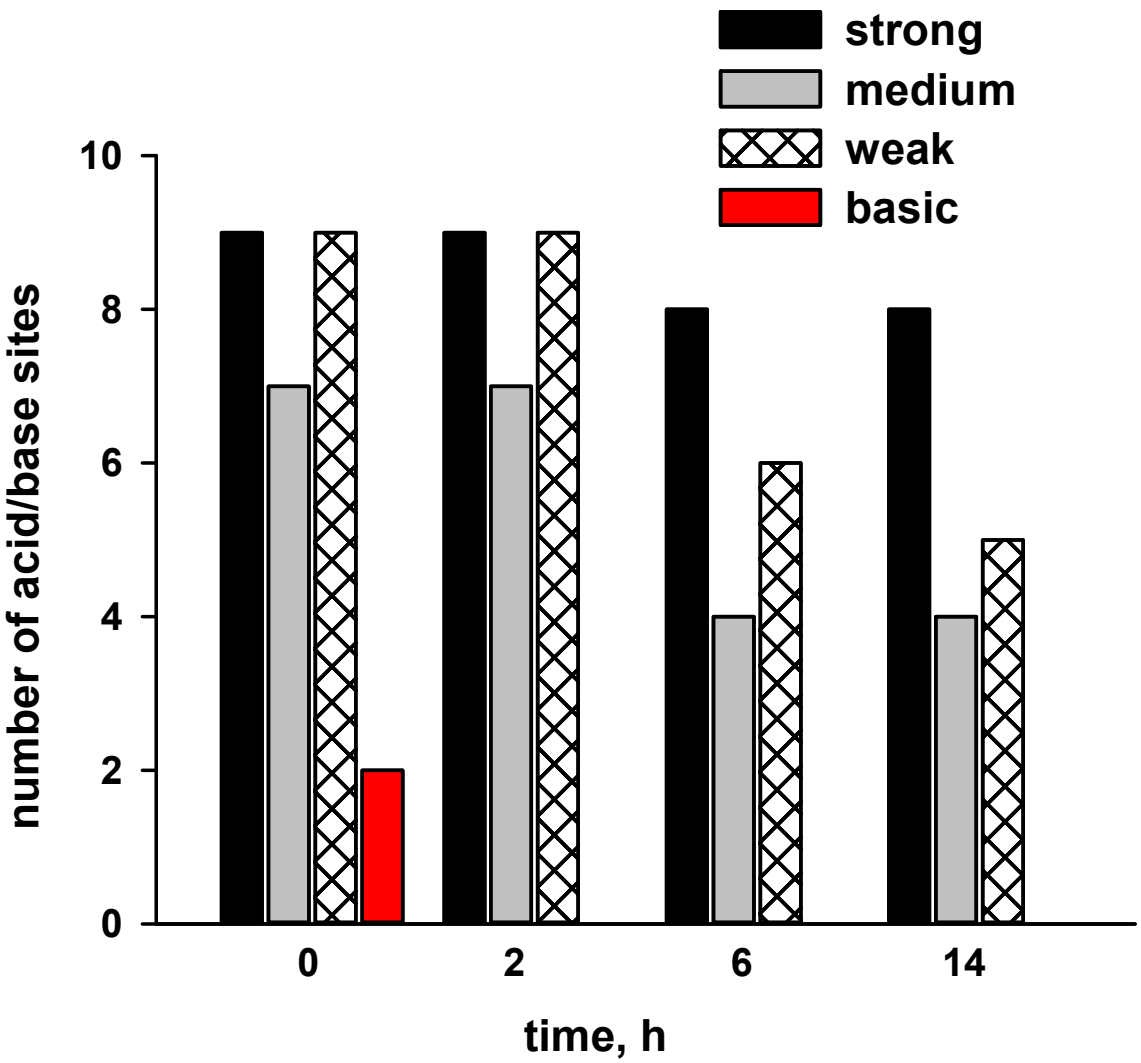

Figure 5.14 Number of acid sites of different strengths and basic sites vs. reaction time

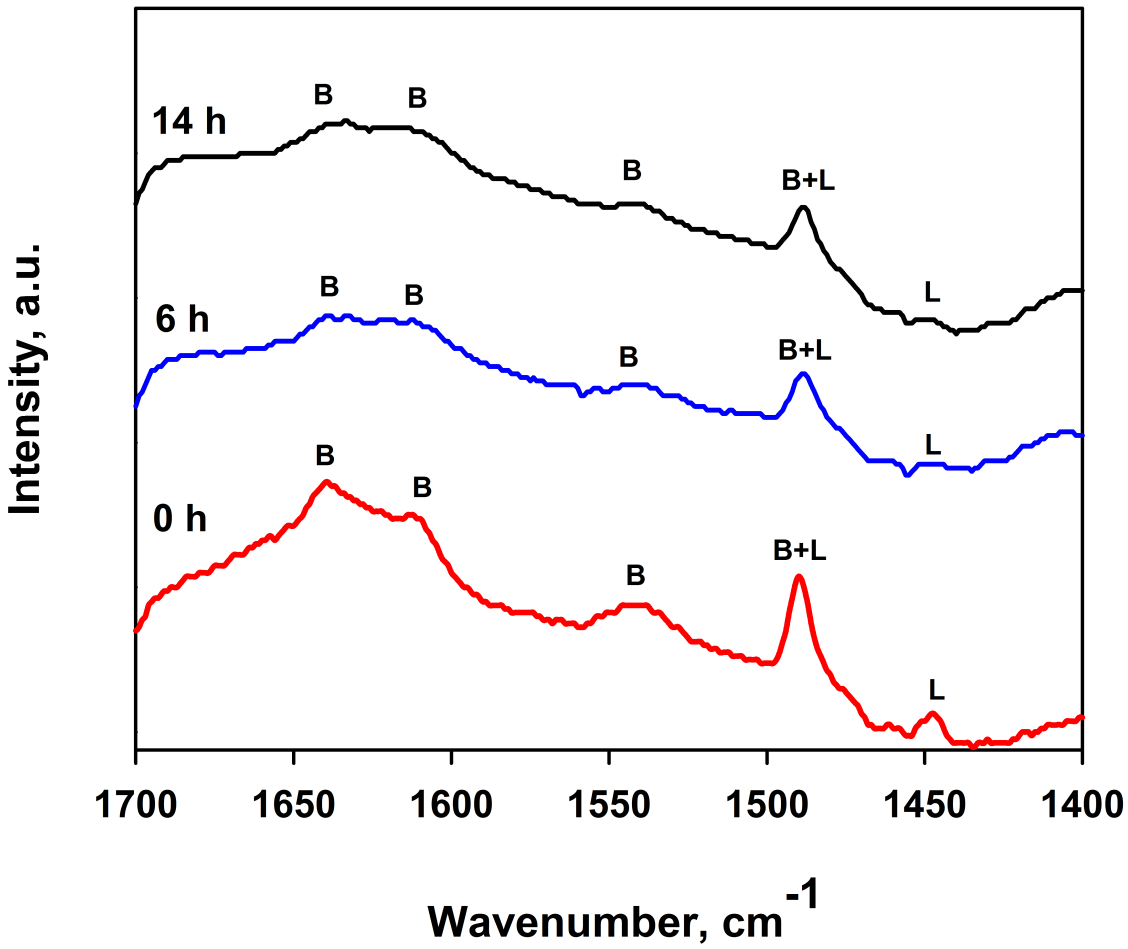

Figure 5.15 FT-IR spectra recorded after pyridine adsorption at room temperature and desorption at 100 °C for fresh and used catalysts. (L : Lewis and B : Brønsted acid sites)

of Lewis and Brønsted acids and the pyridine that was coordinated to Lewis sites on fresh dehydrated catalyst (Py−L) appeared at 1450 cm^{-1} (Martin et al., 1997). For the 6 h sample, the band corresponding to B+L sites was still dominant while the Brønsted acid bands decreased. The peaks of Lewis acidity disappeared while the peaks of Brønsted sites reduced with reaction time. We attribute the drop in the Brønsted and Lewis sites to coke formation. However, there was no noticeable difference in the band intensity between 6 h and 14 h samples suggesting that although the coke forms continuously, after 6 h the acidity of the catalyst remained constant. Consequently, the selectivity of acrolein and by-products was stable after 6 h and the reaction reached steady-state. The coke selectivity (Figure 5.6b) approaches a plateau after 6 h which corresponds to the same trend for the catalyst acid/base properties, acrolein selectivity and coke. This also proves that Lewis acid sites do not contribute to acrolein selectivity.

5.5 Conclusions

Commercial biofuels manufacture from vegetable oil or animal fat has increased the supply of glycerol and subsequently, its price has dropped five fold (or more) in some regions of the world. Glycerol is an attractive feedstock to produce acrolein. Obstacles to commercialize the glycerol-to-acrolein process relate to achieving high selectivity, reducing the by-products and catalyst deactivation but also finding enough supply of glycerol at a price low enough. WO_3/TiO_2 catalyst selectively dehydrates glycerol to acrolein at a selectivity of 73 % in a fluidized bed at 100 % conversion even though coke formed on the surface. It increased steadily from 3 % to the steady state value after 6 h on-stream. Concurrently, the selectivity of acetone and acetaldehyde decreased : acetone selectivity dropped from 10 % in the first hour to zero after 14 h. The acetone selectivity was related to the hydrogen transfer reaction. As less coke formed the acetone and propanal selectivity decreased. In the first hour coke selectivity was 50 % and it dropped to 9 % after 14 hour. Coke covers the catalyst active sites that catalyse the parallel reactions and for this reason acrolein selectivity increased with time-on-stream. After 6 h both the coke rate and acrolein selectivity were constant. The Lewis and Brønsted sites reduced with reaction time based on FT-IR pyridine analysis. Strong acid sites remained constant after 14 h. This could be related to the continuous catalyst regeneration by molecular oxygen or because of coke formation on basic sites to medium acidic sites before reaching the strongly sites. Strong acid sites survive during the reaction time whereas by-products formation decreased with decrease in medium acidic and basic sites of the catalyst.

CHAPTER 6 ARTICLE 3 : COKE PROMOTERS IMPROVED ACROLEIN SELECTIVITY IN THE GAS-PHASE DEHYDRATION OF GLYCEROL TO ACROLEIN

Marjan Dalil, Mahesh Edake, Camille Sudeau, Jean-Luc Dubois and Gregory S. Patience

6.1 Abstract

Commercial processes partially oxidize propylene to acrolein but glycerol can replace the petroleum derived feeds as a bio-feedstock for this large volume specialty chemical. Metal oxides, particularly acid catalysts, dehydrate glycerol at elevated temperature. We tested phosphotungstic acid (HPW) loaded on titania catalysts (a weight fraction of 10, 20 and 30 %) at 280 °C in a fluidized-bed reactor. With time-on-stream, the acrolein selectivity increased and the coke selectivity decreased. As much as 85 % of the glycerol formed coke in the first hour and less than 20 % acrolein. Liquid feed directly sprayed on the catalyst bed and the reaction occurred in the gas phase.

We also compared the performance of pure titania supports with respect to the acrolein selectivity. Acrolein selectivity was 13 % higher on TiO_2 with an average pore diameter of 17.3 nm versus the TiO_2 support with a pore of 5.6 nm. Three times more coke formed on the small pore diameter TiO_2. We treated the catalyst with hydrogen rich coke promoters - tetralin and decalin - to passivate non-selective catalytic sites. This treatment increased acrolein selectivity from 10 % to 30 % in the first 30 min of reaction. As expected, they hydrogenated the intermediates to undesired compounds including acetone and propanaldehyde (propanal).

This article has been submitted to the Applied Catalysis A : General journal.

6.2 Introduction

Renewable feedstocks could replace petroleum to produce energy and chemicals. Researchers and industries endeavour to develop sustainable processes based on bio-resources. Adding biodiesel to petro-diesel is a first step to substitute petroleum fuel with bio-based fuels. Microalgea (Menetrez, 2012) and waste cooking oil (Maddikeri et al., 2012) are possible large volume sources for biodiesel synthesis.

Glycerol is the main co-product of biodiesel synthesis (a mass fraction of 10 %) and with the growing biodiesel industry has overwhelmed the market resulting in low prices. Due to its

multifunctional structure, glycerol is widely applied in various industries such as food, cosmetics, pharmaceuticals and plastics. However, crude glycerol contains NGOM (non-glycerin organic matter), water, methanol and traces of fatty acids and must be purified. Distillation is an extra step in refining and thereby increases the cost of the process. Acrolein is versatile intermediate for the chemical industry and is a feedstock for acrylic acid and its esters, glutaraldehyde, methionine, polyurethanes and polyester resins (Etzkorn et al., 2000; Council, 1981; Bowmer and Smith, 1984). The principal commercial process to synthesize acrolein relies on propylen as a feedstock and multi-tubular fixed bed reactors. Mixed-metal oxide containing Mo and Bi catalyzes this reaction at 250 °C - 400 °C (Cornils, 2004; Callahan et al., 1970).

Due to the availability of glycerol from biodiesel synthesis, dehydration of glycerol to acrolein is a potential economic alternative to propylene oxidation. The early studies of glycerol dehydration was patented in 1930 by Kahlbum (1930). The yield of acrolein was 75 % over lithium phosphate catalyst.

Synthesis of acrolein from glycerol has been studied in both gas and liquid phase reactions. Generally, gas-phase dehydration is preferred due to the environmental and operational issues of liquid-phase reactions.

Several classes of catalysts such as zeolites, mixed-metal oxides and heteropoly acids, dehydrate glycerol to acrolein. Brønsted acids are active and selective in acrolein synthesis, but deactivation of the catalyst is the major drawback in this case. Dubois et al. (2006a) suggested in-situ regeneration of the catalyst by co-feeding of molecular oxygen. They observed that molecular oxygen not only decreased the coking rate, but also improved the acrolein selectivity. Additionally, the catalyst maintained its activity and reduced the by-products such as acetol and phenol. Few studies have focused on the effect of coke formation on catalyst performance. Erfle et al. (2011) analyzed used vanadium based catalysts by FTIR spectroscopy and concluded that coke forms on Brønsted sites. This conclusion was confirmed by Suprun et al. (2009) who evaluated carbon deposits on phosphate catalysts. They also observed that higher reaction temperatures and small pore diameter of the catalyst lead to further carbon formation. Pethan Rajan et al. (2014) characterized spent VPO by TPD-NH_3 and FTIR-pyridine. The results showed that the acidity and Brønsted acidic sites of the catalyst decreased after 40 h time-on-stream. Consequently, the conversion and selectivity of the catalyst decreased. Acrolein selectivity of coked WO_3/TiO_2 catalysts are higher than on fresh catalyst and it remains active even after 6 h reaction time (Dalil et al., 2015). Partial regeneration of the catalyst improved the selectivity of acrolein and less coke formed in the early stages of reaction.

Here, we tested three loadings of tungsten oxide over large pore and narrow pore titania sup-

ports. We focused on the effect of pore diameter on acrolein, by-products and coke selectivity. We treated catalyst with tetralin and decaline as coke promoters to understand the impact of coke on secondary products.

6.3 Methodology

6.3.1 Catalyst preparation

We prepared catalysts with a mass fraction of 10, 20 and 30 % phosphotungstic acid (HPW) on TiO_2 samples on large pore and narrow pore titania supports provided by ARKEMA (Hombikat 11010—HKT-1 and Hombikat 11060 — HKT-2). A LA-950 (Horiba) laser diffractometer measured the particle size distribution (PSD) of the pure titania. The mean particle size of the supports were 95 µm and 106 µm for the HKT-1 and the HKT-2 samples, respectively. The HPW (Nippon Inorganic Color & Chemical Co., Ltd.) dissolved in 10 mL of distilled water in a rotavapor flask (BUCHI R-210). We subsequently loaded 10 g of titania to the flask. The rotavapor mixed the slurry for 2 h at room temperature. We applied a 60 mbar vacuum and heated the flask to 60 °C. The sample then dried for 10 h at 120 °C and calcined for 3 h at 500 °C (Dubois et al., 2013).

6.3.2 Characterization techniques

An Autosorb-1 porosimeter (Quantachrome) measured the N_2 adsorption/desorption isotherms at −196 °C. We assigned the surface area based on the Multi point BET (Brunauer, Emmett and Teller) equation and the pore size and pore volume of the samples on the BJH (Barrett-Joyner-Halenda) equation. A TA-Q50 thermogravimetric analyzer measured the weight loss as a function of temperature. A Platinel II thermocouple placed 2 mm above the sample pan monitored the temperature. For each run, we loaded 20 mg of sample to a 10 µm aluminum crucible. The resolution and accuracy of the balance was 0.1 µg and > ±0.1 %. A Philipps Xpert diffractometer scanned samples at room temperature (Cu anode, K = 0.154 06 nm recorded the patterns at 50 kV voltage and 40 mA current) and produced and the diffraction pattern (XRD) from which we deduced the HPW/TiO_2 crystal phases. The diffraction angle (2 theta range) varied between 20° to 90° at a 0.020° step size. A JEOL JSM-7600TFE Field Emission Scanning Electron Microscopy imaged the samples. The samples were mounted on an aluminium sample holder containing a double graphite adhesive layer to hold the samples. We used both a LEI (lower secondary electron image) and LABE (Low-Angle Backscattered Electron) detectors.

6.3.3 Experimental

Catalytic reaction set-up

HPW/TiO_2 catalysts dehydrated glycerol in a a quartz fluidized-bed reactor. The reactor height was 52 mm and its inner diameter was 8 mm. A 20 µm ceramic frit distributed the gas uniformly across the reactor. Fluidized-beds are ideal reactors to regenerate catalysts : the high solids mixing rate minimizes thermal and concentration gradients. In fixed bed reactors, coke may build up on catalysts preferentially at the entrance of the reactor and in the central region, which complicates interpreting reaction kinetics (Kaarsholm et al., 2007). A three-zone furnace heated the reactor and a thermocouple 100 mm above the distributor monitored the bed temperature (Figure 6.1).

A mixture of argon and oxygen fluidized the catalyst. To determine the minimum fluidization velocity (U_{mf}), we recorded the pressure drop at ascending and descending gas flow rates (Figure 6.2a). The U_{mf} of all samples was 1.4 $cm\,s^{-1}$. The total gas velocity was held three times higher than this value for all the experiments.

The molecular oxygen (a mixture of 21% O_2/Ar) co-fed with glycerol maintains catalyst life time and increases acrolein selectivity while decreasing aromatic and hydrogenated by-products (Dubois et al., 2006a; Dalil et al., 2015).

An HPLC pump injected the glycerol aqueous solution (28 wt% glycerol in water, flow rate : 0.5 $ml\,min^{-1}$) directly into the fluidized-bed of catalyst. The liquid feed entered the reactor through a 1.6 mm nozzle without preheating. A flow of argon assisted the liquid feed to enhance the quality liquid spray. The volumetric ratio of argon/glycerol solution was constant (200) for all the experiments. To ensure that the droplets were uniform, we tested the injector with a series gas/liquid ratios. Large droplets agglomerate the catalyst and block the injector. The flow of Ar in injector should be high enough to spray the liquid feed into the catalyst bed but too high flow rate attrits the catalyst.

The effluent gases from the reactor passed through two quenches to trap all the condensable compounds. A Hanna electrical conductivity meter monitored the product quench (first quench) ; the conductivity is related to the concentration of ionizable solutes. Liquid products trapped in the our quench and their concentration increased with reaction time. Using the conductivity meter we were able to monitor and follow the production rate by reaction time (Figure 6.2b). A Bruker GC (equipped with Hyesep Q, Molsieve 5A and FFAP columns) analyzed the gas and liquid products (Figure 6.1).

The conversion of glycerol ($X_{gly.}$) as well as products selectivities (S_p) were calculated as

follows ;

$$X_{gly.}(mol\%) = \frac{n^{in}_{gly.} - n^{out}_{gly.}}{n^{in}_{gly.}} \times 100 \tag{6.1}$$

$$S_p(mol\%) = \frac{n_p}{n^{in}_{gly.} - n^{out}_{gly.}} \times \frac{z_p}{z_{gly.}} \times 100 \tag{6.2}$$

Where : $n^{in}_{gly.}$ and $n^{out}_{gly.}$ are the molar flow rates of glycerol at reactor entrance and exit. In equation 6.2, n_p is the molar stream of each product. z_p and $z_{gly.}$ represent the number of carbon atoms of the products and glycerol.

6.4 Results and discussion

6.4.1 Catalyst characterization

N_2 adsorption/desorption

The surface area of pure HKT-1 TiO_2 was $71\,m^2\,g^{-1}$, whereas the average pore diameter and total pore volume were 17 nm and $0.22\,cm^3\,g^{-1}$. The HKT-2 TiO_2 surface area was $148\,m^2\,g^{-1}$ with the same pore volume. The average pore diameter, however, was three time smaller than HKT-1 titania (5.6 nm). The tungsten loading and calcination affected the physiochemical properties of TiO_2 : both surface area and pore volume dropped as the tungsten loading increased : tungsten covers the surface and partially fills pores. These calcined samples were lower still. The surface area of TiO_2 dropped by 70 % for HKT-1 and by 40 % for HKT-2, when loaded with 30 % HPW and calcined (Table 6.1). Pore volume also decreased by 80 % and 40 % for HKT-1 and HKT-2, respectively but the pore diameter remained constant. Calcination impacts the surface area and pore volume of the catalysts due to the changes in phases or oxidation states.

Table 6.1 Textural properties of various HPW/TiO_2 catalysts

Sample	SA ($m^2\,g^{-1}$)		v_p ($cm^3\,g^{-1}$)		d_p (nm)	
	not-calcined	calcined	not-calcined	calcined	not-calcined	calcined
Pure TiO_2 (HKT-1)	71	-	0.22	-	17	-
10 wt% HPW/TiO_2	68	64	0.19	0.17	17	17
20 wt% HPW/TiO_2	38	33	0.12	0.10	17	17
30 wt% HPW/TiO_2	25	22	0.08	0.05	17	17
Pure TiO_2 (HKT-2)	148	-	0.20	-	6	-
10 wt% HPW/TiO_2	144	137	0.20	0.18	5	5
20 wt% HPW/TiO_2	121	119	0.18	0.15	5	5
30 wt% HPW/TiO_2	92	88	0.14	0.12	5	5

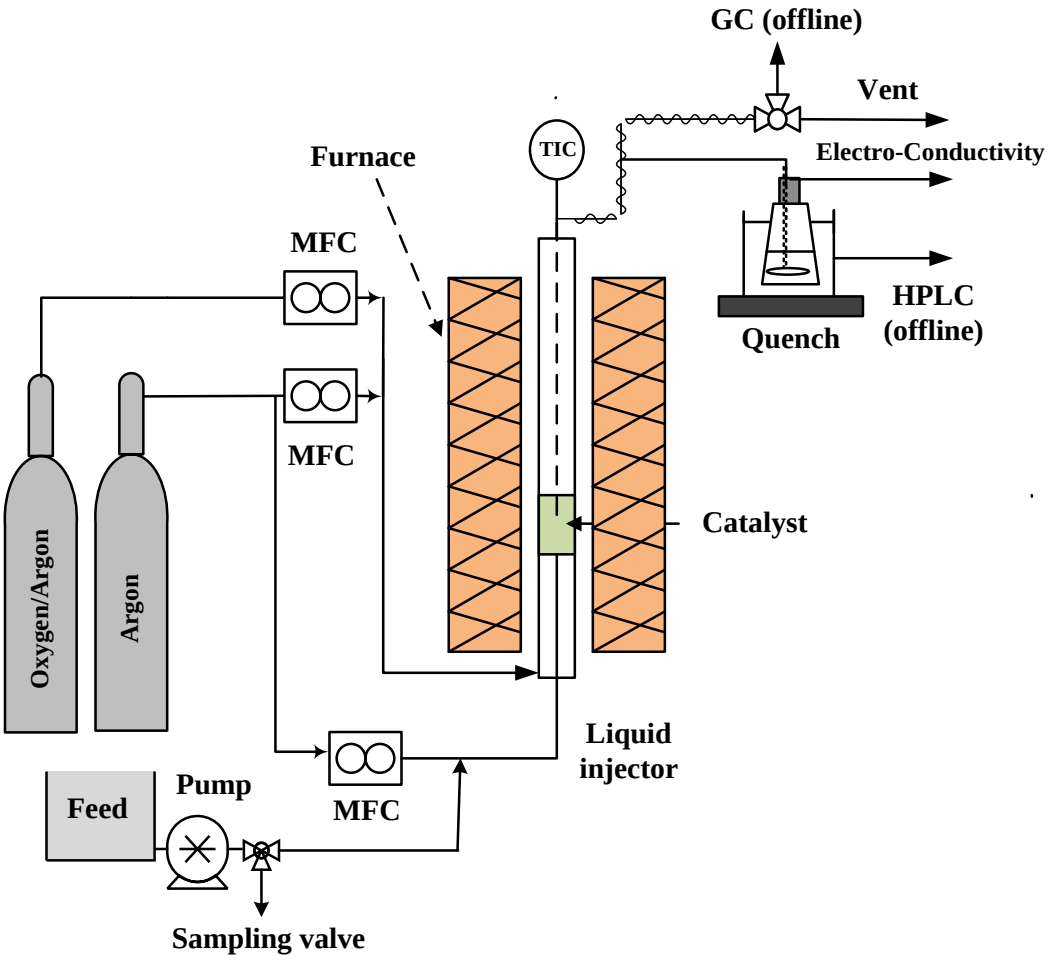

Figure 6.1 Diagram of experimental set-up for dehydration of glycerol

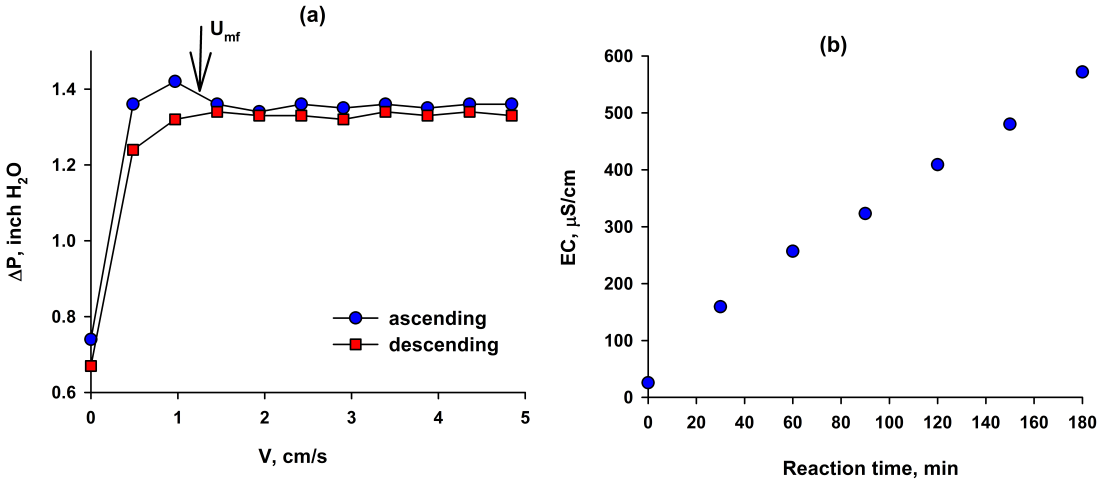

Figure 6.2 (a) Minimum fluidization graph, (b) concentration of product mixture increased as reaction continued

X-ray diffraction

The X-ray diffraction patterns of fresh TiO_2 (HKT-1, HKT-2) and 30 % HPW/TiO_2 suggested that the synthesized catalysts are crystalline (Figure 6.3). All samples exhibited characteristic main relative peaks (101, 004, 200, 211, 204) of the anatase form of TiO_2. We attributed the peaks at 23.4° and 33.4° to crystalline tungsten oxide peaks in 30 %HPW/TiO_2 (HKT-1). 30 %HPW/TiO_2 (HKT-2) catalyst did not show characteristic peaks of W oxide. This could be explained by the higher dispersion on this high surface area support (Table 6.1). Yang et al. (2005) recorded the X-ray diffraction patterns of HPW/TiO_2 with different loadings (0-40 %). They did not report any difference in the patterns of pure titania and the samples when the tungsten content was less than 30 %. The peaks related to the crystalline tungsten oxide appeared when the loading increased to 40 %.

Morphology - FESEM

The high magnification images of the uncalcined and calcined HPW/TiO_2 (FE-SEM) show that they are spheroidal (Figure 6.4) and their diameter varied between 80 µm - 120 µm. The surface was rough. Calcining the catalyst improves the catalytic activity and may distribute the HPW over the TiO_2 since fewer micro-domains of HPW are present on calcined samples (white dots on spheres in Figure 6.4). Catalyst assemblies were closely packed and marginal cracks appeared on the grain surfaces of the calcined samples. The cracks might form due to

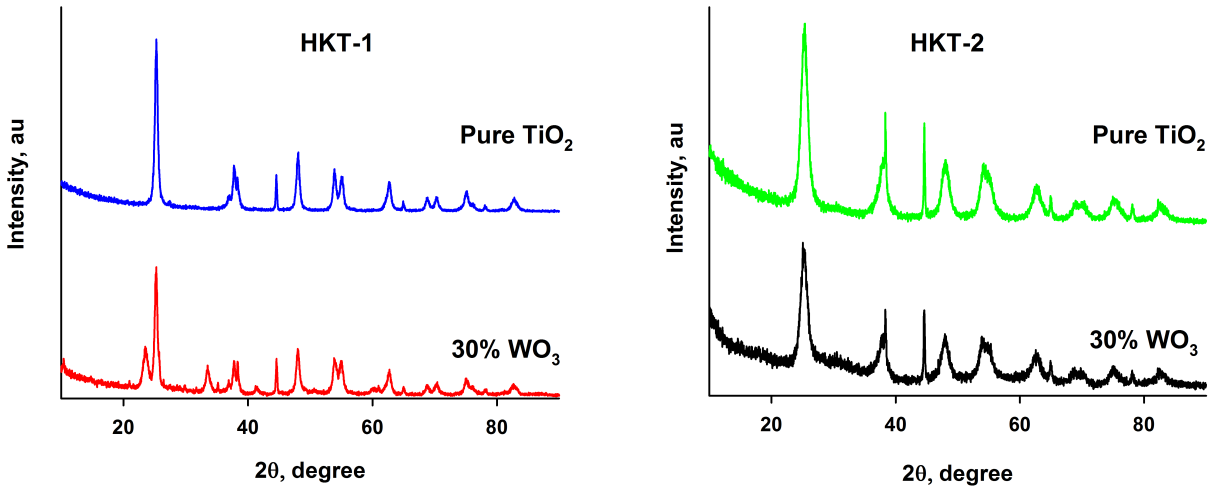

Figure 6.3 XRD patterns for pure titania and 30 % loading of HPW on HKT-1 and HKT-2 supports

the high capillary pressure generated during the impregnation process that manifest themselves when the catalyst is heated. The cracks were less visible on fresh catalyst which may have formed during spray drying.
Energy dispersive X-ray spectroscopy (EDX) confirmed the presence of W and Ti elements in the calcined catalysts (Figure 6.5).

6.4.2 Catalytic reaction over HPW/TiO_2 samples

We tested the performance of all the catalysts to determine the effect of tungsten loading on product selectivity. We loaded the reactor with 1.5 g of catalyst and heated the catalyst bed to 280 °C. The molar ratio of the gas feed was : glycerol/O_2/H_2O/Ar : 0.1/0.01/0.25/0.33. The GC analyzed both liquid and gas samples that we collected every 30 min.

Effect of HPW loading on acrolein selectivity

Every catalyst containing tungsten converted all the glycerol, even in the first 30 min. However, the conversion of glycerol over pure HKT-1 and HKT-2 was only 65 % and 54 %, respectively. Both titania supports, containing 20 % HPW, produced more acrolein than

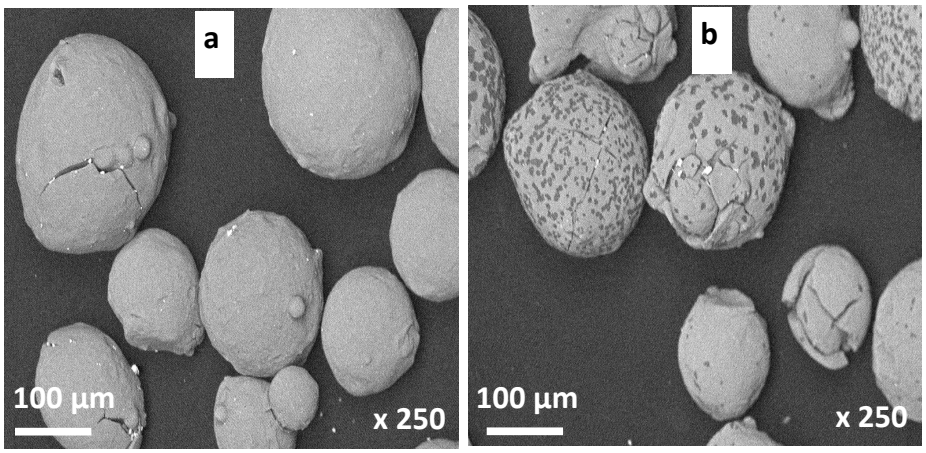

Figure 6.4 FE-SEM images of (a) uncalcined and (b) calcined 30 % HPW on HKT-1 supports

10 % and 30 % catalysts and the maximum acrolein selectivity was 48 %, (20 % HPW on HKT-1 titania). The lowest acrolein yield, on the other hand, was over pure titania samples (Figure 6.6). Pure HKT-1 and HKT-2 titania produced only 8 % and 6 % acrolein.

Low glycerol conversion and acrolein selectivity over pure titania catalysts is attributed to the presence of basic and Lewis acid sites in TiO_2 (Stosic et al., 2012). Lewis sites on the surface of pure TiO_2 may react with steam and generate Brønsted sites (Alhanash et al., 2010). Acrolein is formed over strong Brønsted sites (Benjamin et al., 2010; Alhanash et al., 2010; Stosic et al., 2012). Impregnating HPW over pure titania produced Brønsted sites (Stosic et al., 2012) which favour acrolein selectivity. Brønsted acid protonates the central hydroxyl group of glycerol to release a water molecule and a proton from glycerol. The resulting intermediate, 3-hydroxypropanal, further dehydrates to acrolein (Figure 6.7).

On pure titania surface, basic sites control the reaction pathway. To improve the catalyst, not only Brønsted sites should be available on the surface, but also the concentration of HPW species should be high enough to cover the non-selective sites of the support. Stosic et al. (2012) established a correlation between the number of asic sites of the catalyst and acrolein selectivity. According to SO_2 adsorption results, as the number of basic sites increased, the selectivity of acrolein decreased. 10 wt% tungsten was insufficient to passivate the non-selective sites so more tungsten was required. On the other hand, adding too much tungsten will form HPW crystals and thereby reduce acrolein selectivity.

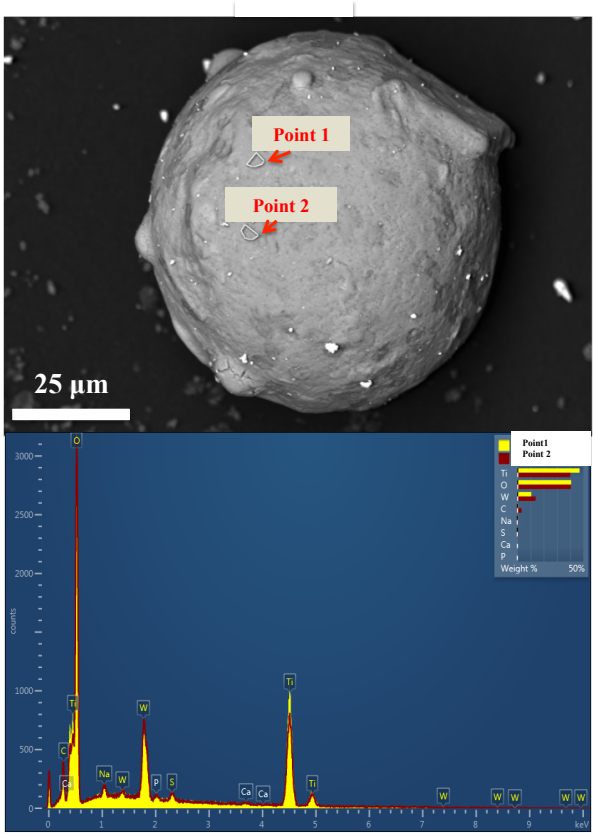

Figure 6.5 Elemental composition of 30 % HPW/TiO_2 catalyst

Effect of tungsten loading on by-products

The major by-products were acetol, acetaldehyde, formic acid, propanal and acetone. The selectivity of acetol decreased in order of : TiO_2 > 10 % > 20 % > 30 % Figure 6.8). Selectivity towards acetol was higher when pure titania catalyzed the reaction. It was 9 % for HKT-1 and 11 % for HKT-2 titania. Adding 10 % HPW to titania, dropped the selectivity to 3 % (Table 6.2). The acid/base properties of titania account for the differences in glycerol conversion and product distribution.
Acetol could be formed over basic sites of titania (Stosic et al., 2012). A possible route for the reaction over basic sites starts with the dehydration of terminal hydroxyl groups resulting in the formation of enol intermediate, which can further undergo rapid rearrangement to acetol (Stosic et al., 2012).

Effect of TiO_2 support on product distribution

The activity of the HKT-1 titania sample (large pore) was higher than that of HKT-2 (smaller pore) (Table 6.2). The performance of 20 wt% samples were compared in order to study the effect of titania support in acrolein production. The acrolein selectivity increased with time-on-stream (Dalil et al., 2015). Catalysts prepared with HKT-1 were more selective towards acrolein compared to those based on HKT-2 and after 3 h, they produced 10 % more acrolein(44 % for HKT-1 vs. 34 % HKT-2). The formation of by-products did not vary significantly as we changed the TiO_2 support. The higher acrolein selectivity could be attributed to the difference of the average pore diameter of the two titania supports (Table 6.1) and confirms the previous work (Dubois et al., 2013; Okumura et al., 2013).

Table 6.2 Selectivity of the products in dehydration of glycerol at 280 °C after 3 h time-on-stream.

Sample	Conversion	$S_{acrolein}$	$S_{propanal}$	$S_{acetone}$	$S_{acetaldehyde}$	$S_{formic\ acid}$	S_{acetol}
Pure TiO_2 (HKT-1)	65.0	8.5	1.5	3.3	3.7	3.2	9.5
10 wt% HPW/TiO_2	96.0	41.3	1.0	2.3	1.6	2.2	3.3
20 wt% HPW/TiO_2	100	48.3	2.0	2.0	2.0	1.4	1.8
30 wt% HPW/TiO_2	100	41.4	1.5	2.0	2.4	1.6	1.5
Pure TiO_2 (HKT-2)	54.2	6.0	2.6	3.7	3.0	3.2	11.7
10 wt% HPW/TiO_2	100	33.0	1.7	1.7	2.2	2	2.9
20 wt% HPW/TiO_2	100	35.3	2.5	1.0	2.6	1.8	1.2
30 wt% HPW/TiO_2	100	31.6	2.5	1.0	2.1	2	1.3

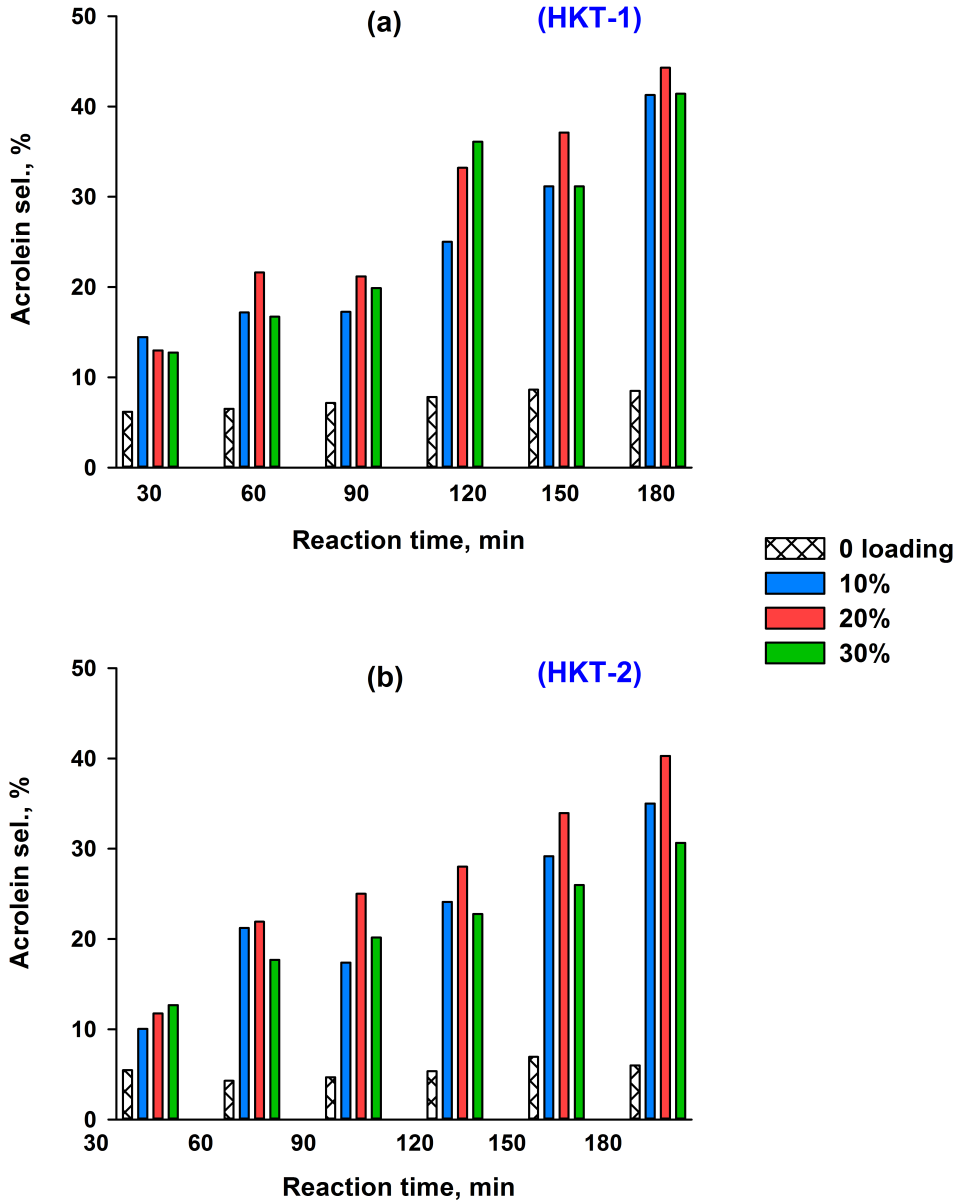

Figure 6.6 Selectivity of acrolein over 10 %, 20 % and 30 % of HPW on (a) HKT-1 and (b) HKT-2 titania supports

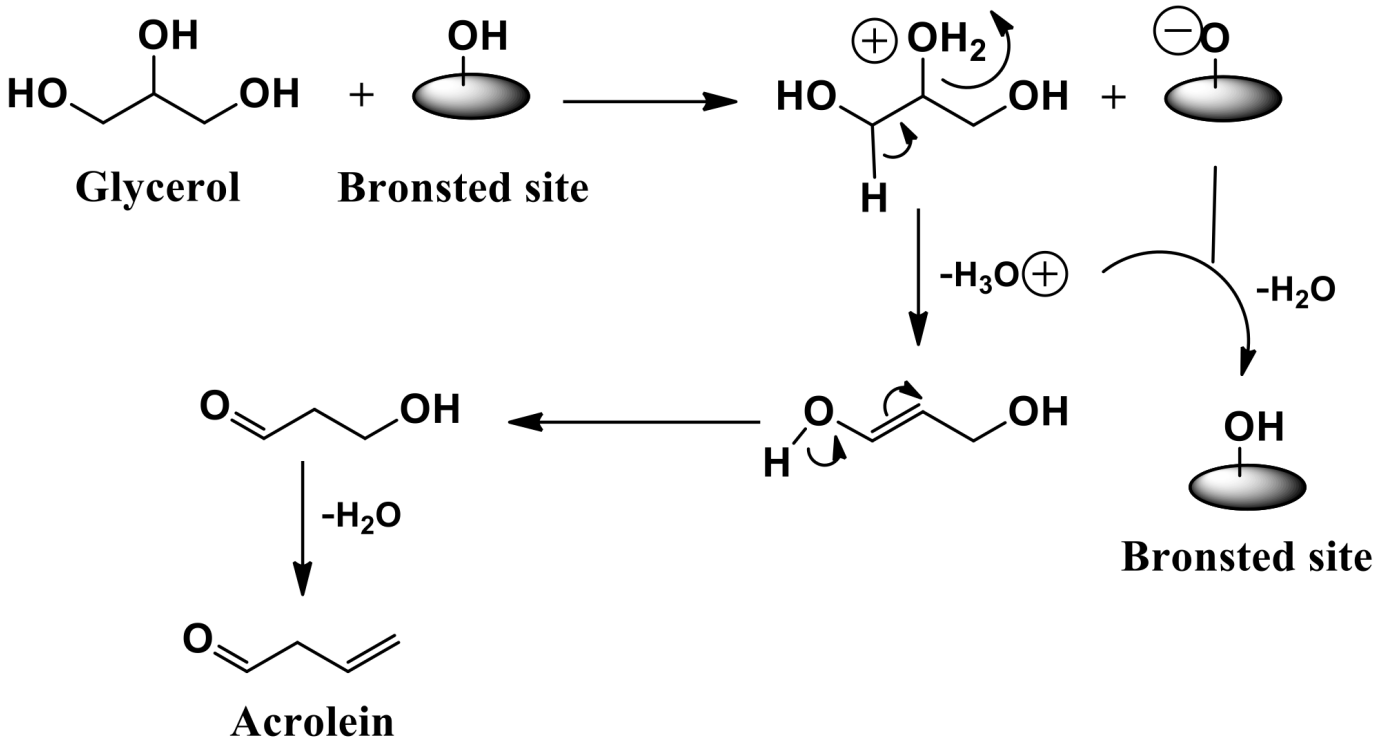

Figure 6.7 Mechanism of glycerol dehydration over Brønsted sites proposed by Kinage et al. (2010)

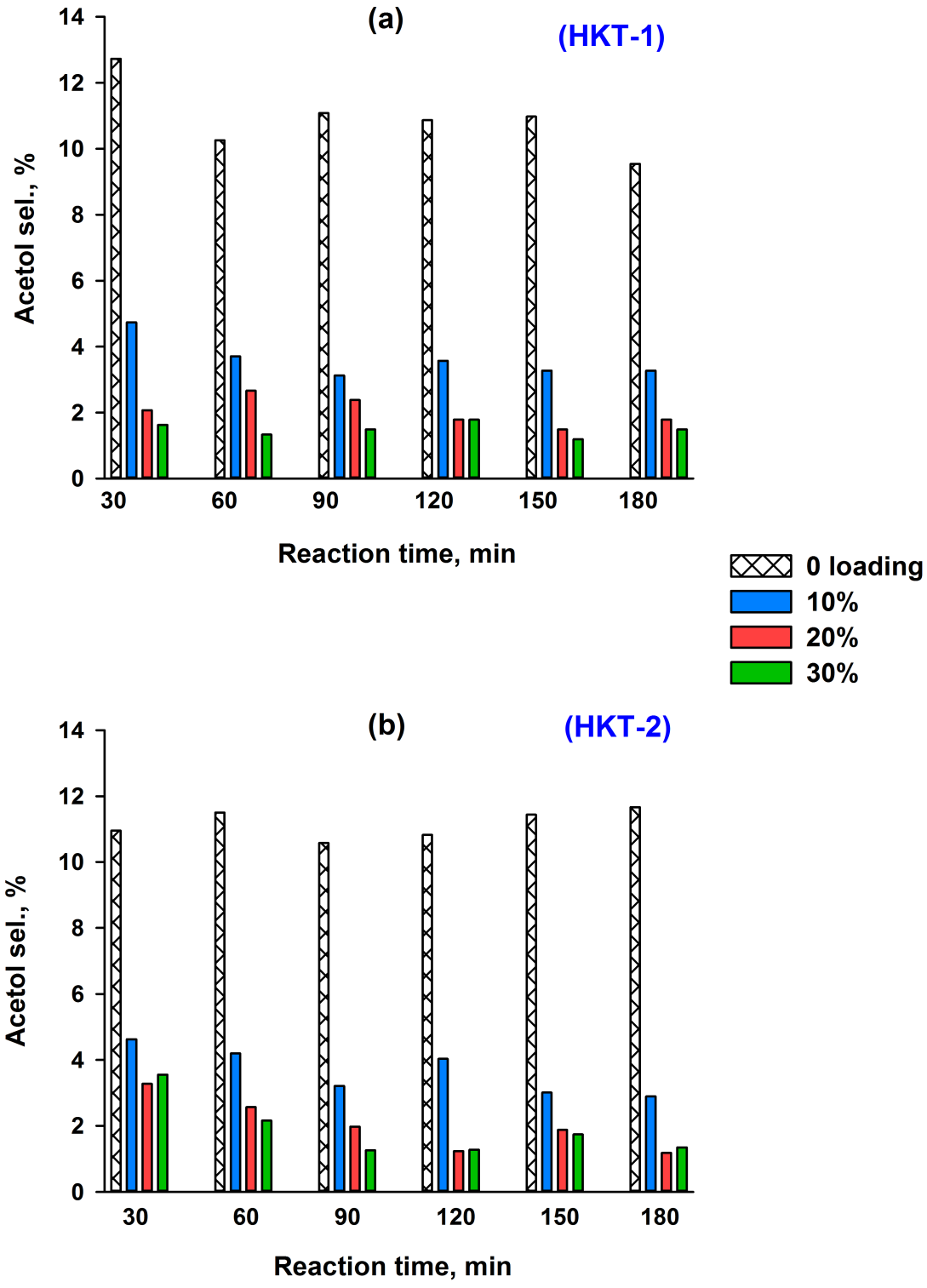

Figure 6.8 Selectivity of acetol over 10 %, 20 % and 30 % of HPW on (a) HKT-1 and (b) HKT-2 titania supports

The pore diameter of HKT-1 is three times larger than that of HKT-2. Therefore, HKT-1 provides more space within its pores for the reactants and the active phase metal to react. Tsukuda et al. (2007) and Atia et al. (2008) reported the same effect of pore size distribution on acrolein yield for silica heteropoly acids.

Coke

To quantify the mass of coke on the catalyst surface, we heated the sample in a TGA and measured the weight loss (Dalil et al., 2015). Coke deposition after 3 h was 0.5 wt% for pure HKT-1 and 0.7 wt% for HKT-2 ; it reached to 3 wt% and 8 wt%, respectively with 30 wt% tungsten. For both supports, as we increased the loading of HPW, more coke formed (Figure 6.9). According to Yang et al. (2005) and Chai et al. (2007a), HPW on pure titania increases the acidity and as a result more coke accumulates.
Coking was higher on the HKT-2 compared to than HKT-1 (Figure 6.9). Smaller pores (Table 6.1) are responsible for the higher coke levels. Glycerol can condense in the pores (capillary condensation). This is favoured when the temperature is low, pores are too narrow and glycerol concentration is rather high (28 %) (Dubois, 2014). The diffusion limitations (steric limitations) could inhibit the effective desorption of the reactants and the products in catalyst framework.

Catalyst treatment with coke promoters

During the first hour of glycerol dehydration, coke selectivity was highest and the acrolein selectivity was lowest. With time-on-stream less coke formed as well as the hydrogenated by-products such as acetone and the acrolein selectivity increased. Partially regenerated catalyst increased the acrolein selectivity from 10 % to 25 % in the first 15 min due to the coverage of the non-selective sites by coke (Dalil et al., 2015). We chose tetralin and decalin as "coke promoters" because these compounds are rich in hydrogen and carbon (Figure 6.10). We were following two objectives by coating the catalysts with decalin and tetralin ; first, to reach higher selectivity of acrolein in the initial phase of reaction and second, to see the effect of various coke promoters on product distribution.

Tetralin and decalin have similar boiling points but very different melting points. We spread 10 g of catalyst in a porcelain dish and placed it inside a desicator. In a separate plate, inside the desicator, we placed 10 g of hydrocarbon and heated the system to 120 °C in an oven. After one hour, the colour of the catalyst turned to dark grey indicating that the product

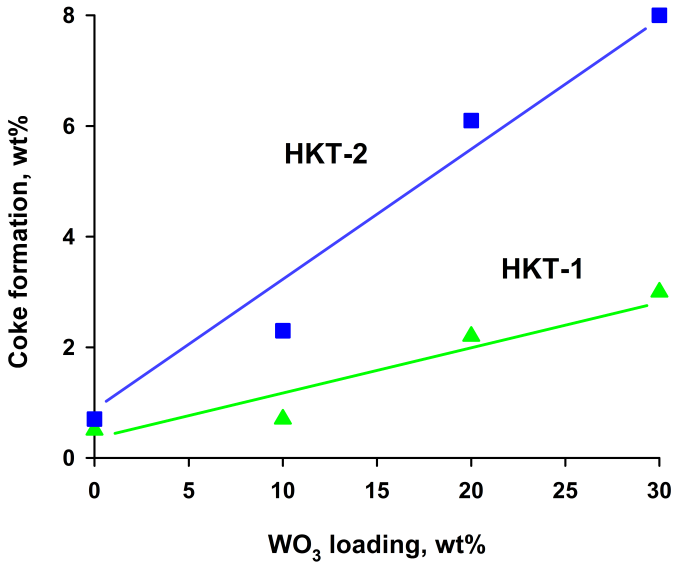

Figure 6.9 Coke deposition over different HPW/TiO_2 catalysts after 3 h. Smaller pore diameter and high loading of HPW increased the coke formation.

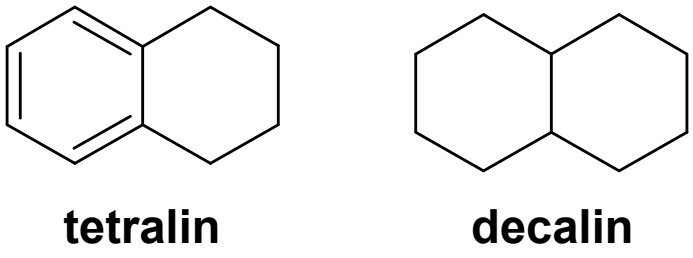

Figure 6.10 tetralin : $C_{10}H_{12}$ and decalin : $C_{10}H_{18}$ used as coke promoters to coat HPW/TiO_2 catalysts.

evaporated and adsorbed on the catalyst surface. We used three different catalysts : 20 wt% phosphotungstic acid on HKT-1 and HKT-2 titania as well as WO_3/TiO_2 (ARKEMA) catalyst.

To assure that the catalyst contained tetralin and deaclin under the reaction condition, the TGA measured the quantity of hydrocarbon deposited on catalyst. First, we heated the samples to 270 °C (ramp : 10 °C min^{-1}) with 40 ml min^{-1} nitrogen. After a 15 min isothermal hold, oxygen substituted the nitrogen and we ramped the temperature to 450 °C and measured the weight loss of the samples in TGA. At this point there was was 3.5 % to 3.9 % on the catalyst (Table 6.3) — each catalyst adsorbed about the same mass of hydrocarbon.

The performance of coated samples was compared to the original catalysts under the same reaction conditions. We loaded the reactor with 1 g of catalyst and operated at 270 °C. The temperature was purposely held low to avoid the decomposition of tetralin and decalin. Each reaction continued for 2 hour. Meanwhile, we colleected gas and liquid samples every 30 min and measured their concentration by GC.

Effect of coke promoters on acrolein selectivity

Adding coke promoters to HPW/TiO_2 catalysts increased acrolein selectivity. After 30 min, over 20 wt% HPW/TiO_2 (HKT-1) catalyst, acrolein selectivity increased from 10 % to 24 % for decalin and to 30 % for tetralin treated samples. Acrolein selectivity was 10 % for untreated 20 wt% HPW/TiO_2 (HKT-2) and reached to 30 % and to 17 % when tetralin and decalin were added, respectively. Acrolein selectivity doubled for tetralin treated WO_3/TiO_2 (ARKEMA) samples and it increased from 15 % to 21 % when decalin was used as coke promoter.

For virgin catalysts, more coke formed than acrolein and by-products at the beginning of

Table 6.3 TGA results measured the weight loss of the treated catalysts caused by the addition of tetralin and decalin

Sample	Hydrocarbon	Weight gain (wt%)
20 wt% HPW/TiO_2 (HKT-1)	tetralin	3.5
20 wt% HPW/TiO_2 (HKT-1)	decalin	3.5
20 wt% HPW/TiO_2 (HKT-2)	tetralin	3.9
20 wt% HPW/TiO_2 (HKT-2)	decalin	3.7
WO_3/TiO_2 (ARKEMA)	tetralin	3.6
WO_3/TiO_2 (ARKEMA)	decalin	3.5

reaction. With time, the selectivity of acrolein increased and the coke selectivity decreased considerably (Dalil et al., 2015). Coke builds-up on the catalyst and passivated non-selective sites. Coke promoters substituted severe coke formation in the first 30 min and the active sites of the catalyst which were selectively producing coke or by-products, were covered by tetralin and decalin, which are large molecules.

Effect of coke promoters on by-products formation

The selectivity of propanal and acetone increased over the catalysts treated with tetralin and decalin. This could be related to the high quantity of hydrogen in these compounds that become hydrogen donors. Propanal and acetone are both hydrogenated products and formed through hydrogen transfer. Acrolein hydrogenates to propanal and glycerol dehydrates to acetol. Acetol hydrogenates to 1,2-propanediol, which can further dehydrate to acetone (Figure 6.12). The selectivity of both propanal and acetone dropped with time (as the hydrogen donor capacity of the tetralin and decalin dropped) but the selectivity of acetaldehyde, formic acid and acetol was constant (Table 6.4).
These results confirm that it is important to keep some coke on the catalyst surface, and that a dehydrogenated coke is better for acrolein selectivity. Note that hydrogenated side products are more important when decalin is used instead of tetralin, since it has more hydrogen available.

6.5 Conclusions

The price of glycerol has dropped due to its overproduction from biodiesel synthesis. Commercial dehydration of glycerol to acrolein is an economic alternative to propylene oxidation

Table 6.4 Product distribution of glycerol dehydration at 2 h over coated HPW/TiO_2 catalysts.

Sample	treatment	Conversion	$S_{acrolein}$	$S_{propanal}$	$S_{acetone}$	$S_{acetaldehyde}$	$S_{formic\ acid}$	S_{acetol}
HPW/TiO_2 (HKT-1)	-	92.5	35.2	2.0	1.2	1.5	1.4	2.6
HPW/TiO_2 (HKT-1)	tetralin	90.3	50.1	4.2	4.0	2.0	0.6	3.5
HPW/TiO_2 (HKT-1)	decalin	90.0	42.0	5.5	6.0	1.0	1.5	3.0
HPW/TiO_2 (HKT-2)	-	88.6	30.4	1.0	2.1	1.0	1.8	2.5
HPW/TiO_2 (HKT-2)	tetralin	87.8	45.8	3.3	4.1	1.2	2.1	3.0
HPW/TiO_2 (HKT-2)	decalin	88.5	43.2	4.5	6.5	2.3	1.4	3.2
WO_3/TiO_2 (ARKEMA)	-	92.0	37.8	1	3.5	2.0	0.9	3.6
WO_3/TiO_2 (ARKEMA)	tetralin	92.0	49.0	2.2	6.7	2.5	1.3	3.0
WO_3/TiO_2 (ARKEMA)	decalin	89.7	42.1	4.0	7.8	2.3	1.3	2.0

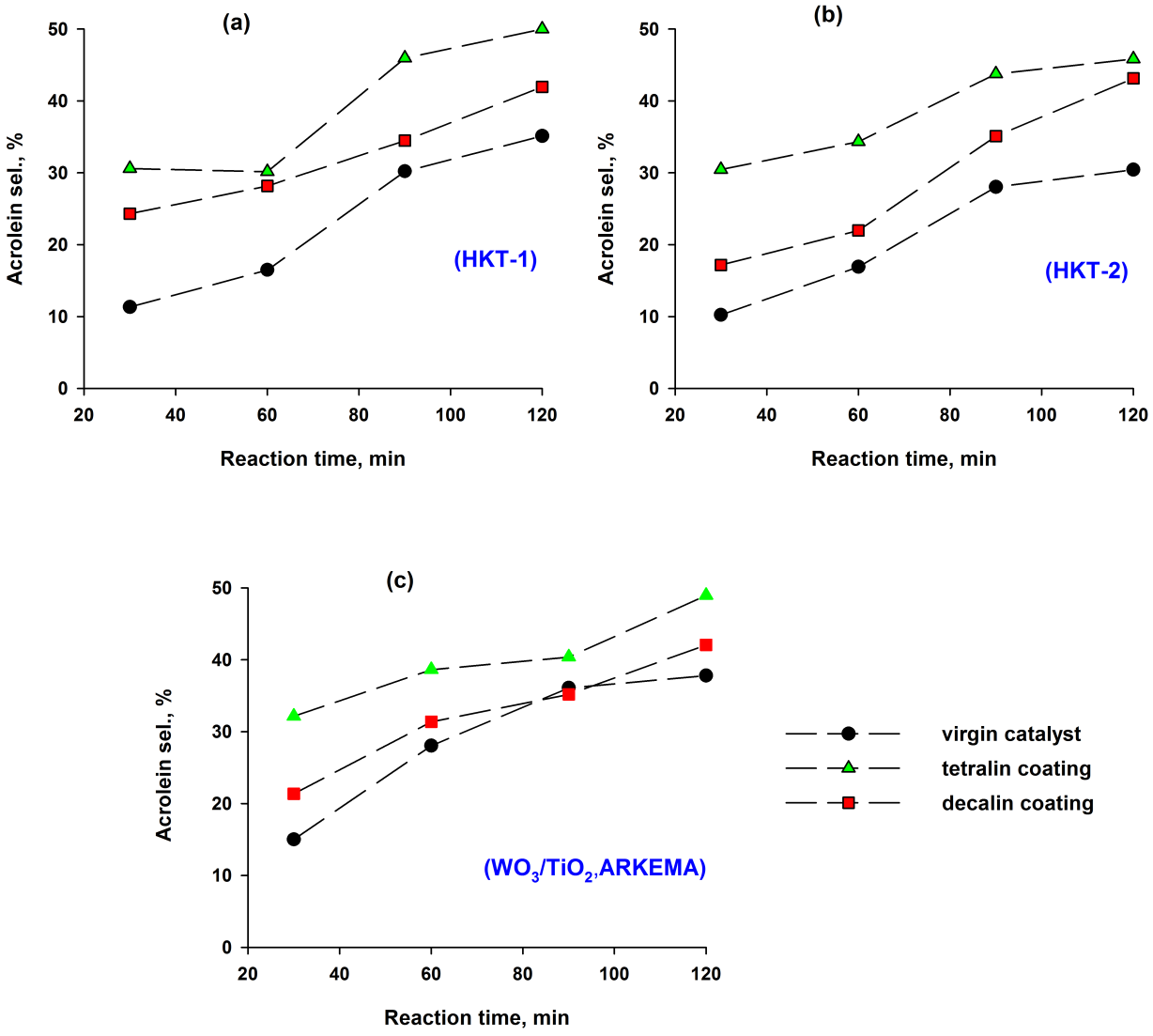

Figure 6.11 Adding tetralin and decalin to HPW/TiO_2 catalysts, increased the selectivity of acrolein at 270 °C. (a) and (b) correspond to the catalysts supported on HKT-1 and HKT-2 titanias, respectively. (●) 20 wt% HPW/TiO_2, (▲) decalin and (■) tetralin treated samples.

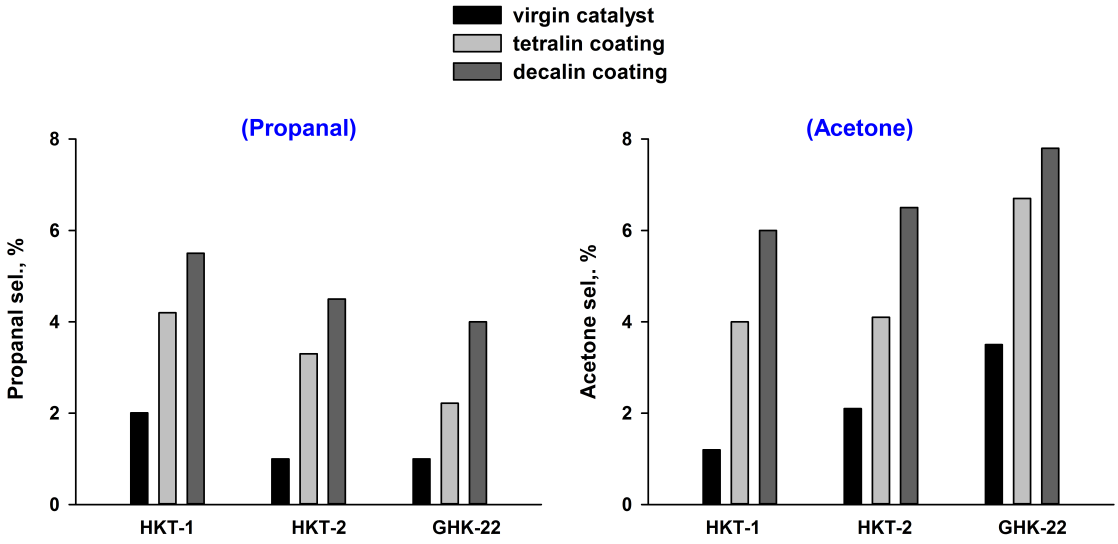

Figure 6.12 Selectivity of propanal and acetone at 2 h for virgin and coated catalysts ; addition of tetralin and decalin to HPW/TiO_2 catalysts, increased the selectivity of hydrogenated by-products at 270 °C.

if catalysts can achieve high acrolein selectivity and resist rapid deactivation. The titania support pore size affects the acrolein selectivity and coke : three times more coke formed in the small pore diameter titania due to glycerol capillary condensation. Acrolein selectivity reached 48 % with 20 wt% HPW at 280 °C. Coke passivates some non-selective sites, which we demonstrated with tetralin and decalin as coke promoters. Furthermore, selectivity increases with time-on-stream as the coke accumulates on the catalyst. In a continuous process, it is then important to keep a constant level of coke for which the fluidized-bed reactors are most suitable as they provide a homogeneous mass and heat distribution and avoid the formation of hot spots and local accumulation of coke. In conventional multi-tubular reactors, oxygen (in a regeneration step) will combust all the coke progressively from the entrance to the exit of the bed. If all of the coke combusts, the acrolein selectivity will be low when the reactor switches from regeneration to glycerol dehydration. Partially regenerating (Dalil et al., 2015), distributing the O_2 supply (Dubois, 2011) and reverse flow regeneration (Dubois, 2012) may mitigate the non-selective reactions.

6.6 Acknowledgements

The authors would like to thank Natural Sciences and Engineering Research Council of Canada (NSERC), Canadian Foundation for Innovation (CFI), CRIBIQ and Mitacs for their

financial support of this study.

CHAPTER 7 GENERAL DISCUSSION

Like any experimental study, this project also encountered various technical and analytical issues that had to be overcome in every single step. This chapter focuses on the problems faced during this thesis. According to the works done, two major categories of problems will be discussed hereafter : technical problems and analytical challenges.

7.1 Technical problems

7.1.1 Injector

Despite all advantages of the liquid injection in fluidized bed reactors such as minimizing hot spot formation, no need for external evaporation, uniform distribution of reactants, and protecting thermally sensitive compounds from degradation, there were some issues involved with this technique. A major problem was the quality of injection, which is a determining factor in long term experiments. A well-atomized liquid continuously evaporates in the catalyst bed providing a homogeneous distribution of the feed. The quality of spraying is evaluated by the size of the droplets formed at the tip of the nozzle. Large size droplets agglomerate the catalyst particles which leads to poor fluidization, blockage of the injector and physical damage to the reactor (Figure 7.1). In the case where the injector was blocked, the pressure increased and caused a back flow of the liquid in the inlet lines.To solve this problem, we used gas assisted liquid injection. The size of the droplets depends on several factors such as concentration of glycerol solution (viscosity), temperature, and gas/liquid ratio.
Before performing glycerol dehydration experiments, it was critical to examine the injection efficacy in order to avoid the aforementioned technical issues. Therefore, optimized gas and liquid flow rates as well as glycerol concentration must be obtained by qualitative tests (Appendix A).

7.1.2 Catalyst attrition

In this project, we tested the WO_3-TiO_2 catalyst (ARKEMA) which was originally designed for fixed-bed reactors. For fluidized-bed application, we crushed the pellets and sieved them to an appropriate size for fluidization. The particles in the range of $90\,\mu m < d_p < 150\,\mu m$ were collected for the reaction. Due to mechanical grinding, the powder was non-uniform in shape and suffered from low resistance to high gas velocities. Consequently, there was a noticeable attrition of solid particles during the reaction which resulted in catalyst loss,

Figure 7.1 Technical issues related to low quality liquid injection : (a) broken reactor, (b) catalyst agglomeration

injector blockage, plugging of the exit lines and MS capillary (Figure 7.2). We, therefore, had to shut down the reactor, clean up all the lines and restart the reaction. To minimize the effect of attrition, we reduced the injection gas velocity. This process was complemented by purging the reactor with a flow of 2000 mL min^{-1} of argon at 300 °C in order to exhaust the fine particles. Nevertheless, this process took 5 - 6 h until there was no more fine particles exiting the reactor. Then, we collected and weighed the catalyst to have an accurate measure of its quantity left for the reaction.

7.1.3 Analytical challenges

Most of our products were volatile compounds (acrolein, acetaldehyde, propionaldehyde and acetone) making them difficult to condense at the exit of the reactor. Volatiles were escaping with the gas products even after a two-step quench. For an accurate quantification of these compounds, we collected and analysed the gaseous products prior to condensation. We also developed a new GC system for the off-line analysis of reaction products. Heavier products such as acetol, acrylic acid and glycerol passed through the quenches and condensed. The configuration of the reactor exit was modified by adding a circulating pump in order to wash the possibly condensed products from the exit line (Figure 7.3).

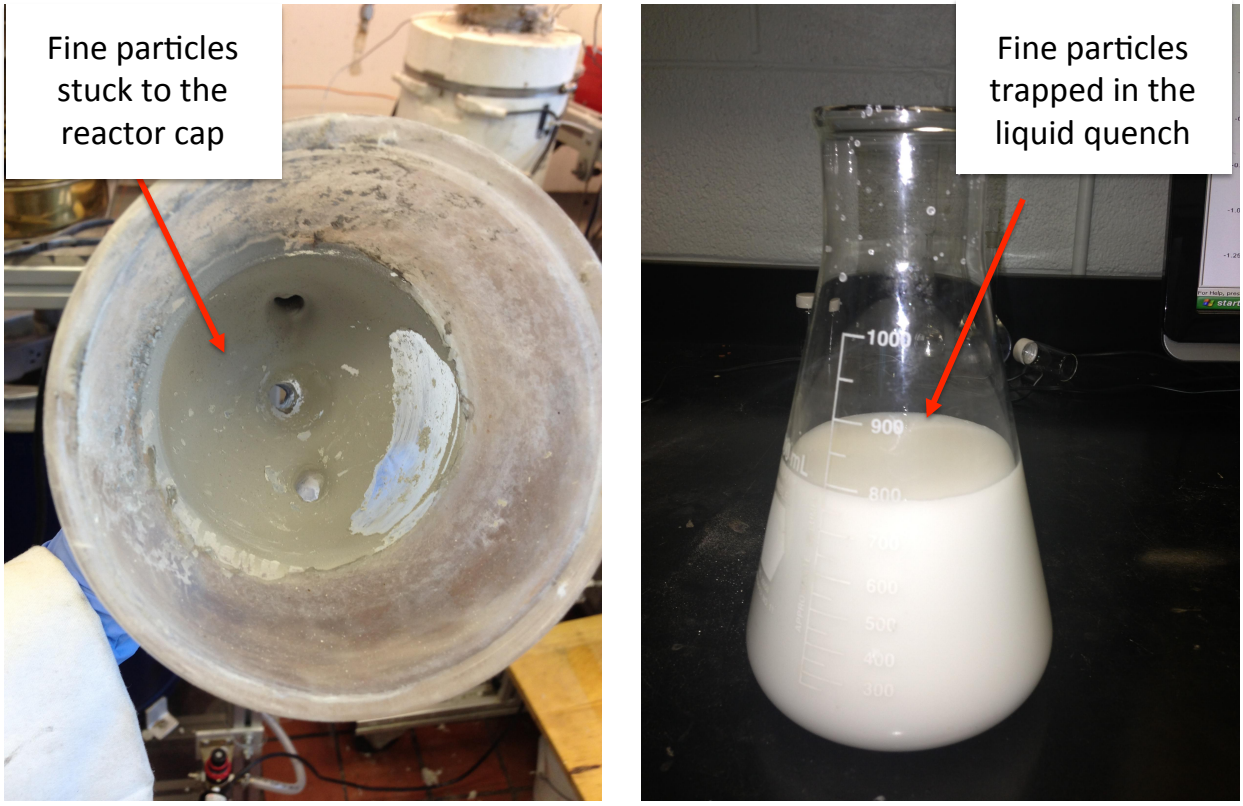

Figure 7.2 Catalyst attrited and transferred by the gas flow. Particles settled in the quench and eventually plugged the reactor exit lines.

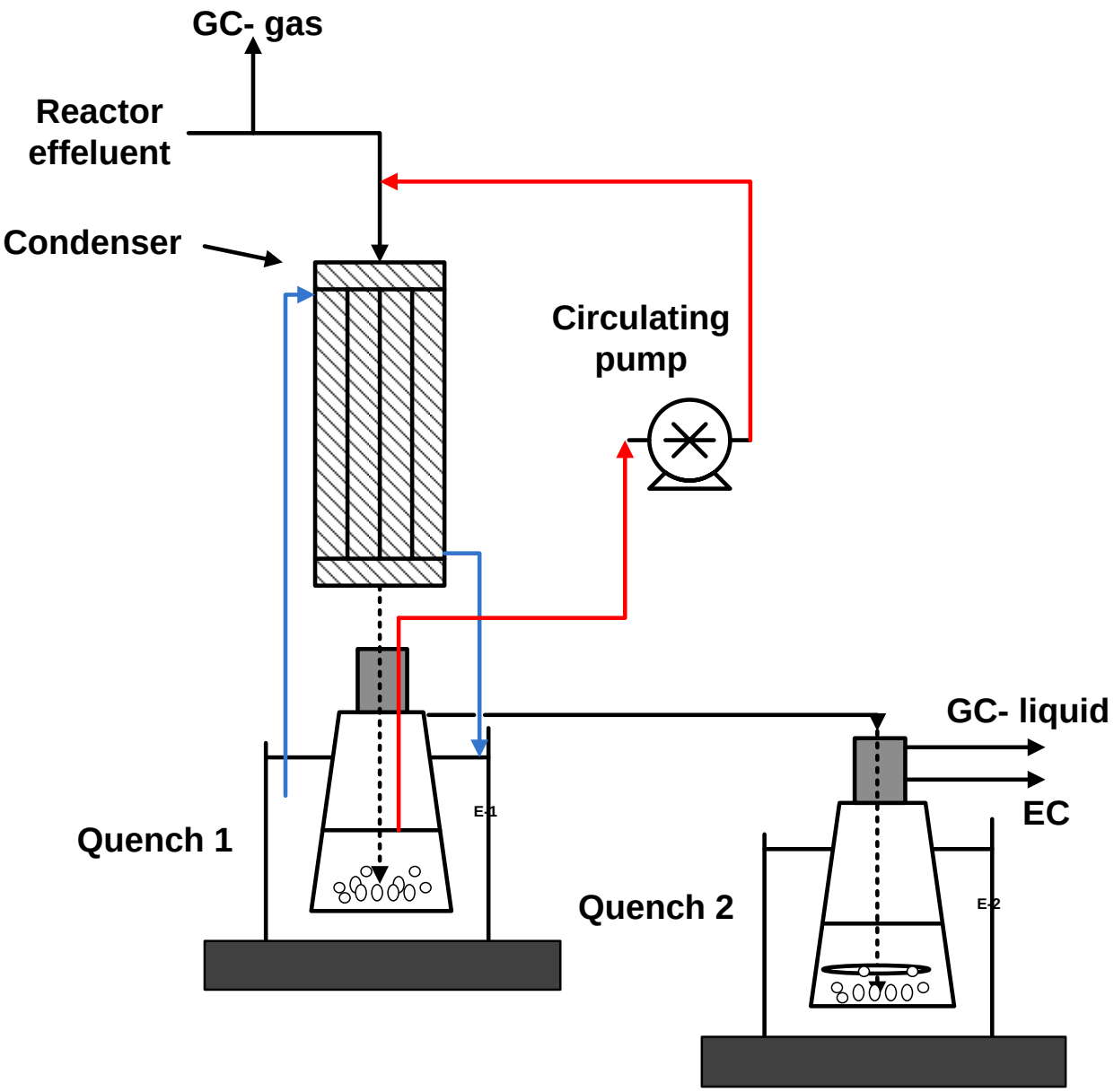

Figure 7.3 Schematic of the quenching step at the reactor exit

CHAPTER 8 CONCLUSION AND RECOMMENDATIONS

The synthesis of commercial biofuels from vegetable oil or animal fat has led to an increase in the supply of glycerol and a five fold (or more) drop in its price. Glycerol is an attractive feedstock for the production of acrolein given the right value proposition. The show-stoppers to commercialize a glycerol-to-acrolein process is attributed to achieving high acrolein selectivity, reducing the selectivity of by-products and decreasing catalyst deactivation.

The main objective of this study was to develop a process to produce acrolein via glycerol dehydration in a fluidized-bed reactor. As a result of this study, new methods were proposed to increase acrolein selectivity despite the coke formation as a major parameter affecting the product distribution.

During the 6 h time-on-stream, the selectivity of acrolein increased from 55% to 73% as the coke formation developed over a WO_3-TiO_2 catalyst. It was observed that the catalyst remained fully active in the 6 h long reaction. A first order kinetic model characterizes the rate of carbon oxidation on the catalyst surface with an activation energy of 100 kJ mol^{-1} ($R^2 > 0.997$). Applying a new approach for regenerating the catalyst increased the selectivity of acrolein from 10% to 25% in the first 30 min of the reaction. Coke formation, on the other hand, reduced from 3.6 g to 0.6 g per 100 g of the catalyst.

As the 6 h long experiment was not sufficient for the selectivity of acrolein to achieve steady state, the reaction was prolonged to 14 h in which the catalyst fully retained its activity (100% conversion). Concurrently, the selectivity of acrolein increased from 36 % in the first hour to 73 % in 14 h, while the selectivities towards acetone and acetaldehyde decreased with time. A dramatic drop in the selectivity of acetone from 10 % in the first hour to zero after 14 h was also observed. On the other hand, the selectivity towards coke deposition decreased from 50 % to 9 %. High selectivity of acetone in the first hour of the reaction was linked to the hydrogen transfer provided by coke formation. After 6 h, the reaction reached steady-state while the selectivity of acrolein remained constant. Additionally, the type of acid sites was constant after 6 h according to the FTIR pyridine analysis. The morphology and texture of the catalyst was not affected by coke deposition. Calorimetry results revealed that the basic sites of the catalyst disappeared while the number of weak and medium acid sites decreased after 2 h in the reaction time-on-stream. However, the number of strong acid sites remained constant which explains the full activity and selectivity of the catalyst at the end of the reaction.

We synthesized catalysts by impregnating 10, 20 and 30 wt% HPW on two types of titania supports. Pure titania catalysts showed the lowest selectivity towards acrolein and the

highest towards acetol. As the tungsten loading increased, selectivity of acetol decreased. On the other hand, for both supports, 20 wt% was the optimal loading for the maximum production of acrolein (48%) at 280 °C.
Pore size of titania support is an important parameter which impacts acrolein selectivity and coke formation. The selectivity towards acrolein was 35% for the small pore diameter (5.6 nm) titania which increased to 48% in the case of the larger pore size was (17.3 nm). The coke formation, on the other hand, was three times higher for the small pore diameter. Glycerol dehydration suffers from low acrolein selectivity in the first hour of the reaction, which was overcome by coating the catalysts with 3.7 wt% tetralin and decalin as coke promoters. As a results, the selectivity of acrolein increased 30% in the first 30 min. Coke promoters covered non-selective sites of the fresh catalyst and increased the acrolein selectivity. In a continuous process, it is then important to keep a constant level of coke on the catalyst for which the fluidized-bed reactors are suitable as they provide a homogeneous mass and heat distribution and avoid the formation of hot spots.

8.1 Limitations of the proposed solutions

The challenges related to the liquid-injection into a fluidized-bed reactor (already mentioned in Section 6), could be a limitation to this technique. Also, for partial regeneration of the catalyst or treatment of the catalyst with coke promoters, the quantity of the carbon retained on the catalyst surface should be consistent in all the runs. However, a protocol with accurate procedures can be devised in order to solve such issue.

8.2 Recommendations for future research

The following recommendations for future work are considered :

1. For the sake of simplicity and to earn the basic knowledge about the performance of treated catalysts, the effect of coke promoters was studied in a micro fluidized-bed reactor. Performing the reactions in 4.6 cm reactor could be of interest. Furthermore, the scale up of the process to a pilot plant would be a big step towards commercialization.
2. We used the technology of direct liquid feed injection in fluidized-bed reactor. The characteristics of the injection can be studied in order to achieve a better understanding of the injection mechanism. Developing a model to estimate the size of the droplets at the nozzle exit is required for high quality liquid injections.
3. As acid catalysts favour the production of acrolein, WO_3-TiO_2 catalyst was designed

for such purpose with a small number of basic sites. After 2 h, there was a major drop in number of basic sites. Thus, the error of calorimetric titration for basic sites was not negligible and we couldn't correlate the rate of coke formation to the number of acidic/basic sites. Acidity/basicity of the catalyst can be tuned during the synthesis process for having more basic sites available on the surface if required. With a more basic catalyst, the error of analysis would be less and we can have a better judgement on the sites responsible for coke formation.

4. In all our experiments, we used purified glycerol as feedstock. As mentioned before, glycerol obtained from biodiesel synthesis contains impurities such as salts, non-glyceric organic matter (NGOM) and water. Performing the reactions with crude glycerol and studying the effect of impurities would be another step towards the commercialization of this process if acceptable yields are obtained.

5. Mores et al. (2008) studied the process of coke formation during the MTO conversion over HZSM-5 zeolites. They suggested that this process occurs within the zeolite and at the outer surface of HZSM-5 zeolite crystals. Using a confocal fluorescence microscope, the authors observed that different laser excitation lines (488 and 561 nm) indicate a distinctive detectable coke species (Figure 8.1).
   Similarly, we tried to monitor the diffusion of carbon deposits inside the pores by fluorescence microscopy. Unfortunately, our microscope was not adjusted for such purpose and did not provide different wavelengths. Moreover, recorded images could only exhibit the changes on the surface of the catalyst and not within the pores. We suggest to prepare ultra fine cuts of the particles and use a more advanced microscope to observe the coke formation pattern. The structure and characterization of formed coke could be studied more in detail as (Guisnet and Magnoux, 2001).

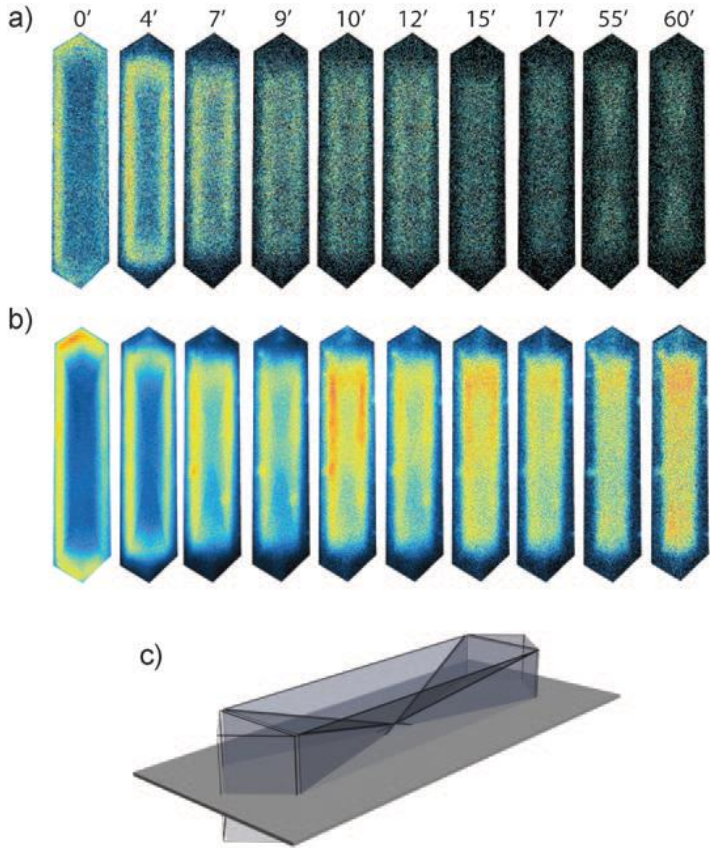

Figure 8.1 Fluorescence intensity profiles of HZSM-5 crystal during MTO reaction captured with time-on-stream at laser excitation (a) 488 nm, (b) 561 nm, and (c) Schematic representation of HZSM-5 slice at which the confocal fluorescence measurement has been performed (Mores et al., 2008).

REFERENCES

A. Alhanash, E. F. Kozhevnikova, et I. V. Kozhevnikov, "Gas-phase dehydration of glycerol to acrolein catalysed by caesium heteropoly salt", *Applied Catalysis A : General*, vol. 378, no. 1, pp. 11–18, 2010.

H. An, W. E. Wilhelm, et S. W. Searcy, "Biofuel and petroleum-based fuel supply chain research : A literature review", *Biomass and Bioenergy*, vol. 35, no. 9, pp. 3763–3774, 2011.

E. Aransiola, T. Ojumu, O. Oyekola, T. Madzimbamuto, et D. Ikhu-Omoregbe, "A review of current technology for biodiesel production : state of the art", *Biomass and Bioenergy*, vol. 61, pp. 76–297, 2014.

Y. Arita, H. Kasuga, et M. Kirishiki, "Method for regenerating catayst for dehydrating glycerine", Brevet JP2 008 110 298, 2008.

H. Atia, U. Armbruster, et A. Martin, "Dehydration of glycerol in gas phase using heteropolyacid catalysts as active compounds", *Journal of Catalysis*, vol. 258, no. 1, pp. 71–82, 2008.

A. Auroux, éd., *Calorimetry and thermal methods in catalysis*. Springer, 2013.

R. T. Baker, C. H. Bartholomew, et D. B. Dadyburjor, *Stability of Supported Catalysts : Sintering and Redispersion*. Catalytic Studies Devision, 1991.

C. Bartholomew, *Catalyst Deactivation and Regeneration*. John Wiley Sons, Inc., 2000.

D. Bavykin et F. C. Walsh, "Titanate and titania nanotubes : Synthesis, properties and applications". Royal Society of Chemistry, 2010, p. 60.

K. Benjamin, P. Sebastien, C. Mickael, L. Christine, B.-B. Virginie, R. Patrick, et D. Franck, "A long-life catalyst for glycerol dehydration to acrolein", *Green Chem.*, vol. 12, pp. 1922–1925, 2010.

H. Bi, N. Ellis, I. Abba, et J. Grace, "A state-of-the-art review of gas–solid turbulent fluidization", *Chemical Engineering Science*, vol. 55, no. 21, pp. 4789–4825, 2000.

G. Bing, S. Hangyan, S. Kangying, Z. Yaowu, et N. Wensheng, "The study of the relationship between pore structure and photocatalysis of mesoporous TiO_2", *Journal of Chemical Sciences*, vol. 121, no. 3, pp. 317–321, 2009.

K. H. Bowmer et G. H. Smith, “Herbicides for injection into flowing water : acrolein and endothal-amine”, *Weed Research*, vol. 24, no. 3, pp. 201–211, 1984.

S. Bruhns et J. Werther, “An investigation of the mechanism of liquid injection into fluidized beds”, *AIChE Journal*, vol. 51, no. 3, pp. 766–775, 2005.

W. Buhler, E. Dinjus, H. Ederer, A. Kruse, et C. Mas, “Ionic reactions and pyrolysis of glycerol as competing reaction pathways in near- and supercritical water”, *The Journal of Supercritical Fluids*, vol. 22, no. 1, pp. 37–53, 2002.

J. L. Callahan, R. K. Grasselli, E. C. Milberger, et H. A. Strecker, “Oxidation and ammoxidation of propylene over bismuth molybdate catalyst”, *Product R&D*, vol. 9, pp. 134–142, 1970.

F. Cavani, S. Guidetti, L. Marinelli, M. Piccinini, E. Ghedini, et M. Signoretto, “The control of selectivity in gas-phase glycerol dehydration to acrolein catalysed by sulfated zirconia”, *Applied Catalysis B : Environmental*, vol. 100, no. 1–2, pp. 197–204, 2010.

S.-H. Chai, H.-P. Wang, Y. Liang, et B.-Q. Xu, “Sustainable production of acrolein : investigation of solid acid-base catalysts for gas-phase dehydration of glycerol”, *Green Chem.*, vol. 9, pp. 1130–1136, 2007.

——, “Sustainable production of acrolein : Gas-phase dehydration of glycerol over Nb_2O_5 catalyst”, *Journal of Catalysis*, vol. 250, no. 2, pp. 342–349, 2007.

W. Chu, X. Yang, Y. Shan, X. Ye, et Y. Wu, “Immobilization of the heteropoly acid (hpa) $H_4SiW_{12}O_{40}$ (SiW_{12}) on mesoporous molecular sieves (HMS and MCM−41) and their catalytic behavior”, *Catalysis Letters*, vol. 42, no. 3-4, pp. 201–208, 1996.

Z. Chun-Jiao, H. Cai-Juang, Z. Wen-Gui, Z. He-Sheng, W. Hai-Long, et C. Zi-Sheng, “Synthesis of micro-and mesoporous ZSM−5 composites and their catalytic application in glycerol dehydration to acrolein”, *Studies in surface science and catalysis*, vol. 165, pp. 527–530, 2006.

A. Corma, G. W. Huber, L. Sauvanaud, et P. O’Connor, “Biomass to chemicals : Catalytic conversion of glycerol/water mixtures into acrolein, reaction network”, *Journal of Catalysis*, vol. 257, no. 1, pp. 163–171, 2008.

B. Cornils, *Handbook of Commercial Catalysts. Heterogeneous Catalysts.* By Howard F. Rase. Angewandte Chemie International Edition, 2004.

N. R. Council, *Formaldehyde and other aldehydes*. National academy press, 1981.

M. Dalil, D. Carnevali, J.-L. Dubois, et G. S. Patience, "Transient acrolein selectivity and carbon deposition study of glycerol dehydration over WO_3/TiO_2 catalyst", *Chemical Engineering Journal*, vol. 270, no. 0, pp. 557–563, 2015.

A. S. de Oliveira, S. J. Vasconcelos, J. R. de Sousa, F. F. de Sousa, J. M. Filho, et A. C. Oliveira, "Catalytic conversion of glycerol to acrolein over modified molecular sieves : Activity and deactivation studies", *Chemical Engineering Journal*, vol. 168, no. 2, pp. 765–774, 2011.

F. F. de Sousa, A. C. Oliveira, J. M. Filho, G. S. Pinheiro, M. Giotto, N. A. Barros, H. S. Souza, et A. C. Oliveira, "Metal oxides nanoparticles from complexes on sba-15 for glycerol conversion", *Chemical Engineering Journal*, vol. 228, no. 0, pp. 442–448, 2013.

J. Deleplanque, J.-L. Dubois, J.-F. Devaux, et W. Ueda, "Production of acrolein and acrylic acid through dehydration and oxydehydration of glycerol with mixed oxide catalysts", *Catalysis Today*, vol. 157, no. 1–4, pp. 351–358, 2010.

J.-F. Devaux et J.-L. Dubois, "Improved process for manufacturing acrolein/acrylic acid", Brevet EP2 673 252 A1, 2013.

J.-L. Dubois, "procédé de préparation d'acroléine", Brevet FR2 897 058, 2007.

——, "Method for producing acrolein by means of dehydration of glycerol", Brevet WO2 009 156 664 A3, 2009.

——, "Process of manufacturing acrolein from glycerol", Brevet WO2 010 046 227 A1, 2010.

——, "Plate-type reactor with in-situ injection", Brevet US2 014 094 617, 2011.

——, "Catalytic reaction with reverse-flow regeneration", Brevet US20 150 141 703A1, 2012.

——, "Sustainable glycerine dehydration to acrolein". Presented at American Oil Chemists Society (AOCS), San Antonio, USA, 2014.

J.-L. Dubois, C. Duquenne, et W. Hoelderlich, "Process for dehydrating glycerol to acrolein", Brevet WO2 006 087 083 A2, 2006.

J.-L. Dubois, C. Duquenne, W. Hoelderich, et J. Kervennal, "Process for dehydrating glycerol to acrolein", Brevet WO2 006 087 084 A2, 2006.

J.-L. Dubois, Y. Magatani, et K. Okumura, “Process for manufacturing acrolein from glycerol”, Brevet WO2 009 127 889 A1, 2009.

——, “Process for manufacturing acrolein or acrylic acid from glycerin”, Brevet WO2 009 128 555 A3, 2009.

J.-L. Dubois, K. Okumura, Y. Kobayashi, et R. Hiraoka, “Improved process of dehydration reactions”, Brevet WO2 013 017 942 A2, 2013.

D. Eley, H. Pines, et P. B. Weisz, éds., *Selective Oxidation of Propylene*, série Advances in Catalysis. Academic Press, 1979, vol. 27.

S. Erfle, U. Armbruster, U. Bentrup, A. Martin, et A. Bruckner, “Impact of redox properties on dehydration of glycerol to acrolein over heteropolyacids assessed by operando-EPR spectroscopy”, *Applied Catalysis A : General*, vol. 391, no. 1–2, pp. 102–109, 2011.

W. G. Etzkorn, S. E. Pedersen, et T. E. Snead, *Acrolein and Derivatives*. John Wiley Sons, Inc., 2000.

L.-S. Fan, R. Lau, C. Zhu, K. Vuong, W. Warsito, X. Wang, et G. Liu, “Evaporative liquid jets in gas–liquid–solid flow system”, *Chemical Engineering Science*, vol. 56, no. 21–22, pp. 5871–5891, 2001.

Y. Fan, C. E, M. Shi, C. Xu, J. Gao, et C. Lu, “Diffusion of feed spray in fluid catalytic cracker riser”, *AIChE Journal*, vol. 56, no. 4, pp. 858–868, 2010.

B. C. H. Farrauto R. J., *Fundamentals of Industrial Catalytic Processes*. Kluwer Academic Publishers, London, 1997.

J. Gao, C. Xu, S. Lin, G. Yang, et Y. Guo, “Simulations of gas-liquid-solid 3-phase flow and reaction in FCC riser reactors”, *AIChE Journal*, vol. 47, no. 3, pp. 677–692, 2001.

M. Guisnet et P. Magnoux, “Organic chemistry of coke formation”, *Applied Catalysis A : General*, vol. 212, no. 1–2, pp. 83–96, 2001.

A. Gupta et D. S. Rao, “Effect of feed atomization on FCC performance : simulation of entire unit”, *Chemical Engineering Science*, vol. 58, no. 20, pp. 4567–4579, 2003.

T. Haas, A. Neher, D. Arntz, H. Klenk, et W. Girke, “Process for the simultaneous production of 1,2- and 1,3-propanediol”, Brevet US5 426 249 A, 1993.

G. Hearne et G. H. P. A, “Process of converting a polyhydric alcohol to a carbonyl compound”, Brevet US2 042 224 A, 1936.

S. Heinrich et L. Mörl, “Fluidized bed spray granulation—a new model for the description of particle wetting and of temperature and concentration distribution”, *Chemical Engineering and Processing : Process Intensification*, vol. 38, no. 4–6, pp. 635–663, 1999.

H. E. Hoyt et T. H. Manninen, “Production of acrolein from glycerol”, Brevet US2 558 520 A, 1951.

Y. Izumi, R. Hasebe, et K. Urabe, “Catalysis by heterogeneous supported heteropoly acid”, *Journal of Catalysis*, vol. 84, no. 2, pp. 402–409, 1983.

O. Jacque et W. Henry, éds., *Deactivation and Poisoning of Catalysts*. Marcel Dekker Inc., New york, 1985.

C.-J. Jia, Y. Liu, W. Schmidt, A.-H. Lu, et F. Schuth, “Small-sized HZSM−5 zeolite as highly active catalyst for gas phase dehydration of glycerol to acrolein”, *Journal of Catalysis*, vol. 269, no. 1, pp. 71–79, 2010.

M. Kaarsholm, F. Joensen, J. Nerlov, R. Cenni, J. Chaouki, et G. S. Patience, “Phosphorous modified ZSM−5 : Deactivation and product distribution for MTO”, *Chemical Engineering Science*, vol. 62, no. 18–20, pp. 5527–5532, 2007.

S. Kahlbum, “Procédé de fabrication d’acroléine”, Brevet FR 695 931 (A), 1930.

B. Katryniok, S. Paul, M. Capron, et F. Dumeignil, “Towards the sustainable production of acrolein by glycerol dehydration”, *ChemSusChem*, vol. 2, no. 8, pp. 719–730, 2009.

B. Katryniok, S. Paul, V. Belliere-Baca, P. Rey, et F. Dumeignil, “Glycerol dehydration to acrolein in the context of new uses of glycerol”, *Green Chem.*, vol. 12, pp. 2079–2098, 2010.

B. Katryniok, S. Paul, M. Capron, C. Lancelot, V. Belliere-Baca, P. Rey, et F. Dumeignil, “A long-life catalyst for glycerol dehydration to acrolein”, *Green Chem.*, vol. 12, pp. 1922–1925, 2010.

Y. T. Kim, K.-D. Jung, et E. D. Park, “Gas-phase dehydration of glycerol over ZSM−5 catalysts”, *Microporous and Mesoporous Materials*, vol. 131, no. 1–3, pp. 28–36, 2010.

A. K. Kinage, P. P. Upare, P. Kasinathan, Y. K. Hwang, et J.-S. Chang, “Selective conversion of glycerol to acetol over sodium-doped metal oxide catalysts”, *Catalysis Communications*,

vol. 11, no. 7, pp. 620–623, 2010.

I. V. Kozhevnikov, "Sustainable heterogeneous acid catalysis by heteropoly acids", *Journal of Molecular Catalysis A : Chemical*, vol. 262, no. 1–2, pp. 86–92, 2007, polyoxometalates in Catalysis.

O. L. Kuni Daizo, *Fluidization Engineering*. Butterworth-Heinemann, 1991.

X. Li, C. Zhang, C. Qin, C. Chen, et J. Shao, "Process for preparing acrolein by glycerin dewatering", Brevet CN101 070 276 B, 2007.

L. Liu, X. P. Ye, et J. J. Bozell, "A comparative review of petroleum-based and bio-based acrolein production", *ChemSusChem*, vol. 5, no. 7, pp. 1162–1180, 2012.

Q. Liu, Z. Zhang, Y. Du, J. Li, et X. Yang, "Rare earth pyrophosphates : Effective catalysts for the production of acrolein from vapor-phase dehydration of glycerol", *Catalysis Letters*, vol. 127, no. 3–4, pp. 419–428, 2009.

G. L. Maddikeri, A. B. Pandit, et P. R. Gogate, "Intensification approaches for biodiesel synthesis from waste cooking oil : A review", *Industrial and Engineering Chemistry Research*, vol. 51, no. 45, pp. 14 610–14 628, 2012.

S. Maronga et P. Wnukowski, "Establishing temperature and humidity profiles in fluidized bed particulate coating", *Powder Technology*, vol. 94, no. 2, pp. 181–185, 1997.

D. W. Marquardt, "An algorithm for least-squares estimation of non-linear parameters", *Journal of society for industrial mathematics*, vol. 11, no. 2, pp. 431–441, 1963.

C. Martin, G. Solana, V. Rives, G. Marci, L. Palmisano, et A. Sclafani, "Physico-chemical properties of WO_3/TiO_2 systems employed for 4-nitrophenol photodegradation in aqueous medium", *Catalysis Letters*, vol. 49, no. 3–4, pp. 235–243, 1997.

M. Y. Menetrez, "An overview of algae biofuel production and potential environmental impact", *Environmental Science and Technology*, vol. 46, no. 13, pp. 7073–7085, 2012.

P. Menon, "Coke on catalysts-harmful, harmless, invisible and beneficial types", *Journal of Molecular Catalysis*, vol. 59, no. 2, pp. 207–220, 1990.

D. Mores, E. Stavitski, M. H. F. Kox, J. Kornatowski, U. Olsbye, et B. M. Weckhuysen, "Space- and time-resolved in-situ spectroscopy on the coke formation in molecular sieves :

Methanol-to-olefin conversion over HZSM−5 and HSAPO−34", *Chemistry European Journal*, vol. 14, pp. 11 320–11 327, 2008.

M. Nasrin, A. Alireza, R. Reza, M. Tangestani, R. Eghtesadi, et A. S. Nejad, "Large-scale biodiesel production using microalgae biomass of nannochloropsis", *Biomass and Bioenergy*, vol. 39, pp. 449–453, 2012.

A. Neher, T. Haas, D. Arntz, H. Klenk, et W. Girke, "Process for the production of acrolein", Brevet US5 387 720 A, 1995.

L. Ning, Y. Ding, W. Chen, L. Gong, R. Lin, L. Yuan, et Q. Xin, "Glycerol dehydration to acrolein over activated carbon-supported silicotungstic acids", *Chinese Journal of Catalysis*, vol. 29, no. 3, pp. 212–214, 2008.

P. Oconnor, C. A. Corma, G. Huber, et L. A. Savanaud, "Process for production of acrolein and other oxygenated compounds from glycerol in transported bed reactor", Brevet WO2 008 052 993 A2, 2008.

K. Okumura, Y. Kaypbashi, R. Hiraoka, et J.-L. Dubois, "Improved process of dehydration reactions", Brevet WO2 013 018 915A3, 2013.

M. Okuno, E. Matsunami, T. Takahashi, H. Kasuga, M. Okada, et M. Kirishiki, "Production method of acrolein", Brevet WO2 007 132 926 A1, 2007.

C. M. O'Neil et E. E. Wolf, "Yield improvements in membrane reactors for partial oxidation reactions", *Industrial and Engineering Chemistry Research*, vol. 45, no. 8, pp. 2697–2706, 2006.

L. Ott, M. Bicker, et H. Vogel, "Catalytic dehydration of glycerol in sub- and supercritical water : a new chemical process for acrolein production", *Green Chem.*, vol. 8, pp. 214–220, 2006.

M. Pagliaro et M. Rossi, *The Future of Glycerol*. The Royal Society of Chemistry, 2010.

K. Pathak, K. M. Reddy, N. Bakhshi, et A. Dalai, "Catalytic conversion of glycerol to value added liquid products", *Applied Catalysis A : General*, vol. 372, no. 2, pp. 224–238, 2010.

G. S. Patience, Y. Farrie, J.-F. Devaux, et J.-L. Dubois, "Oxidation kinetics of carbon deposited on cerium-doped $FePO_4$ during dehydration of glycerol to acrolein", *Chemical Engineering and Technology*, vol. 35, no. 9, pp. 1699–1706, 2012.

G. Patience et P. Mills, "Modelling of propylene oxidation in a circulating fluidized-bed reactor", dans *New Developments in Selective Oxidation II Proceedings of the Second World Congress and Fourth European Workshop Meeting*, série Studies in Surface Science and Catalysis, V. C. Corberán et S. V. Bellón, éds. Elsevier, 1994, vol. 82, pp. 1–18.

N. Pethan Rajan, G. S. Rao, V. Pavankumar, et K. V. R. Chary, "Vapour phase dehydration of glycerol over VPO catalyst supported on zirconium phosphate", *Catalysis Science and Technology*, vol. 4, pp. 81–92, 2014.

J. A. Posada, L. E. Rincon, et C. A. Cardona, "Design and analysis of biorefineries based on raw glycerol : Addressing the glycerol problem", *Bioresource Technology*, vol. 111, no. 0, pp. 282–293, 2012.

S. Ramayya, A. Brittain, C. DeAlmeida, W. Mok, et M. J. A. Jr, "Acid-catalysed dehydration of alcohols in supercritical water", *Fuel*, vol. 66, no. 10, pp. 1364–1371, 1987.

H. Redlingshofer, O. Krocher, W. Bock, K. Huthmacher, et G. Emig, "Catalytic wall reactor as a tool for isothermal investigations in the heterogeneously catalyzed oxidation of propene to acrolein", *Industrial and Engineering Chemistry Research*, vol. 41, no. 6, pp. 1445–1453, 2002.

H. Redlingshofer, A. Fischer, C. Weckbecker, K. Huthmacher, et G. Emig, "Kinetic modeling of the heterogeneously catalyzed oxidation of propene to acrolein in a catalytic wall reactor", *Industrial and Engineering Chemistry Research*, vol. 42, no. 22, pp. 5482–5488, 2003.

L. Shen, Y. Feng, H. Yin, A. Wang, L. Yu, T. Jiang, Y. Shen, et Z. Wu, "Gas phase dehydration of glycerol catalyzed by rutile TiO_2-supported heteropolyacids", *Journal of Industrial and Engineering Chemistry*, vol. 17, no. 3, pp. 484–492, 2011.

L. Shen, H. Yin, A. Wang, X. Lu, et C. Zhang, "Gas phase oxidehydration of glycerol to acrylic acid over Mo/V and W/V oxide catalysts", *Chemical Engineering Journal*, vol. 244, no. 0, pp. 168–177, 2014.

L. Shen, H. Yin, A. Wang, X. Lu, C. Zhang, F. Chen, Y. Wang, et H. Chen, "Liquid phase catalytic dehydration of glycerol to acrolein over brønsted acidic ionic liquid catalysts", *Journal of Industrial and Engineering Chemistry*, vol. 20, no. 3, pp. 759–766, 2014.

D. A. Simonetti, J. Rass-Hansen, E. L. Kunkes, R. R. Soares, et J. A. Dumesic, "Coupling of glycerol processing with fischer-tropsch synthesis for production of liquid fuels", *Green Chem.*, vol. 9, pp. 1073–1083, 2007.

K. S. W. Sing, D. H. Everett, R. A. W. Haul, L. Moscou, R. A. Pierotti, J. Rouquerol, et T. Siemieniewska, “Reporting physisorption data for gas/solid systems with special reference to the determination of surface area and porosity (recommendations 1984)”, *Pure and Applied Chemistry*, vol. 57, no. 4, pp. 603–619, 1985.

R. R. Soares, D. A. Simonetti, et J. A. Dumesic, “Glycerol as a source for fuels and chemicals by low-temperature catalytic processing”, *Angewandte Chemie International Edition*, vol. 45, no. 24, pp. 3982–3985, 2006.

N. O. Sonntag, “Glycerolysis of fats and methyl esters—status, review and critique”, *Journal of the American Oil Chemists Society*, vol. 59, no. 10, pp. 795A–802A, 1982.

D. Stosic, S. Bennici, S. Sirotin, C. Calais, J.-L. Couturier, J.-L. Dubois, A. Travert, et A. Auroux, “Glycerol dehydration over calcium phosphate catalysts : Effect of acidic–basic features on catalytic performance”, *Applied Catalysis A : General*, vol. 447-–448, pp. 124–134, 2012.

W. Suprun, M. Lutecki, T. Haber, et H. Papp, “Acidic catalysts for the dehydration of glycerol : Activity and deactivation”, *Journal of Molecular Catalysis A : Chemical*, vol. 309, no. 1–2, pp. 71–78, 2009.

L. Z. Tao, S. H. Chai, Y. Zuo, W. T. Zheng, Y. Liang, et B. Q. Xu, “Sustainable production of acrolein : Acidic binary metal oxide catalysts for gas-phase dehydration of glycerol”, *Catalysis Today*, vol. 158, no. 3–4, pp. 310–316, 2010.

K. N. Theologos et N. C. Markatos, “Advanced modeling of fluid catalytic cracking riser-type reactors”, *AIChE Journal*, vol. 39, no. 6, pp. 1007–1017, 1993.

K. Theologos, A. Lygeros, et N. Markatos, “Feedstock atomization effects on FCC riser reactors selectivity”, *Chemical Engineering Science*, vol. 54, no. 22, pp. 5617–5625, 1999.

M. Timofeeva, “Acid catalysis by heteropoly acids”, *Applied Catalysis A : General*, vol. 256, no. 1–2, pp. 19–35, 2003, heteropoly Acids Special Issue.

E. Tsukuda, S. Sato, R. Takahashi, et T. Sodesawa, “Production of acrolein from glycerol over silica-supported heteropoly acids”, *Catalysis Communications*, vol. 8, no. 9, pp. 1349–1353, 2007.

M. R. Tyson KS, *Biodiesel handling and use guide*, 3e éd. Springfield, 2006.

A. Ulgen et W. Hoelderich, “Conversion of glycerol to acrolein in the presence of WO_3/ZrO_2 catalysts”, *Catalysis Letters*, vol. 131, no. 1–2, pp. 122–128, 2009.

A. Ulgen et W. F. Hoelderich, “Conversion of glycerol to acrolein in the presence of WO_3/TiO_2 catalysts”, *Applied Catalysis A : General*, vol. 400, no. 1–2, pp. 34–38, 2011.

S. J. Vasconcelos, C. L. Lima, J. M. Filho, A. C. Oliveira, E. B. Barros, F. F. de Sousa, M. G. Rocha, P. Bargiela, et A. C. Oliveira, “Activity of nanocasted oxides for gas-phase dehydration of glycerol”, *Chemical Engineering Journal*, vol. 168, no. 2, pp. 656–664, 2011.

E. Vasiliadou et A. Lemonidou, “Kinetic study of liquid-phase glycerol hydrogenolysis over Cu/SiO_2 catalyst”, *Chemical Engineering Journal*, vol. 231, no. 0, pp. 103–112, 2013.

M. J. Verhoef, P. J. Kooyman, J. A. Peters, et H. van Bekkum, “A study on the stability of MCM−41-supported heteropoly acids under liquid- and gas-phase esterification conditions”, *Microporous and Mesoporous Materials*, vol. 27, no. 2–3, pp. 365–371, 1999.

S. Vyazovkin, A. K. Burnham, J. M. Criado, L. A. Pérez-Maqueda, C. Popescu, et N. Sbirrazzuoli, “ICTAC kinetics committee recommendations for performing kinetic computations on thermal analysis data”, *Thermochimica Acta*, vol. 520, no. 1–2, pp. 1–19, 2011.

C. Wang, H. Jiang, C. Chen, R. Chen, et W. Xing, “Solvent effect on hydrogenolysis of glycerol to 1,2-propanediol over Cu-ZnO catalyst”, *Chemical Engineering Journal*, vol. 264, pp. 344–350, 2015.

F. Wang, J.-L. Dubois, et W. Ueda, “Catalytic dehydration of glycerol over vanadium phosphate oxides in the presence of molecular oxygen”, *Journal of Catalysis*, vol. 268, no. 2, pp. 260–267, 2009.

——, “Catalytic performance of vanadium pyrophosphate oxides (VPO) in the oxidative dehydration of glycerol”, *Applied Catalysis A : General*, vol. 376, no. 1–2, pp. 25–32, 2010.

M. Watanabe, T. Iida, Y. Aizawa, T. M. Aida, et H. Inomata, “Acrolein synthesis from glycerol in hot-compressed water”, *Bioresource Technology*, vol. 98, no. 6, pp. 1285–1290, 2007.

G. E. William, *Acrolein and Derivatives*. John Wiley Sons, Inc., 2000.

Y. Wu, X. Ye, X. Yang, X. Wang, W. Chu, et Y. Hu, “Heterogenization of heteropolyacids : A general discussion on the preparation of supported acid catalysts”, *Industrial and Engineering Chemistry Research*, vol. 35, no. 8, pp. 2546–2560, 1996.

S. Xia, Z. Yuana, L. Wangb, P. Chena, et Z. Houa, “Catalytic production of 1,2-propanediol from glycerol in bio-ethanol solvent”, *Bioresource Technology*, vol. 104, no. 0, pp. 814–817, 2012.

W. Yan et G. J. Suppes, “Low-pressure packed-bed gas-phase dehydration of glycerol to acrolein”, *Industrial and Engineering Chemistry Research*, vol. 48, no. 7, pp. 3279–3283, 2009.

W. C. Yang, *Handbook of fluidization and fluid-particles systems : CRS Press*. Siemens Westinghouse Power Corporation Pittsburgh, Pennsylvania, U.S.A, 2003.

X. L. Yang, W. L. Dai, C. Guo, H. Chen, Y. Cao, H. Li, H. He, et K. Fan, “Synthesis of novel core-shell structured WO_3/TiO_2 spheroids and its application in the catalytic oxidation of cyclopentene to glutaraldehyde by aqueous H_2O_2”, *Journal of Catalysis*, vol. 234, no. 2, pp. 438–450, 2005.

Z. Yuan, J. Wang, L. Wang, W. Xie, P. Chen, Z. Hou, et X. Zheng, “Biodiesel derived glycerol hydrogenolysis to 1,2-propanediol on Cu/MgO catalysts”, *Bioresource Technology*, vol. 101, no. 18, pp. 7088–7092, 2010.

Z. Zakaria, J. Linnekoski, et N. Amin, “Catalyst screening for conversion of glycerol to light olefins”, *Chemical Engineering Journal*, vol. 207–208, no. 0, pp. 803–813, 2012.

APPENDIX A Liquid injection evaluation

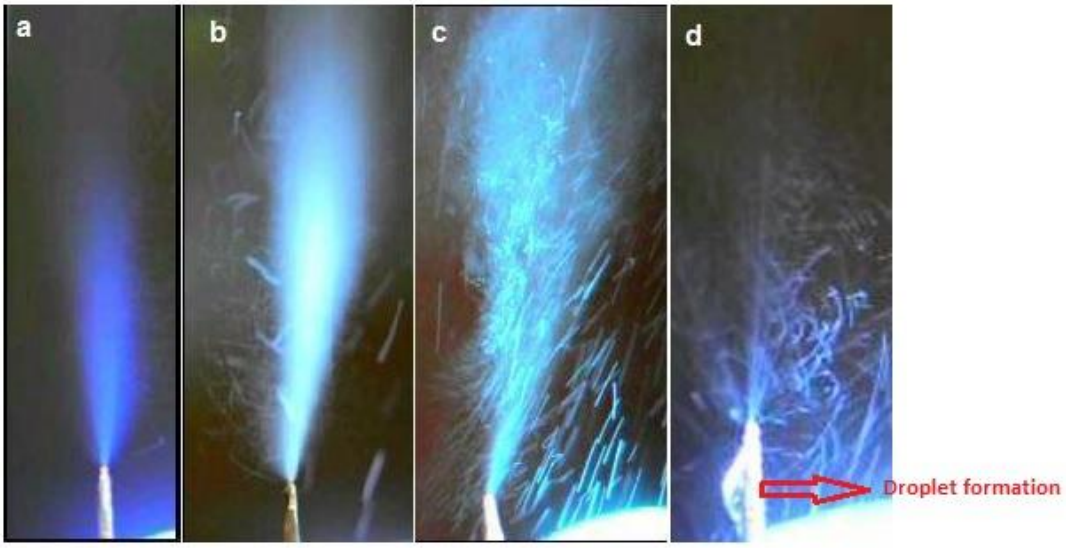

Figure A.1 Injection quality for 30 wt% glycerol aqueous solution

Table A.1 Dependancy of injector pressure drop to gas/liquid flow rates for 10 wt% glycerol/water solution

Q liq. $mL\,min^{-1}$	Q Ar $mL\,min^{-1}$	Δp psi
0.1	200	16
0.1	300	26
0.1	500	38
0.1	700	48
0.1	1000	70
0.1	1500	74
0.3	200	58
0.3	300	62
0.3	500	68
0.3	700	72
0.3	1000	75
0.5	200	75
0.5	500	75

Table A.2 Dependancy of injector pressure drop to gas/liquid flow rates for 30 wt% glycerol/water solution

Q liq. $mL\,min^{-1}$	Q Ar $mL\,min^{-1}$	Δp psi
0.1	200	12
0.1	300	14
0.1	500	16
0.1	700	40
0.1	1000	56
0.1	1500	70
0.3	200	11
0.3	300	17
0.3	500	30
0.3	700	46
0.3	1000	66